Kirsi Spoof-Tuomi

An evaluation of renewable fuels´ potential to reduce global and local emissions in non-road and heavy-duty on-road sectors

ACTA WASAENSIA 514

Vaasan yliopisto
UNIVERSITY OF VAASA

ISBN 978-952-395-097-9 (print)
978-952-395-098-6 (online)

ISSN 0355-2667 (Acta Wasaensia 514, print)
2323-9123 (Acta Wasaensia 514, online)

URN https://urn.fi/URN:ISBN:978-952-395-098-6

Hansaprint Oy, Turenki, 2023.

ACADEMIC DISSERTATION

To be presented, with the permission of the Board of the School of Technology and Innovations of the University of Vaasa, for public examination on the 6th of September, 2023, at noon.

Article based dissertation, School of Technology and Innovations, Energy Technology

Author Kirsi Spoof-Tuomi https://orcid.org/0000-0002-6212-9630

Supervisor(s) Professor Seppo Niemi
University of Vaasa, School of Technology and Innovations, Energy Technology.

Dr Jukka Kiijärvi
University of Vaasa. School of Technology and Innovations, Energy Technology.

Custos Professor Seppo Niemi
University of Vaasa. School of Technology and Innovations, Energy Technology

Reviewers Dr Jyrki Ristimäki
Royal Caribbean International.

Professor Anders Christiansen Erlandsson
DTU - Technical University of Denmark, Department of Civil and Mechanical Engineering, Thermal Energy.

Opponent Adjunct Professor, Dr Mika Huuhtanen
University of Oulu, Faculty of Technology, Environmental and Chemical Engineering.

Tiivistelmä

Hiilineutraaliuuden saavuttaminen EU:ssa vuoteen 2050 mennessä vaatii kasvihuonekaasujen merkittävää vähentämistä koko liikennesektorilta. Sähköistys ja hybridisaatio ovat kasvavia trendejä kevyissä ajoneuvoissa. Sen sijaan raskaan runkoliikenteen ja laivaliikenteen vaatimat suuret energiamäärät on vaikea korvata sähköllä. Liikkuvien työkoneiden kohdalla sähköistystä vaikeuttaa puuttuva latausinfrastruktuuri. Polttomoottoreiden kasvihuonekaasupäästöihin voidaan kuitenkin merkittävästi vaikuttaa polttoainevalinnoilla. Tämän vuoksi siirtyminen vaihtoehtoisiin polttoaineisiin on yksi keskustelun kohteena olevista strategioista.

Tässä tutkimuksessa selvitettiin biometaanin ja mäntyöljypohjaisen uusiutuvan dieselpolttoaineen käytön vaikutuksia päästöihin. Kasvihuonekaasupäästöjen lisäksi selvitettiin polttoaineiden poltosta aiheutuvat haitalliset paikallispäästöt. Biometaania tutkittiin Itämerellä liikennöivään matkustaja-autolauttaan kohdistuvalla tapaustutkimuksella. Lisäksi tutkittiin biometaanikäyttöisen kaupunkibussin ajonaikaisia päästöjä todellisissa ajo-olosuhteissa. Uusiutuvalla dieselillä päästömittaukset tehtiin työkonedieselmoottorikokeilla laboratorio-olosuhteissa.

Kasvihuonekaasupäästöt laskettiin polttoaineiden koko elinkaaren ajalta. Tulokset osoittivat, että kestävistä biomassalähteistä tuotettujen uusiutuvien polttoaineiden käyttö voi vähentää elinkaaren aikaisia kasvihuonekaasupäästöjä 65–90 % fossiilisiin polttoaineisiin verrattuna. Lisäksi biometaanilla ja uusiutuvalla dieselillä voidaan välittömästi parantaa paikallista ilmanlaatua, koska polton aikaiset paikallispäästöt vähenevät. Nesteytetty biometaani pienensi meriliikenteen hiukkaspäästöjä 80 % dieselöljykäyttöön verrattuna. Rikkidioksidipäästöt vähenivät 99 % dieselöljyyn verrattuna ja typen oksidit olivat alhaiset. Uusiutuvalla dieselillä kaikki säännellyt kaasumaiset paikallispäästöt olivat hieman pienempiä kuin dieselöljyllä. Uusiutuvalla dieselillä hiukkaslukumäärä laski jopa 26 % perinteiseen fossiiliseen dieseliin verrattuna.

Biometaani ja uusiutuva diesel osoittautuivat tehokkaiksi keinoiksi vähentää liikenteen kasvihuonekaasupäästöjä lyhyellä ja keskipitkällä aikavälillä vaikeasti sähköistettävässä liikenteessä. Biometaanin ja uusiutuvan dieselin ensisijainen huolenaihe on niiden rajallinen saatavuus. Kestävästi tuotettujen polttoaineiden tarjonnan lisäämiseksi ja välttämättömien investointien nopeuttamiseksi tarvitaan päättäväistä pitkän aikavälin politiikkaa.

Asiasanat:
biometaani, uusiutuva diesel, elinkaarikasvihuonekaasupäästöt, paikallispäästöt, hiilenpoisto

Abstract

Achieving carbon neutrality in the European Union by 2050 requires deep reductions in greenhouse gas emissions in all forms of transport. Powertrain electrification and hybridisation are growing trends for light vehicles. Instead, electrification of maritime and heavy long-distance transport is far more difficult due to their massive energy needs. Battery technology is also problematic for mobile non-road machinery operating for long periods far from the charging infrastructure. However, fuel choices can significantly influence greenhouse gas emissions from internal combustion engines. Therefore, a transition to alternative fuels is one of the strategies under discussion.

This study investigated the emission performance of two alternative fuels: biomethane and tall oil-based renewable diesel. In addition to greenhouse gas emissions, the harmful local emissions originating from fuel combustion were investigated. Biomethane was evaluated through a case study of a RoPax vessel operating in the Baltic Sea. In addition, real-driving emissions from a biomethane-powered city bus were measured. The study of renewable diesel´s emissions was carried out with engine experiments on an off-road diesel engine under laboratory conditions.

Greenhouse gas emissions were calculated over the entire life cycle of the fuels. The results showed that using renewable fuels derived from sustainable biomass sources can reduce life-cycle greenhouse gas emissions by 65–90 % compared with fossil fuels. In addition, biomethane and renewable diesel can immediately improve local air quality by reducing local emissions. Burning liquefied biomethane reduced particulate matter by 80 % relative to marine diesel oil. Sulphur dioxide emissions were negligible and NO_x emissions were low. Renewable diesel slightly reduced all regulated local gaseous emissions. The reduction in particulate number was more significant, at up to 26 % compared with conventional market diesel.

Biomethane and renewable diesel proved to be effective ways to decarbonise transport in the short to medium term in hard-to-abate sectors with no immediate alternatives. The primary concern with biomethane and renewable diesel today is their limited availability. Guaranteed long-term policy is needed to scale up the supply of sustainably produced biofuels and accelerate the necessary investments.

Keywords:
biomethane, renewable diesel, life-cycle greenhouse gas emissions, local emissions, decarbonisation

ACKNOWLEDGEMENT

This dissertation has been developed mainly based on three research projects conducted at the University of Vaasa during 2018–2022. In addition to the support I received from academic colleagues, this thesis benefited from the advice and expertise of several business partners. I want to express my gratitude to everyone who made this dissertation possible.

First, I owe my deepest gratitude to my supervisors, Professor Seppo Niemi and Dr Jukka Kiijärvi, for their guidance, first with my master's degree and then with this dissertation. We have made a long and fruitful journey. Seppo, accept my heartfelt gratitude for your time, support, and encouragement throughout my studies. Jukka, your excellent advice during the finalisation of this dissertation ensured the thesis's highest possible overall quality. Thank you both gentlemen: I could not have had better supervisors than you.

I thank my preliminary examiners, Dr Jyrki Ristimäki and Professor Anders Christiansen Erlandsson, for their constructive feedback. Warm thanks also to Adjunct Professor, Dr Mika Huuhtanen for agreeing to be my opponent.

I have had the privilege of being part of a great research team. Thanks go to Dr Teemu Ovaska, Mrs Sonja Heikkilä, Mrs Michaela Hissa, Mr Olav Nilsson, and Dr Katriina Sirviö, among others. Furthermore, I want to thank all co-authors who have contributed to the publications.

I want to express my gratitude to Business Finland, the Regional Council of Ostrobothnia, and the European Regional Development Fund for financial support for the research projects in question. I would also thank Gasum Oy and the Finnish Foundation for Technology Promotion for awarding a personal encouragement grant to support my postgraduate studies.

I wish to thank the University of Vaasa for giving me the necessary working time for the research work and for finalising the dissertation. In addition, I thank AGCO Power Finland and the Novia University of Applied Sciences for providing the equipment and facilities necessary for the laboratory experiments, and UPM Biofuels for delivering renewable diesel fuel for the research. I also wish to thank Wasaline/NLC Ferry Ab Oy for allowing the use of its ferry traffic for the case study. Thanks also go to Scania Vaasa, Oy Wasa Citybus Ab, and the City of Vaasa for their collaboration in the real-driving emission measurement campaigns performed in this study.

Last but not least, I wish my most loving thanks to Ville for your love and support through the years.

Vaasa, June 2023

Kirsi Spoof-Tuomi

Contents

Figures

Tables

Abbreviations

CBG	compressed biomethane, also referred to as compressed biogas
CH_4	methane
CNG	compressed natural gas
CO	carbon monoxide
CSS	crude sulphate soap
CTO	crude tall oil
DFO	diesel fuel oil
GHG	greenhouse gas
GWP	global warming potential
HC	hydrocarbon emissions
IMO	International Maritime Organization
LBG	liquefied biomethane, also referred to as liquefied biogas
LCI	life-cycle inventory

LNG	liquefied natural gas
MDO	marine diesel oil
N_2O	nitrous oxide
NH_3	ammonia
NO_x	nitrous oxides
PM	particulate matter
PM_{10}	fine particulate matter with a diameter of less than 10 µm
RD	renewable diesel derived from crude tall oil
RD50	blend containing 50 vol.-% crude tall oil-derived renewable diesel and 50 vol.-% fossil diesel
RD100	neat crude tall oil-derived renewable diesel (same as RD)
RED II	EU Renewable Energy Directive
SCR	selective catalytic reduction
SO_2	sulphur dioxide

Publications

This doctoral dissertation summarises the following four original research articles, referred to in the text by their Roman numerals:

I. Spoof-Tuomi, K. & Niemi, S. (2020). Environmental and Economic Evaluation of Fuel Choices for Short Sea Shipping. *Clean Technologies,* 2(1), 34–52. https://doi.org/10.3390/cleantechnol2010004

II. Spoof-Tuomi, K., Arvidsson, H., Nilsson, O., Niemi, S. (2022). Real-Driving Emissions of an Aging Biogas-Fueled City Bus. *Clean Technologies*, 4(4), 954–971. https://doi.org/10.3390/cleantechnol4040059

III. Spoof-Tuomi, K., Vauhkonen, V., Niemi, S., Ovaska, T., Lehtonen, V., Heikkilä, S. & Nilsson O. (2021). Effects of Crude Tall Oil Based Renewable Diesel on the Performance and Emissions of a Non-Road Diesel Engine. *SAE Technical Paper* 2021-01-1197. https://doi.org/10.4271/2021-01-1197

IV. Spoof-Tuomi, K., Vauhkonen, V., Niemi, S., Ovaska, T., Lehtonen, V., Heikkilä, S. & Nilsson, O. (2021). Crude Tall Oil based Renewable Diesel: Performance, Emission Characteristics and Storage Stability. *SAE Technical Paper* 2021-01-1208, 2021. https://doi.org/10.4271/2021-01-1208

Author's contribution

Paper I: Spoof-Tuomi is the lead author. As the corresponding author, Spoof-Tuomi designed the study, collected and analysed the data, visualised the results and wrote the article. Niemi provided valuable comments on the paper and supervised the study.

Paper II: Spoof-Tuomi is the lead author and the corresponding author who designed the study and organised the experiments. Arvidsson and Nilsson performed the emission measurements. Arvidsson preprocessed the data: Spoof-Tuomi analysed the data, visualised the results and wrote the article. Niemi provided valuable comments and supervised the study.

Paper III: Spoof-Tuomi is the main author. Vauhkonen and Niemi designed the study. Spoof-Tuomi implemented the engine experiment with Nilsson, Ovaska, and Heikkilä. Spoof-Tuomi, Ovaska and Lehtonen analysed the data and visualised the results. Spoof-Tuomi wrote the paper, together with Vauhkonen and Ovaska. Niemi contributed to the discussions and provided valuable comments on the paper.

Paper IV: Spoof-Tuomi is the main author. Vauhkonen and Niemi designed the study. Spoof-Tuomi implemented the engine experiment with Nilsson, Ovaska, and Heikkilä. Spoof-Tuomi, Ovaska, and Lehtonen analysed the data and visualised the results. Spoof-Tuomi wrote the paper, together with Vauhkonen and Ovaska. Niemi contributed to the discussions and provided valuable comments on the paper.

1 INTRODUCTION

1.1 Background

Climate change is one of the biggest environmental, economic and humanitarian challenges our society has ever faced. The main cause of climate change is the release of greenhouse gases (GHG) into the atmosphere. Energy consumption is by far the largest source of human-caused GHG emissions. Worldwide data from 2019 indicates that the energy sector was responsible for 75 % of total GHG emissions. In the European Union, the share of GHG emissions from the energy sector was even higher, at 87 %. Within the energy sector, transport was responsible for 30 % of EU-wide GHG emissions (Climate Watch, 2022).

There is a global consensus that greenhouse gas emissions must be significantly reduced to avoid the worst impacts of climate change. Various laws and regulations have already been implemented to combat and respond to global warming. For example, in July 2021, the European Commission adopted an extensive legislative package, “Fit for 55”, to reduce the economy-wide GHG emissions by at least 55 % by 2030 from the 1990 level. This ambitious goal for the current decade is expected to put Europe on a balanced path to becoming climate neutral by 2050, meaning an economy with net-zero GHG emissions (EU COM 2020/562).

“Fit for 55” includes a proposal to revise the EU Renewable Energy Directive (RED II) to support development of sustainable biofuels. The currently applicable RED II sets a binding overall EU target, whereby at least 32 % of the EU's total final energy consumption energy must come from renewable sources in 2030. The binding target for renewable energy in the transport sector by 2030 is 14 %. The share of advanced biofuels and biogas within this minimum share shall be at least 3.5 % by 2030 (EU 2018/2001). RED II also defines a set of sustainability and GHG emission criteria for biofuels, so that contribute to the RED II targets. The new revision, RED III, is expected to tighten both the renewable energy targets and the sub-targets for advanced biofuels after 2023, aligning them with the 55 % GHG emission reduction target by 2030.

Shipping is also approaching a pivotal moment on the journey to reduce global GHG emissions. The International Maritime Organization’s (IMO) initial reduction strategy was adopted in 2018, aiming to cut the global fleet´s GHG emissions by 50 % by 2050 from 2008 levels, despite growing traffic volumes (IMO, 2018). The IMO strategy will be updated in 2023, moving from short-term energy

efficiency measures to mid- and long-term measures, including actions to promote the transition from fossil fuels to low- and zero-carbon fuels (IMO, 2019). The European Commission wants renewable and low-carbon fuels to account for 6–9 % of international maritime transport´s fuel mix in 2030, and 86–88 % by 2050, thus contributing to the EU economy-wide GHG emissions reduction targets (EU, 2021/562).

Although the global environmental agenda is increasingly shifting to focus on climate change, tackling local air pollutants remains an important issue. The quality of the air can significantly impact our health and the environment. Air pollution is claimed to be the single largest environmental health risk in Europe (EEA, 2022b). Pollutants with the strongest evidence for public health concern include particulate matter (PM), carbon monoxide (CO), sulphur dioxide (SO_2), and oxides of nitrogen (NO_x) (WHO, 2023). In addition to the harmful effects on human health, air pollution has adverse effects on terrestrial and aquatic ecosystems, degrading environments and reducing biodiversity (EEA, 2023a).

1.2 Pathways towards more sustainable transport

Reducing the total GHG emissions from the transport and non-road sector in accordance with the European Commission's targets is possible through a combination of multiple decarbonisation measures – powertrain electrification and hybridisation, energy efficiency- and energy-saving measures, and the introduction of renewable fuels produced from sustainable feedstocks.

Powertrain electrification is a growing trend in vehicular applications (Niemi et al., 2019). However, full electrification seems to be relevant primarily to the light-duty vehicle sector (Kalghatgi, 2018). Electrification of heavy-duty and maritime transport will be difficult due to their massive energy needs (ERTRAC, 2016). Battery technology may be even more problematic for non-road machinery operating for long periods far from the charging infrastructure. Thus, efficient and mature internal combustion engine technology is expected to continue to play a central role for heavy-duty and non-road applications in the coming decades (Kalghatgi, 2018).

Although engine technology is undergoing further improvements to increase efficiency (Santos et al., 2021), it is clear that these alone are not enough to achieve GHG reductions of the required magnitude. Using renewable fuels in internal combustion engines is a viable option for reducing GHG emissions from the transport sector (Santos et al., 2021). Significant GHG savings stem from the fact that combustion of renewable fuels releases only biogenic CO_2, which is considered

carbon neutral in terms of climate effects if the fuel is derived from a sustainable source (Sitra, 2022). Hence, renewable fuels, both liquid and gaseous, are expected to play an increasingly important role in heavy-duty transport where electrification may not be feasible (Gray et al., 2021). Drop-in renewable fuels, such as biomethane and renewable paraffinic diesel oils, can be used directly in existing fleets with internal combustion engines. Their infrastructure or engines do not need any modifications (IEA-AMF, 2020), enabling rapid deployment of these fuels. Biofuels can also be mixed with their fossil counterparts.

It has been argued (e.g., Panoutsou et al., 2021) that advanced biofuels derived from organic waste materials and residues are the only immediately available solution for heavy-duty transport to meet the 2030 GHG reduction targets. This is on the basis that large-scale electrification of heavy-duty applications is difficult and because hydrogen technology is still nascent in this time horizon. An additional advantage of second-generation biofuels is that waste is efficiently utilised, following the principles of circular economy. Use of energy from renewable sources also promotes security of energy supply while providing environmental, social and health benefits (EU, 2018/2001).

1.3 Research objectives

Using renewable fuels derived from sustainable biomass sources is an effective way to decarbonise transport in the short to medium term in hard-to-abate sectors with no immediate alternatives. Furthermore, high-quality, bio-based fuels can immediately improve local air quality by reducing local emissions.

The primary objective of this dissertation was to demonstrate the emission reduction potential of two sustainably produced renewable fuels in the transport sector. One gaseous and one liquid fuel were investigated. The gaseous fuel was biomethane, produced from organic municipal waste. The liquid fuel was renewable diesel, made from wood-based tall oil. The study paid particular attention to greenhouse gas emissions, reflecting the global environmental agenda´s focus on climate change. In addition, the study evaluated local air pollutants, such as PM, NO_x, CO, and hydrocarbon (HC) emissions.

Testing renewable diesel, the emission measurements were carried out with engine experiments with an off-road diesel engine at an internal combustion engine laboratory. Biomethane was used in two ways; compressed at 200–250 bar and cooled down to a liquid at −162 °C. Liquefied biomethane was evaluated through a case study of a ro-ro/passenger ship operating in the Baltic Sea. Compressed biomethane was studied by measuring real-driving emissions from a biomethane-

fuelled city bus. Examination of emissions of a six-year-old bus also provided important information concerning the activity loss of a three-way catalyst over time. Catalyst activity loss has a crucial effect on emissions.

In addition to achieving acceptable emission levels, fuels are expected to remain stable and high-quality, even after long-term storage. Another goal of this study was to verify renewable diesel's storage stability through comprehensive fuel analyses.

A critical factor for the uptake of new fuels is their continuous availability. Thus, the thesis also discusses the current status and future prospects of renewable diesel and biomethane availability. Finally, the thesis calls attention to certain weaknesses in the current emission regulatory framework identified during the research.

1.4 Research design

The findings of this doctoral thesis are based mainly on four research papers in which the results were originally presented.

Paper I, entitled *"Environmental and Economic Evaluation of Fuel Choices for Short Sea Shipping"*, investigated the emission characteristics and environmental impacts of three marine fuel alternatives. The fuels studied were liquefied biomethane, also referred to as liquefied biogas (LBG); liquefied natural gas (LNG); and conventional marine diesel oil (MDO), combined with a proper exhaust aftertreatment system for NO_x reduction. The environmental impact categories considered were the global warming potential (GWP), acidification and eutrophication potentials and impacts on human health. Additionally, the study made an economic evaluation of LBG as a marine fuel, a topic hitherto lacking in the literature. Availability of LBG was also discussed.

Paper II, *"Real-Driving Emissions of an Aging Biogas-Fueled City Bus"*, presents the results of real-driving emissions measurements from a biomethane-fuelled city bus. Methane (CH_4) and other gaseous emissions were measured using a portable emissions measurement system in real-traffic conditions on a regular bus line in Vaasa. Examining a six-year-old bus fills the emission data gap closer to vehicles' service life. In addition, the lifetime carbon intensity of compressed biomethane, also referred to as compressed biogas (CBG), was calculated and compared with its fossil counterpart, compressed natural gas (CNG), and to traditional diesel fuel.

Paper III was entitled *"Effects of Crude Tall Oil Based Renewable Diesel on the Performance and Emissions of a Non-Road Diesel Engine"*. The paper investigated how renewable diesel derived from crude tall oil (CTO) affects the performance and exhaust emissions of a high-speed diesel engine designed for off-road use. The renewable diesel was studied in both its neat form and as a 50 % blend with conventional fossil diesel fuel oil (DFO). Exhaust emission evaluation included gaseous emissions, particulate number and particle size distribution. A combustion analysis was also performed.

Paper IV, *"Crude Tall Oil based Renewable Diesel: Performance, Emission Characteristics and Storage Stability",* examined the influence of long-term storage on CTO-derived renewable diesel. The paper reported the results of fuel analyses in a fresh state and after four years of storage. Additionally, the study included measurements of gaseous emissions, particulate number and particulate size distributions, plus basic engine performance.

As new material, this dissertation also investigated the life-cycle GHG emissions of renewable diesel derived from crude tall oil.

2 MATERIALS AND METHODS

This chapter introduces the investigated fuels and their production routes, and explains the data collection and data analysis methods used in the studies.

2.1 Fuels

2.1.1 Biomethane

Biomethane is the purified form of raw biogas and can be used directly as a substitute for fossil natural gas. Biogas, the pre-stage of biomethane, can be sourced from a wide variety of organic matter. Wet organic matter with a low lignocellulose content, such as organic waste and sewage sludge, is appropriate for biogas production through anaerobic digestion (Strauch et al., 2013). This is currently the most common way to produce biogas.

Biomethane is an effective tool for mitigating climate change. It offers significant GHG emission reduction potential in several ways. First, it replaces fossil fuels. Second, it avoids methane emissions from decomposing wastes. Third, it entails production of green fertiliser which replaces carbon-intensive chemical fertilisers (EBA, 2020). Most local emissions, such as particulate and sulphur emissions, are also low (Pérez-Camacho et al., 2019).

This thesis investigated biomethane produced via anaerobic digestion of locally collected municipal organic waste. Following anaerobic digestion, the biogas is purified and upgraded to 97–98 % methane. Biomethane was used in two ways; compressed at 200–250 bar (CBG, Paper II) and cooled down to a liquid at –162 °C (LBG, Paper I). The main advantage of LBG over CBG is its high energy density: LBG is three times as energy-dense and space-efficient than CBG at 200 bar, making it easier to transport and store. High energy density makes LBG a practical choice, especially for large engines, such as heavy vehicles and shipping.

To understand the GHG benefits of biomethane, we need to understand the concept of "short carbon cycle". Unlike natural gas, biomethane is produced from fresh organic materials, either directly (e.g., agricultural residues) or indirectly (e.g., sewage sludge, biowaste). During its growth, the biomass absorbs a certain amount of CO_2 from the atmosphere via photosynthesis. This captured CO_2 is returned to the atmosphere during biomethane combustion, after which the newly growing biomass recaptures it, and so on. Therefore, burning biomethane does not increase the amount of CO_2 in the atmosphere, but causes it to circulate in short

carbon cycles. So, we are talking about biogenic CO_2, as opposed to fossil CO_2. The latter is released after millions of years of underground storage, being previously inaccessible. (EBA, 2020.)

Biomethane production from organic waste materials has no unwanted side effects related to land use or food security (Scarlat et al., 2018). Municipal biowaste as a feedstock meets the EU RED II sustainability criteria (EU 2018/2001, Annex IV, Part A).

2.1.2 Crude tall oil-based renewable diesel

The fuel investigated in Papers III and IV was renewable diesel produced by the Finnish forest company UPM. The production process of UPM's renewable diesel, BioVerno, is based on the hydrotreatment of crude tall oil. This oil is a residue of the chemical pulp-making process (Heuser et al., 2013). Pulping pine trees produces a residue called black liquor, which is an aqueous mixture of lignin residues, hemicellulose and inorganic chemicals used in the pulping process. The last-mentioned are valuable chemicals which are fed back into the pulping process. For this, a layer of soap called crude sulphate soap (CSS) must be removed to avoid evaporator malfunctions and to guarantee good pulp yield. Crude sulphate soap can be either burned as process fuel or acidulated to produce crude tall oil. Due to certain technical issues associated with burning CSS, most plants prefer to transform CSS into CTO. (Heuser et al., 2013; Peters & Stojcheva, 2017.) Production of renewable diesel entails a final refining process for the CTO, including hydrogenation treatment, fractionation and distillation (Heuser et al., 2013).

As with biomethane, combustion of CTO-derived renewable diesel is considered carbon neutral, as it simply returns the carbon captured through biomass growth to the atmosphere. In addition, use of crude tall oil as feedstock does not compete with food production, and there is no indirect land use change (Heuser et al., 2013). Thus, CTO feedstock meets the EU RED II sustainability criteria (EU 2018/2001, Annex IV, Part A).

2.2 Engines

As the case ship, Paper I used a RoPax vessel operating in the Baltic Sea Emission Control Area. The calculation was based on information received from the shipping company about the new ferry, which would be commissioned by the beginning of summer 2021. The vessel was supposed to be equipped with medium-speed, four-stroke, dual-fuel engines, with a total power of 16 MW. Four-stroke engines are

typically used on ferries that operate from city centers, so studying the emissions from four-stroke marine engines is of utmost importance. Dual-fuel technology enables the engine to be operated on gaseous and liquid marine fuels. In gas mode, a small amount of liquid fuel is used to ignite the gaseous methane-air mixture.

In Paper II, the CBG-fuelled city bus was equipped with a five-cylinder, spark-ignition gas engine. The maximum power of the engine was 206 kW. The vehicle was equipped with exhaust gas recirculation and a three-way catalytic converter. Table 1 lists the main technical data of the engine. The accumulated distance travelled was 375,000 km in Test 1, and 400,000 km in Test 2.

The research for Papers III and IV was conducted in the engine laboratory of the Technobothnia laboratory unit in Vaasa, Finland. The test engine was a high-speed, four-cylinder diesel engine designed for non-road applications. Table 1 gives the main specifications of the engine. The test engine was mounted on a test bench and loaded with a Horiba WT300 eddy current dynamometer. The engine was not equipped with exhaust gas aftertreatment, so the tests recorded raw engine-out emissions.

Table 1. Test engines specifications

Paper	II	III, IV
Engine	Scania OC09 101	AGCO Power 44 AWI
Engine type	spark-ignition engine	compression-ignition engine
Fuel	CNG/CBG	diesel
Cylinder number	5	4
Total displacement	9.3 L	4.4 L
Compression ratio	12.6:1	16.5:1
Rated speed	1900 rpm	2200 rpm
Maximum power	206 kW@1900 rpm	103 kW@2200 rpm
Maximum torque at rated speed	1040 Nm@1900 rpm	446 Nm@2200 rpm
Engine peak torque	1350 Nm@1000–1400 rpm	560 Nm@1500 rpm

2.3 Local air pollutants

Local emissions were evaluated from the tank-to-propeller or tank-to-wheels perspective, i.e., only the emissions released during vessel or vehicle operation were considered.

2.3.1 Paper I: A literature review and a case study

The starting point of Paper I was a literature review to gain a thorough knowledge of the environmental impacts of fuel choices. The review results were then illustrated in a case study to provide an in-depth environmental analysis of LBG and two fossil fuels, LNG and MDO, in short sea shipping.

The local environmental impacts assessed in the case study were acidification potential, eutrophication potential, formation of fine particles and human health damage. The main causes of acidification are oxides of sulphur and nitrogen, and ammonia, while eutrophication is mainly related to NO_x and NH_3 emissions. Air pollutants harmful to human health include fine particles with a diameter of less than 10 μm (PM_{10}), NH_3, NO_x and SO_2 (Van Zelm et al., 2008). In addition to total PM_{10} emissions, the disability-adjusted life year concept was applied as a more accurate method for evaluating the effects on human life. Disability-adjusted life years are the sum of years lost due to disease, disability or early death (Keoleian & Spitzley, 2006).

The emission data (in g/MJ of fuel) were sourced mainly from peer-reviewed articles, augmented with data from the Third IMO GHG study (Smith et al. 2015). The functional unit considered in the case study was one year of RoPax ferry operation in the Baltic Sea. Calculation of the acidification potential of each fuel was based on SO_2-equivalent, and the eutrophication potential calculation was based on NO_x-equivalent emissions per one year of ferry operation. The SO_2- and NO_x-equivalent factors were retrieved from the scientific literature. The human health damage stemming from combustion of the studied fuels was calculated similarly, using specific characterisation factors for the health effects of PM, NH_3, NO_x and SO_2 emissions.

2.3.2 Paper II: Real-driving emissions measurements

The real-driving emissions measurements were performed on a regular bus line in Vaasa in normal traffic and with normal driving patterns and common passenger loads. To minimize the variables, the measurements were started in the morning at the same time and the same driver from Wasa Citybus was used in both measurement campaigns. The total duration of one test was approximately 3 hours. The route included both urban (<50 km/h) and rural (50–75 km/h) driving. The main focus was on CH_4 emissions, but NO_x, CO and CO_2 were also measured. Emissions were recorded with an onboard VARIO plus Industrial device. This measures CH_4, CO and CO_2 concentrations using a non-dispersive infrared sensor, and NO_x concentrations via electrochemical cells.

Engine parameters, including engine speed, torque, lambda, airflow, coolant temperature and vehicle speed, were recorded from the vehicle's engine control unit, using Scania Diagnosis & Programmer SDP3 software. Lambda is defined as the ratio of the actual air-to-fuel ratio to the stoichiometric air-to-fuel ratio. An external global positioning system (GPS) recorded the vehicle's location and vehicle speed data. A dedicated weather station registered ambient temperature, pressure and relative humidity. An external power unit supplied the electrical power to the portable emissions-measurement system. Figure 1 depicts the measurement system set-up.

Figure 1. Portable emission-measurement system installed on the bus

All data were recorded with a frequency of 1 Hz, which was considered sufficient for a three-hour measurement. The emission data and the GPS and weather data were stored with the DEWESoft data acquisition system. The SDP3 and DEWESoft data were carefully synchronised before data processing.

The first measurement campaign took place in March 2022, and the second in June 2022. Only hot-start emissions were investigated in June, but the measurements in March studied both cold-start and hot-start emissions. Recording of hot-start emissions began when coolant temperature had stabilised within ±2 °C over 5 minutes. Cold-start emissions were recorded from the moment the coolant temperature reached 30 °C for the first time, and continued until the coolant

temperature was stabilised within ±2 °C over 5 minutes, according to EU Regulation 582/2011 (EU COM, 2011/582).

The specific emissions were calculated in both g/kWh and g/km, i.e., the total mass of each pollutant over the test cycle was divided by the engine work or by the distance covered in km over the test cycle. The results were defined separately for the total trip, urban and rural sections of the route.

2.3.3 Papers III and IV: Engine experiments in laboratory conditions

In Papers III and IV, the measurement setup for regulated gaseous emissions consisted of a non-dispersive infrared analyser for recording CO and CO_2 concentrations; a chemiluminescence detector for NO_x; and a heated flame ionisation detector for recording hydrocarbon concentration. In addition, a Fourier transformation infrared analyser recorded three unregulated emissions: CH_4, nitrous oxide (N_2O) and formaldehyde. The total particulate number concentrations and particle size distributions were measured using an engine exhaust particle sizer spectrometer, capable of measuring particles from 5.6 to 560 nm. Table 2 summarises the analytical devices used for the measurements. During the studies, the exhaust gas samples were processed in terms of temperature, flow rate and dilution, according to the inlet gas requirements of each measuring device.

Table 2. Analytical instruments in engine laboratory experiments

Parameter	Measuring device	Technology
NO_x	Eco Physics CLD 822 M hr	chemiluminescence detector
CO, CO_2	Siemens Ultramat 6	non-dispersive infrared analyser
Hydrocarbons	J.U.M. VE7	heated flame ionization detector
Particulate number and particle size distribution	TSI EEPS 3090	engine exhaust particle sizer spectrometer
Unregulated gaseous emissions	Gasmet DX4000	Fourier transformation infrared analyser

In addition to emissions, the laboratory tests recorded engine speed, torque and several fluid temperatures and pressures. The sensor data were collected by the engine manufacturer´s own engine management software. Engine settings were kept the same for all fuels, and engine warm-up and measurement procedures were also identical for all fuels.

A standardised eight-mode ISO 8178-4 C1 test cycle was used to ensure similar engine operating conditions for all fuels (ISO 8178-4, 2020). Table 3 lists the loading points (modes), the corresponding engine speeds, loads and torques, together with the weighting factor for each mode. The engine was allowed to stabilise at each load point before starting the measurements. The main criterion for this was that the exhaust gas temperature was stable.

Table 3. Experimental matrix in engine laboratory measurements

Mode	1	2	3	4	5	6	7	8
Speed (rpm)	2200	2200	2200	2200	1500	1500	1500	860
Load (%)	100	75	50	10	100	75	50	0
Torque (Nm)	446	334	223	45	560	420	280	1
Weighting factor	0.15	0.15	0.15	0.1	0.1	0.1	0.1	0.15

The brake-specific emission results were calculated from the recorded pollutant concentration data, following the ISO 8178 standard (ISO 8178-1, 2020). The total particulate number and particle size distributions at each load point were averaged, based on the particle counts measured over three-minute periods. Only instantaneous values were obtained at each load point for gaseous emissions.

Combustion analysis entailed calculating the heat release rate and the mass fraction of burned fuel. These were computed based on the cylinder pressure data, measured with a piezoelectric Kistler 6125C pressure sensor. A Kistler 2614B1 crank-angle encoder recorded the crankshaft position. The heat release rate and the mass fraction of burned fuel were calculated via the AVL Concerto data post-processing tool using the Thermodynamics2 macro.

A summary of the studied local pollutants is shown in Table 4.

Table 4. Summary of the studied local air pollutants

Paper	I	II	III	IV
NO_x	x	x	x	x
CO		x	x	x
HC			x	x
NH_3	x			
SO_2	x			
PM_{10}	x			
Particulate number and particle size distribution			x	x

2.4 Greenhouse gas emissions – a life-cycle approach

The life-cycle approach is the most comprehensive method to assess the global environmental impacts of fuels. In addition to emissions released from fuel combustion, fuels always emit pollutants at earlier stages of their life cycle. This thesis applied life-cycle GHG accounting to evaluate the global warming potential of the studied fuels. Data on GHG emissions were collected for all processes along the fuel supply chains. The total GHG intensity of each fuel was calculated as CO_2-equivalents per MJ of fuel, enabling a consistent comparison of fuels.

GHG emission calculations used the global warming potential values of a 100-year time-horizon (GWP100) given in the IPCC Fifth Assessment Report (AR5). In AR5 (Myhre et al., 2013), the GWP100 for methane is listed as either 28 (without climate-carbon feedback) or 34 (with climate-carbon feedback). For N_2O, the corresponding values are 265 or 298. Climate-carbon feedback refers to the effect of a changing climate on the carbon cycle (Gasser et al., 2017). Concretely, climate warming reduces the carbon absorption capacity of the oceans and the terrestrial biosphere – i.e., the carbon sinks – increasing the CO_2 concentration in the atmosphere and further intensifying climate change (Schwinger & Tjiputra, 2018).

In Paper I, the life-cycle chain of MDO includes crude oil extraction and processing; transport by sea; refining in the EU; distribution; and finally, combustion of MDO in a dual-fuel marine engine. The LNG supply chain consisted of natural gas extraction from the North Sea; pre-treatment and liquefaction near the source; transport to a central hub in Finland; storage; distribution; and combustion of LNG in a marine engine.

The life-cycle chain of LBG differed from those of MDO and LNG because CO_2 emissions from LBG combustion were ignored due to their biogenic nature. The well-to-tank stage for LBG covered biogas production through anaerobic digestion of locally collected municipal organic waste; purification and upgrading; liquefaction; storage; and distribution. Well-to-tank GHG emission data for LBG were retrieved from Kollamthodi et al. (2016), assuming methane leakage of 1.2 % for anaerobic digestion and 0.5 % for upgrading the biogas to biomethane. Tank-to-propeller GHG emissions of LBG consisted only of CH_4 and N_2O emissions from combustion, and a small amount of fossil CO_2 associated with the MDO pilot fuel. The study assumed a methane slip rate of 2 % from fuel combustion and a pilot fuel share of 1.4 % of the fuel input energy for ignition for both LNG and LBG.

For all three fuels, the total GHG emissions from each of the three species considered – CO_2, CH_4, and N_2O – were presented as CO_2-equivalent tonnes per year of RoPax ferry operation. In the investigation, the carbon-climate feedback effect was

included to avoid underestimating the impacts of non-CO_2 greenhouse gases. Thus, the GWP100 factor of 34 for CH_4 and 298 for N_2O were used (Myhre et al., 2013).

Paper II´s system boundary for CBG comprised feedstock collection and transport; biogas production; biogas processing to biomethane; biomethane compression; and finally, combustion in a gas-powered city bus. The CBG was produced at Stormossen waste treatment plant near Vaasa. For calculating CBG´s well-to-tank GHG emissions, the non-biogenic emissions from collection, transport and processing were computed. Methane leakages during anaerobic digestion and upgrading were also counted in well-to-tank GHG emissions. Tank-to-wheels GHG emissions for the gas-fuelled bus were determined from the study´s real-driving emission measurement recordings. Only CH_4 emissions were considered, because the biogenic nature of CO_2 emissions from CBG combustion meant they could be ignored.

The well-to-wheels analysis used the functional unit of vehicle kilometre, i.e., the life-cycle greenhouse gases were presented in grams of CO_2-equivalents per km driven by the bus. In Paper II, non-CO_2 greenhouse gas emissions were converted to CO_2-equivalents using the GWP100 of 28 for methane and 265 for N_2O (Myhre et al., 2013). The GHG benefits associated with the transition from fossil-based fuels to biomethane were calculated by comparing CBG's life-cycle GHG emission relative to its fossil counterpart, compressed natural gas, and to conventional diesel fuel. GHG emission factors for fossil fuels were retrieved from the JRC Well-to-wheels study (JRC, 2014) and Statistics Finland's data (StatFin, 2021).

Papers III and IV mainly dealt with local emissions from fuel combustion. However, to get a broader view of the emission benefits of CTO-derived renewable diesel, this dissertation expands the review to include life-cycle greenhouse gas calculations for this renewable diesel.

Life-cycle emissions data for CTO production were sourced from Cashman et al. (2015), representing the life-cycle inventory (LCI) data from 90 % of the European CTO distillery industry. Due to the lack of life-cycle inventory data on renewable diesel production from CTO, publicly available LCI data on diesel production from crude rapeseed oil was used. The author acknowledges that the LCI data for CTO-based renewable diesel is subject to uncertainty because the data is based on a model with a different feedstock. However, based on Cashman et al. (2015), this was considered the most relevant and best available life-cycle inventory data for the hydrotreatment technology used for CTO.

Crude sulphate soap (CSS) was treated as a process residue (Peters & Stojcheva, 2017) in the calculations, so all GHG emissions from biomass collection, pre-treatment and pulping were allocated to the pulp, and none to the CSS. Thus, the system boundary for renewable diesel derived from CTO consists of the following steps:

1. CSS pre-treatment and acidulation: CSS first undergoes cleaning and homogenisation to uniform the material and to make CTO processing easier to manage. Homogenised CSS is then reacted with sulphuric acid to produce crude tall oil (Peters & Stojcheva, 2017). GHG emission data for this stage are based on Cashman et al. (2015).
2. CTO supply to the tall oil refinery: The GHG emission factor for CTO transport is based on the European average, retrieved from Cashman et al. (2015).
3. Renewable fuel production, including:
   (a) pre-treatment to remove solid particles and other contaminants,
   (b) hydrotreatment, where the pre-treated CTO is fed, together with hydrogen, to the reactor to modify the chemical structure of CTO, and,
   (c) fractionation, where the remaining hydrogen sulphide and non-condensable gases are removed (Heuser et al., 2013).

   GHG emission data for the hydrotreatment step were taken from Prussi et al. (2020), assuming hydrogen production via natural gas steam reforming.
4. Distilling: The remaining liquid is distilled to separate renewable diesel. GHG emission data for distilling were taken from Cashman et a. (2015).
5. Renewable diesel distribution: An average transport distance of 300 km was assumed. The following GHG emission data were obtained from Prussi et al. (2020): road truck (40 t) diesel energy consumption of 0.81 MJ/t.km; GHG emission factor for diesel B7 fuel of 87 g CO_2-equivalents per MJ of fuel.
6. Combustion in a diesel engine.

Figure 2 illustrates the system boundary used in the study, and Table 5 summarises the well-to-tank GHG data. The final well-to-wheels results, based on engine experiments, are reported in both grams of CO_2-equivalents per MJ of fuel, and grams of CO_2-equivalents per kWh engine out.

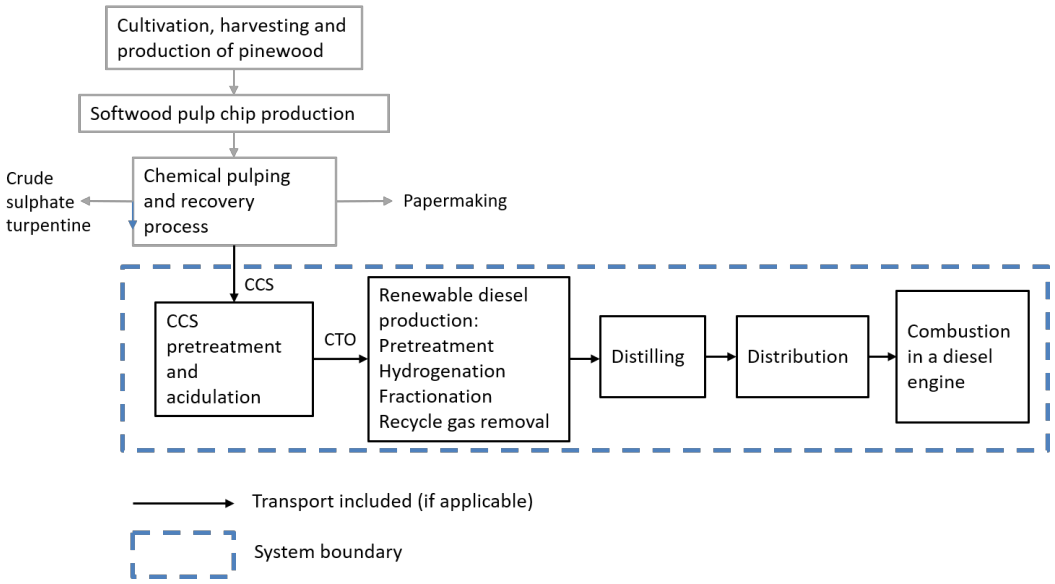

Figure 2. System boundary for the well-to-wheels GHG analysis for CTO-derived renewable diesel

Table 5. Indicative well-to-tank GHG emissions of renewable diesel produced by hydrotreatment of crude tall oil

Well-to-tank GHG emissions in CO_2-eq.	g/MJ	Notes
CSS acidulation	2.4*	On average, in Europe
CTO transport	0.8*	On average, in Europe
Renewable fuel production (hydrogenation)	6.9	Hydrogen via natural gas steam reforming
Distillation	1.2*	On average, in Europe
Renewable diesel distribution	1.0	Road truck (40 t), 300 km
Total non-renewable GHG emissions	12.3	

* *Calculated from the initial values expressed in kilograms of CO_2-equivalents per tonne of CTO, using CTO consumption of 1.23 tonnes per tonne of renewable diesel and the lower heating value of 38.4 MJ/kg for the produced renewable fuel (Cashman et al., 2015).*

3 RESULTS

3.1 Environmental impacts of liquefied biomethane as a marine fuel

Paper I assessed the environmental benefits of liquefied biomethane in short sea shipping. GHG emissions were investigated throughout the entire life cycle of the fuels (well-to-propeller). Local emissions considered were only those released during vessel operation, i.e., the tank-to-propeller stage.

Figures 3 and 4 illustrate the local environmental impacts in terms of acidification and eutrophication potential of LBG compared with its fossil counterpart, LNG, and to conventional marine diesel oil (0.1 % sulphur) combined with selective catalytic reduction (SCR). It is apparent from Figures 3 and 4 that the local environmental impacts were closely related to NO_x emissions. The two gaseous fuels, LBG and LNG, produced comparable NO_x emissions. MDO could not match these gaseous fuels, despite SCR's proven NO_x reduction benefits. Potential ammonia slip from the SCR system also contributes a small incremental increase to MDO's acidification and eutrophication potentials. The acidifying potential of both gaseous fuels was about half that of MDO. The SO_2 produced in MDO combustion is a significant addition to this fuel´s acidification potential.

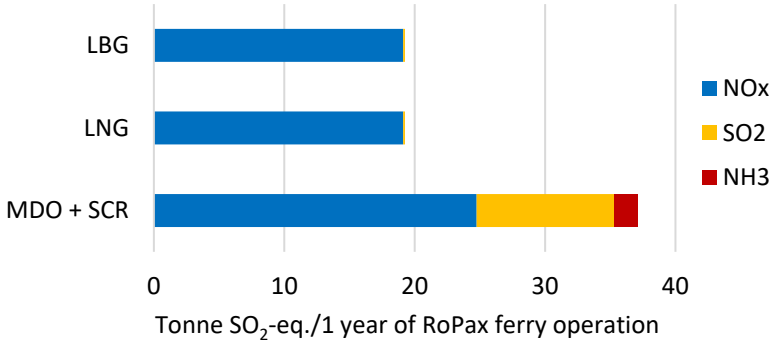

Figure 3. Tank-to-propeller acidifying emissions for LBG, LNG and MDO: emissions converted into SO_2-equivalents

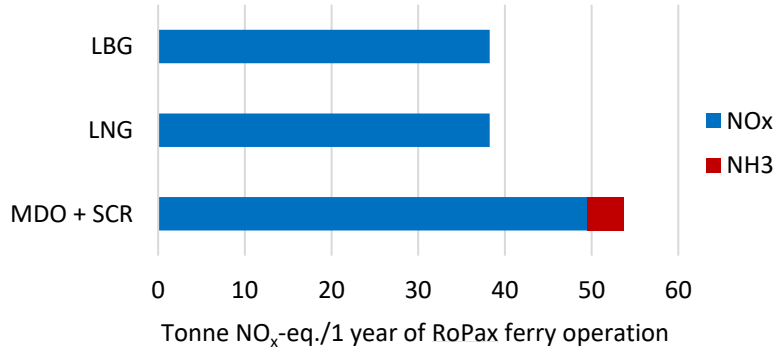

Figure 4. Tank-to-propeller eutrophying emissions in NO_x-equivalents for LBG, LNG and MDO

Figure 5 shows that total PM_{10} emissions from burning gaseous fuels were approximately 80 % lower than for MDO. Figure 6 depicts human health damage, in terms of years lost due to illness, disability or early death, for each year of RoPax ferry operation. The health damage value with MDO was almost double that of LBG or LNG.

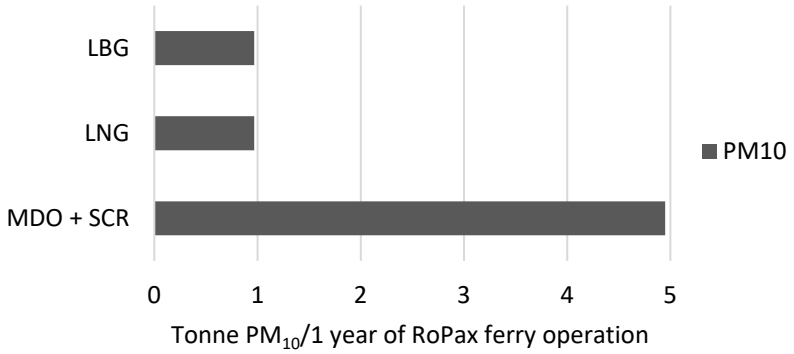

Figure 5. Tank-to-propeller PM_{10} emissions for LBG, LNG and MDO

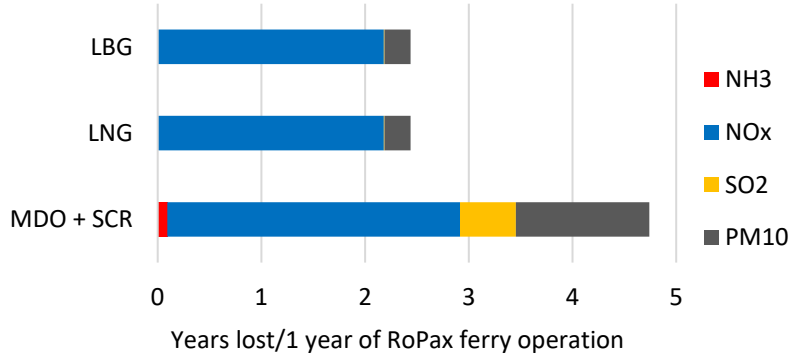

Figure 6. Impact of emissions on human health for LBG, LNG and MDO

GHG emissions were investigated throughout the entire life cycle of the fuels. Using IPCC AR5 emission factors, replacing fossil fuels with LBG reduced lifetime GHG emissions by 60 %. As seen in Figure 7, the substantial GHG benefits of LBG were during the tank-to-propeller phase. Since the biogenic CO_2 from burning waste-based renewable fuels are assumed to have no climate impacts, LBG's tank-to-propeller GHG emissions were almost exclusively due to methane slip from the engine, plus a small amount of fossil CO_2 from the MDO pilot fuel. Replacing this pilot MDO with renewable diesel would yield an additional 1 % GHG saving. LBG's well-to-tank GHG emissions arose from sources such as methane leakages and electricity used during LBG production.

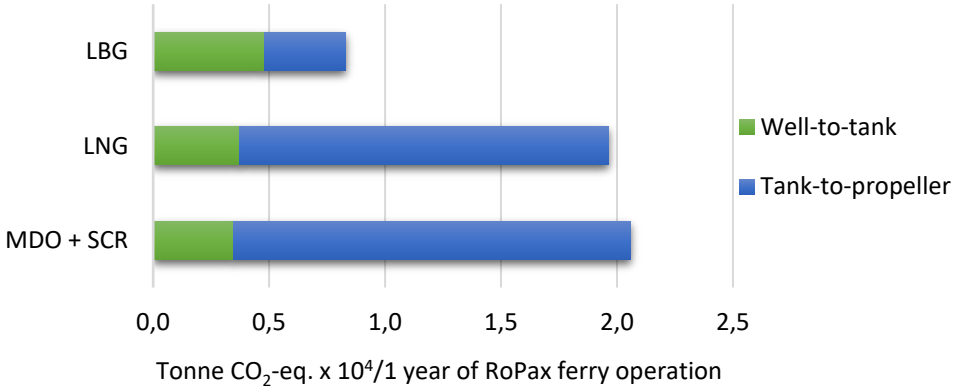

Figure 7. Life-cycle GHG emissions for LBG, LNG and MDO divided into well-to-tank and tank-to-propeller stages

Figure 8 is the contribution analysis, showing how the three different climate gases contributed to the global warming impact of each fuel. CO_2 was the main contributor to the GWP100 for the two fossil fuels. The climate impact contribution from CH_4 emissions was significant for both methane-based fuels, LBG and LNG. For LBG, CH_4 emissions represented 69 % of the total life-cycle GWP100. This underscores the importance of stringent CH_4 emission control throughout the LBG supply chain and, in particular, from the engines.

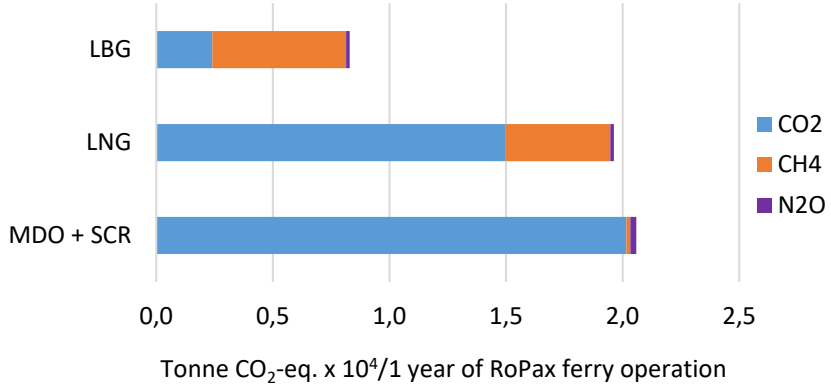

Figure 8. Life-cycle GHG emissions for LBG, LNG and MDO, divided into the different contributing emissions

Figure 9 demonstrates the criticality of limiting CH_4 slip during LBG combustion. For example, with zero CH_4 slip, LBG would cut life-cycle GHG emissions by 75 % compared with MDO.

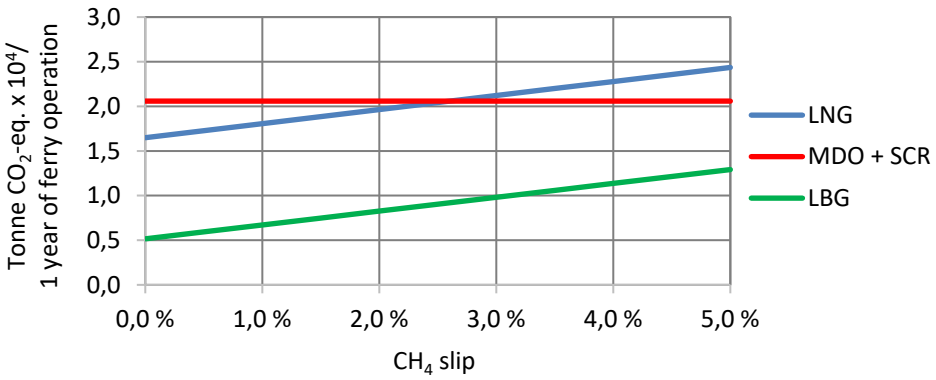

Figure 9. Life-cycle GHG emissions as a function of CH4 slip from combustion

3.2 Real-driving emissions of biomethane-fuelled city bus

Paper II´s aim was to demonstrate the emission benefits of biomethane use in urban traffic by measuring real-driving emissions from a CBG-fuelled city bus. Figures 10 and 11 present the specific CH_4 and NO_x emissions in g/kWh in hot-start tests during two measurement campaigns. Although the tests performed did not fully reflect the Euro VI standard's in-service conformity tests in terms of boundary conditions and route requirements, Euro VI´s in-service conformity limits are also presented for comparative purposes. In-service conformity testing refers to field measurements carried out by manufacturers on in-use vehicles to

ensure that the exhaust gas emissions of the vehicle type continue to comply with emission regulations throughout the vehicle´s expected lifetime (EU COM, 2011/582).

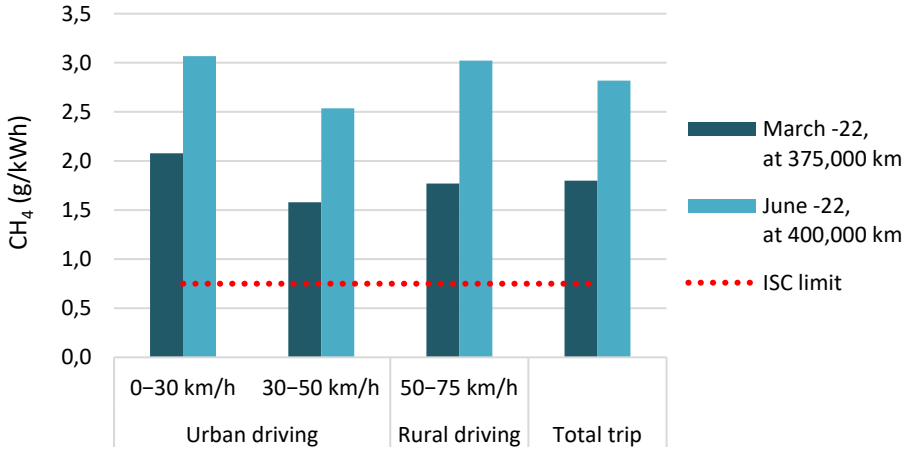

Figure 10. Specific CH_4 emissions in hot-start tests of the biomethane-fuelled urban bus: dotted line denotes in-service conformity limit

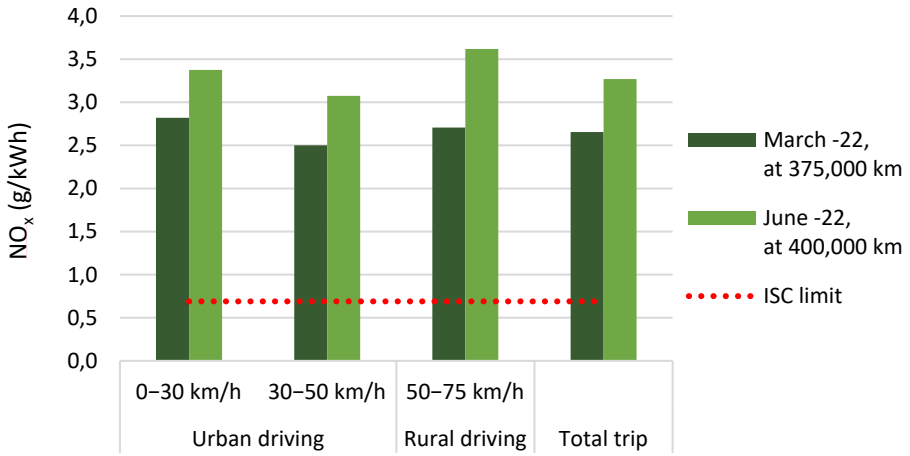

Figure 11. Specific NO_x emissions in hot-start tests of the biomethane-fuelled urban bus: dotted line denotes in-service conformity limit

Test 1´s, in March 2022, relatively high specific CH_4 and NO_x emissions indicated a loss of catalytic activity of the three-way catalyst after its 375,000 km lifetime. Test 2´s results in June 2022, at 400,000 km, revealed further deterioration of catalyst efficiency. CO emissions were well below the in-service conformity limit of 6 g/kWh in both tests.

It should be noted that exceeding the ISC limits was not due to the fuel used but to the deactivation of the catalyst; with a deactivated catalyst, emissions from fossil natural gas would also exceed the ISC limits. High temperatures and temperature

gradients, fluctuating exhaust composition and the presence of catalyst poisons and other impurities in the exhaust gas all increase the possibility of catalyst deactivation (Lassi, 2003). In a deactivated catalyst, temperatures of up to 500–600 °C (Auvinen et al., 2021) may be required to break the strong carbon-hydrogen bonds in CH_4. At low loads, common in the driving profile of a city bus, the exhaust temperature was too low to allow the deactivated catalyst to work effectively. Consequently, the low CH_4 reactivity also meant that methane-based reducing agents for NO_x reduction did not work, resulting in substantial NO_x breakthrough from the catalyst.

The catalyst´s temperature sensitivity was also evident in the cold-start test, when CH_4 emissions were 2.3 times and NO_x emissions 1.4 times higher than during a hot-start (Figure 12). Over the combined cold- and hot-start cycles, CH_4 emissions increased by 30 %, NO_x by 13 %, and CO by 33 % compared with hot-start-only measurements.

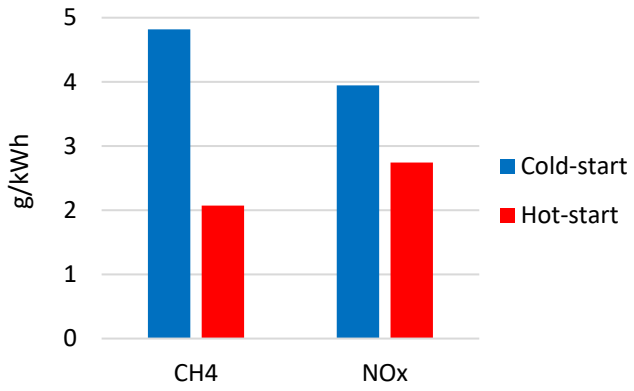

Figure 12. Cold-start versus hot-start emissions in real-driving emission measurements of a CBG-fuelled city bus

In addition to catalyst deactivation, another probable cause of the impaired catalyst performance was the fluctuating air-to-fuel ratio. The engine must be operated within a very narrow air-to-fuel ratio window for its three-way catalytic converter to achieve simultaneous complete conversion of NO_x, CO and hydrocarbon species. If the mixture is not very close to stoichiometric, there is a rapid drop of NO_x conversion efficiency in fuel-lean conditions, and incomplete hydrocarbon conversion in fuel-rich conditions. Figure 13 shows that lambda was outside the optimal range for a significant part of the time, likely reducing catalyst efficiency.

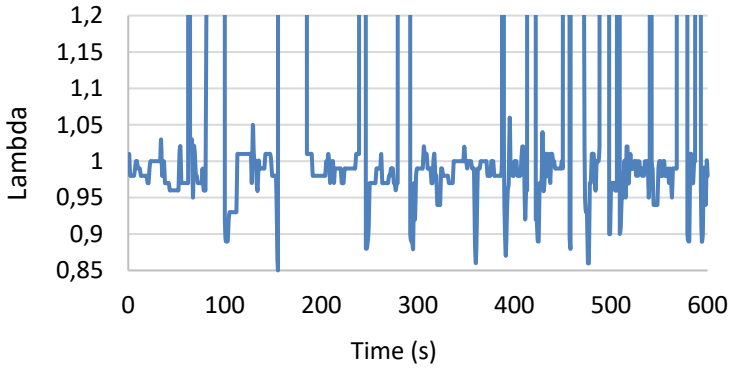

Figure 13. Fluctuating lambda values under real-driving conditions

Again, total GHG emissions were studied over the fuel´s life cycle. The functional unit used in the well-to-wheels analysis was vehicle kilometre. Table 6 summarises the well-to-tank GHG calculations for biomethane production at Stormossen waste treatment plant.

Table 6. CBG's well-to-tank GHG emissions

Parameter	Value	Unit	CH_4 g/MJ	CO_2-eq. g/MJ
Feedstock collection and transportation				
Diesel trucks, diesel B7 fuel	40	km		1.95
Biogas production and refining				
Total biogas production	2,716,000	m^3 (NTP)		
52 % of raw gas for upgrading	1,412,320	m^3 (NTP)		
Methane content (62 %)	875,638	m^3 (NTP)		
Total biomethane production	31,522,982	MJ		
Heat demand *				
• Anaerobic digestion	0.19	kWh/m^3 (NTP) of raw gas		
• Upgrading	0.119	kWh/kWh of bio-CH_4		
Electricity demand *				
• Anaerobic digestion	0.14	kWh/m^3 (NTP) of raw gas		
• Upgrading	0.0136	kWh/kWh of bio-CH_4		
Methane losses				
• Anaerobic digestion, 1 %	6368	kg	0.202	5.66
• Upgrading, 0.1 %	630	kg	0.020	0.56
Compression				
Electricity demand	0.25	kWh/m^3 (NTP)		0.48
Well-to-tank GHG emissions				8.65

** Covered internally by the plant's own CHP biogas engine.*

Table 7 presents the final results of the well-to-wheels GHG analysis for CBG, CNG and diesel B7. Well-to-tank GHG emission factors for CNG and diesel fuel were

retrieved from the European Commission Joint Research Centre's report version 4.a (JRC, 2014). Specific tank-to-wheels GHG emissions for gaseous fuels were calculated from the real-driving CO_2 and CH_4 emissions recorded in this study. CO_2 from combustion of CBG was ignored because this is biogenic carbon, not considered to contribute to global warming. Tank-to-wheels CO_2 emission factor for diesel B7 was taken from StatFin (2021). The average fuel energy consumption in the real-driving measurements was 20.8 MJ/km, applied for both CBG and CNG. Diesel consumption was set at 80 % of that of gas buses, reflecting the well-known higher thermal efficiency of compression-ignition diesel engines compared with spark-ignition gas engines. The 80 % estimation was based on the report by VTT (Technical Research Centre of Finland) evaluating the continuous, multi-year performance of city buses in Helsinki Metropolitan Area (Söderena et al., 2019).

Table 7. Well-to-wheels greenhouse gas emissions of CBG, CNG, and diesel B7

	Unit	CBG	CNG	Diesel B7
Well-to-tank GHG in CO_2-eq.	g/MJ of fuel	8.65	13.0	14.7
Tank-to-wheels GHG				
• Fossil CO_2	g/MJ of fuel	-	46.6	68.4
• CH_4	g/MJ of fuel	0.171	0.171	
Well-to-wheels GHG in CO_2-eq.	g/MJ of fuel	13.4	64.4	83.1
Fuel consumption	MJ/km	20.8	20.8	16.7
Specific life-cycle GHG in CO_2-eq.	g/km	279	1342	1385

The results listed in Table 6 and depicted in Figure 14 confirmed GHG emissions are cut by 80 % by switching from conventional diesel to renewable CBG produced from sustainable sources. These GHG savings would move towards 90 % with more effective CH_4 emission control.

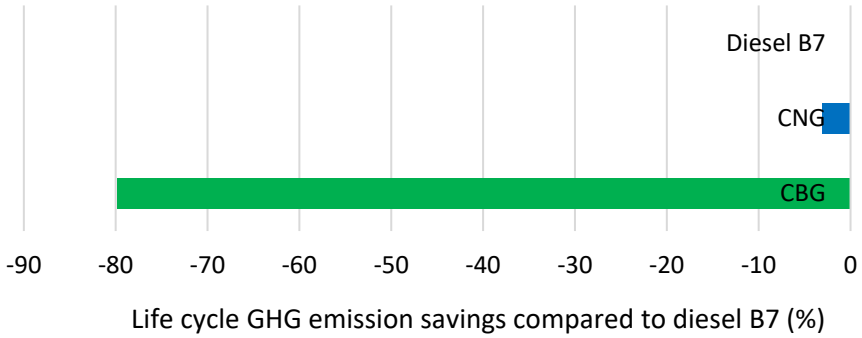

Figure 14. Percentage changes in specific life-cycle GHG emissions of CBG and CNG compared with diesel B7 fuel

3.3 Crude tall oil derived renewable diesel: performance and emission characteristics

Paper III investigated the effect of CTO-derived renewable diesel fuel on the performance and exhaust emissions of a non-road diesel engine. The renewable diesel was studied as neat (RD100) and as a 50 % blend (RD50) with conventional fossil diesel fuel oil. Neat low-sulphur DFO served as the reference fuel. Please note that in the original research article, the fuels were differently named: the neat renewable diesel was called BVN, and the blend BVN-DFO. Renewable diesel and the blend were given more descriptive names in this dissertation.

The combustion analysis showed that combustion propagated in a very similar way with all three fuels examined. Table 8 shows 10 %, 50 %, and 90 % points of the mass fraction of burned fuel for each fuel, at rated speed at 75 % load. Neat renewable diesel had the earliest crank angle position (°CA) of 10 % mass fraction burned, consistent with the highest cetane number of RD100, and presumably, a shorter ignition delay. The latest 90 % mass fraction burned, and a slightly longer combustion duration, was measured for the RD50 blend. Otherwise, no differences in combustion durations were observed.

Table 8. Mass fraction of burned fuel (MFB), standard deviations and combustion durations at rated speed at 75 % load

2200 rpm 75 % load	MFB 10%	Stdev	MFB 50%	Stdev	MFB 90%	Stdev	Combustion duration MFB 10-90%
	°CA	°CA	°CA	°CA	°CA	°CA	°CA
DFO	8.0	0.090	17	0.12	32	0.47	24
RD50	8.0	0.095	17	0.12	33	0.48	25
RD100	7.8	0.094	17	0.11	32	0.39	24

The engine brake thermal efficiency was almost identical with all fuels throughout the load-speed range of the test engine.

Typically, diesel engines have low HC and CO emissions. However, using CTO-derived renewable diesel instead of DFO gave rise to even fewer of these two emissions. CO reduced by 9 % with neat renewable diesel, and by 3 % with the blend. RD100 and RD50 also produced the lowest HC: 0.12 g/kWh for both fuels. This was assumed to be due to the better ignitability of renewable diesel, limiting the over-leaning effect.

RD100 and RD50 also slightly reduced NO_x emissions. The NO_x over the measurement cycle was 7.9 g/kWh for DFO; 7.7 g/kWh for neat renewable diesel; and

7.6 g/kWh for the blend. All three results indicate that the engine was tuned for high efficiency – and consequently, high NO_x – and so designed to be supplemented by an efficient catalytic converter system for NO_x reduction. The lower NO_x for neat renewable diesel and the blend was due primarily to these fuels´ low aromatic content. Formation of thermal NO_x is reduced with fuels having low aromatic content because aromatic compounds have higher adiabatic flame temperatures than paraffinic ones and, thus, higher local combustion temperatures (Glaude et al., 2010).

Figure 15 summarises the percentage changes in gaseous emissions relative to DFO.

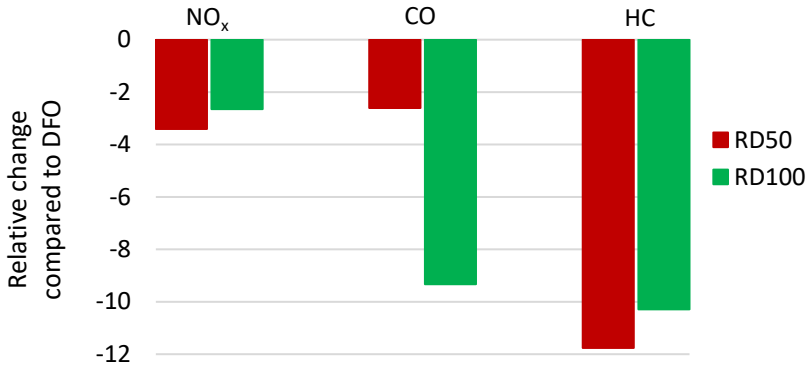

Figure 15. Percentage changes in cycle-weighted brake specific emissions of neat renewable diesel and RD50 blend compared with DFO

Figure 16 depicts the weighted total particulate number emission within the size range of 5.6–560 nm, measured over the eight-mode ISO 8178-4 C1 test cycle. Fuelling with neat renewable diesel cut total particulate number by 10 % compared with DFO. The beneficial hydrocarbon structure and low aromatics content of renewable diesel explained this decrease, because a higher hydrogen-to-carbon ratio likely resulted in more complete combustion, and near-zero aromatics limited poly-cyclic aromatic hydrocarbons (PAH) acting as soot precursors. It also has been reported (Labeckas et al., 2017) that improved ignition quality of high-cetane fuels may lead to cleaner combustion and lower soot formation. An even greater particulate number reduction, of 20 %, was observed for the blend. The lower 95 % distillation point of RD50 (358 °C) compared with RD100 (372 °C) could explain this improved total particulate number outcome relative to neat renewable diesel. A lower distillation temperature results in better evaporation and reduced soot formation rates (McCaffery et al. 2022).

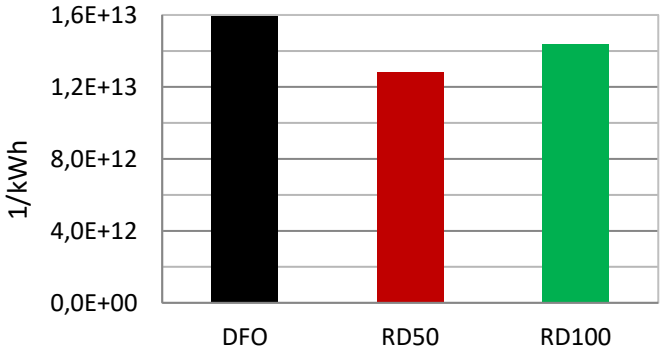

Figure 16. Weighted total particle number over the test cycle for neat renewable diesel, RD50 blend and DFO

No consistent trend was observed in the particle size distributions between fuels at higher loads. In contrast, at low loads, both RD100 and RD50 showed a clear reduction of particles in the 10 nm size category (Figure 17).

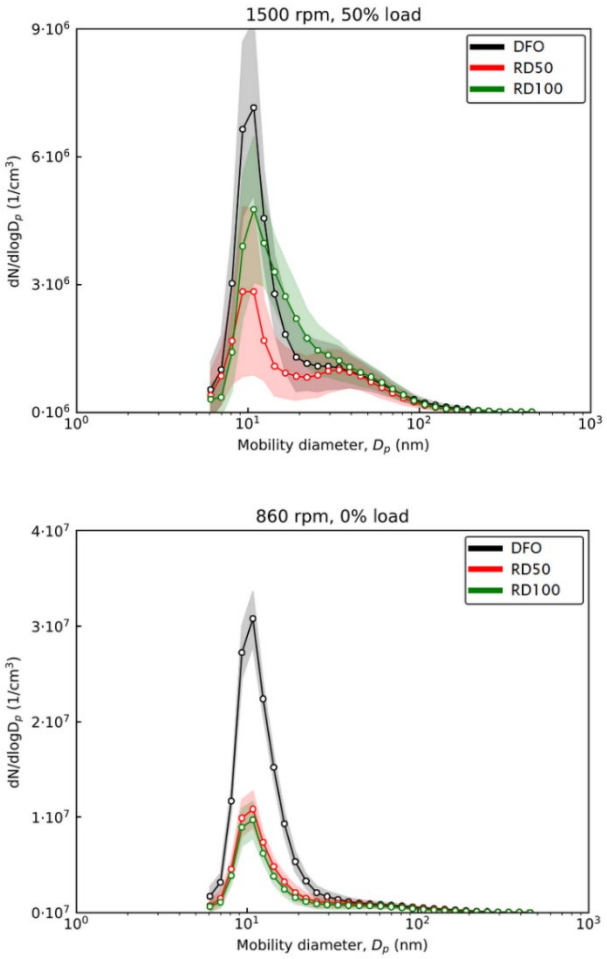

Figure 17. Particle size distribution at low loads for neat renewable diesel, RD50 blend, and DFO: shaded area depicts standard deviation

Table 9 summarises the life-cycle GHG emissions of the three fuels studied, both in grams of CO_2-equivalents per MJ of fuel and grams of CO_2-equivalents per kWh, engine-out. Lower heating values are based on fuel analyses conducted in Paper III. Fuel consumption and specific emissions are averages of values measured in modes 1–7 in the performed engine experiments. The neat renewable diesel reduces life-cycle GHG emission by 86 % relative to fossil diesel.

Table 9. Specific life-cycle GHG emissions of DFO, RD50 and RD100

	Unit	DFO	RD50	RD100
Lower heating value	MJ/kg	42.8	43.2	43.4
Specific fuel oil consumption	g/kWh	262.3	260.3	264.0
Well-to-tank GHG in CO_2-eq.	g/MJ of fuel	18.9*	15.6	12.3
Tank-to-wheels GHG				
• Fossil CO_2	g/MJ of fuel	73.7	36.8	-
• CH_4	g/MJ of fuel	0.00031	0.00009	0.00024
• N_2O	g/MJ of fuel	0.00079	0.00037	0.00061
Tank-to-wheels GHG in CO_2-eq.	g/MJ of fuel	73.9	36.9	0.17
Well-to-wheels GHG emissions in CO_2-eq.	g/MJ of fuel	92.8	52.5	12.5
Well-to-tank GHG in CO_2-eq.	g/kWh	212.3	173.1	136.4
Tank-to-wheels GHG				
• Fossil CO_2	g/kWh	827.5	414.0	-
• CH_4	g/kWh	0.0035	0.0010	0.0028
• N_2O	g/kWh	0.0089	0.0042	0.0070
Tank-to-wheels GHG in CO_2-eq.	g/kWh	830.0	415.1	1.9
Well-to-wheels GHG emissions in CO_2-eq.	g/kWh	1042	590	143
Relative to DFO			-43 %	-86 %

**Source: Prussi et al. (2020)*

Figure 18 illustrates the life-cycle GHG emissions in grams of CO_2-equivalents per kWh, divided into well-to-tank and tank-to-wheels stages.

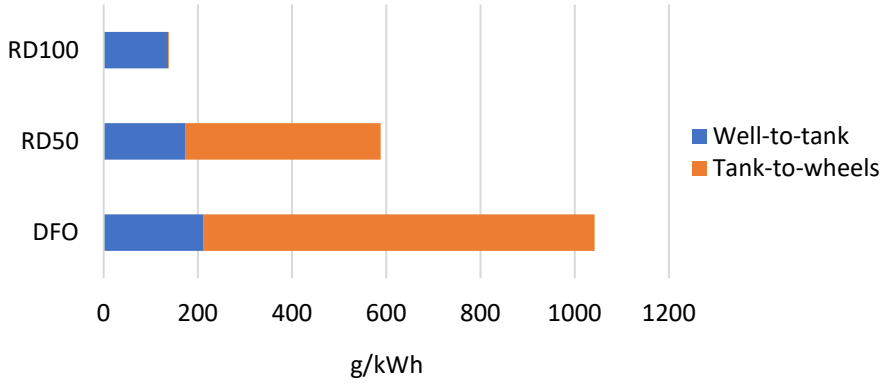

Figure 18. Life-cycle CO_2-equivalent emissions of neat renewable diesel, RD50 blend, and DFO divided into well-to tank and tank-to-wheels stages

3.4 Storage stability of crude tall oil-based renewable diesel

Paper IV extended the research on CTO-derived renewable diesel to also address the effect of long-term storage on this fuel´s properties. In addition, local gaseous and particulate emissions, plus basic engine performance, also were determined. The renewable diesel (RD) was studied in neat form, and conventional DFO served as the reference fuel. Again, in the original research article, the renewable diesel was differently named, as BVO. The more descriptive term of renewable diesel (RD) is used in this dissertation.

The investigated renewable diesel fuel was produced at the end of 2016. Table 10 shows the comprehensive results of fuel analyses in a fresh state in 2016, and in 2020, i.e., after four years, stored in an airtight chemical container at a constant 20 °C temperature. The fuel had been treated with a lubricity additive before storage. This additive is required to compensate for the poor lubricity of hydrotreated renewable diesel, attributed to its absence of sulphur. More specifically, the additive enables the renewable fuel to meet the high frequency reciprocating rig (HFRR) specification of <460 µm, the lubricity test within the European diesel standard EN 590 (DIN EN 590, 2017). The additive is also needed for conventional sulphur-free diesel fuel to protect fuel injection equipment from excessive wear (Neste, 2020). The fuel analyses were made by ASG Analytik-Service GmbH.

Oxidation stability is the key quality parameter when evaluating a fuel´s storage properties. The studied renewable diesel showed a slightly unstable behaviour in

the oxidation tests of the fresh fuel in 2016. A small number of deposits formed in the EN ISO 12205 oxidation stability test, although the level of deposits was clearly below the 25 g/m^3 limit specified in the European diesel standard EN 590. No deposit formation was found in the 2020 fuel analyses.

Overall, the changes in the fuel properties during the four-year storage period were small and partly negligible. This indicated that renewable diesel derived from hydrotreated CTO can be stored under controlled conditions for extended periods without compromising fuel quality.

The engine performance results of this stored renewable diesel were in line with the findings in Paper III: no significant differences in combustion analysis were detected between renewable diesel and DFO. Slightly lower heat release rate peaks in the premixed combustion phases were observed with RD, presumably associated with its higher cetane number and faster ignition. The engine's brake thermal efficiency was also very similar for both fuels at all loads.

Table 10. CTO-derived renewable diesel properties in a fresh state and after four years of storage

	RD in 2020	RD in 2016	Unit	Test method
Cetane Number	61.6	60.8	-	EN 17155 (in 2020) EN 15195 (in 2016)
Density (15 °C)	812.7	812.6	kg/m^3	EN ISO 12185
PAH content	0.1	1.0	% (m/m)	EN 12916
Sulphur content	<5	<5(<1)	mg/kg	EN ISO 20884
Flash Point	73.0	72.0	°C	EN ISO 2719
Carbon residue (10 % Dist.)	<0.10	0.02	% (m/m)	EN ISO 10370
Ash Content (775 °C)	<0.001	<0.005	% (m/m)	EN ISO 6245
Water content	22	<30	mg/kg	EN ISO 12937
Total contamination	<12	6	mg/kg	EN 12662
Copper strip corrosion	1	1	Korr.-Grad.	EN ISO 2160
FAME content	<0.01	<0.1	% (V/V)	EN 14078
Oxidation stability	<1	7	g/m^3	EN ISO 12205
• filterable insolubles		4	g/m^3	EN ISO 12205
• adherent insolubles		3	g/m^3	EN ISO 12205
HFRR (Lubricity at 60°C)	380	361	µm	EN ISO 12156-1
Kin. Viscosity (40°C)	2.8	2.8	mm^2/s	EN ISO 3104
% (V/V) recovery at 250°C	33.2	33.1	% (V/V)	EN ISO 3924
% (V/V) recovery at 350°C	92.8	92.6	% (V/V)	EN ISO 3924
95% (V/V) recovery	367	369	°C	EN ISO 3924
Cold filter plugging point	-8	-9	°C	EN 116
Manganese	<0.5	<0.5	mg/l	EN 16576
Calorific value, lower	43.6	43.3	MJ/kg	DIN 51900-2

Turning to emissions, combustion of the stored renewable diesel resulted in lower brake-specific emissions for all emission species examined, compared with fossil diesel. The NO_x reduction was 9 % over the standardised ISO 8178-4 C1 test cycle, attributed to the lower flame temperature associated with renewable diesel´s low aromatic content. CO and HC emissions were reduced by 7 % compared with DFO.

Figure 19 depicts the averages of particulate number emissions within the particle size range of 5.6 to 560 nm at different speed and load combinations. The most significant particulate number reductions with renewable diesel were detected at minor loads. The reduction of total particulate number, weighted over the eight-mode test cycle, was 26 % compared with DFO, due to RD's beneficial hydrocarbon structure, near-zero sulphur and low aromatics content.

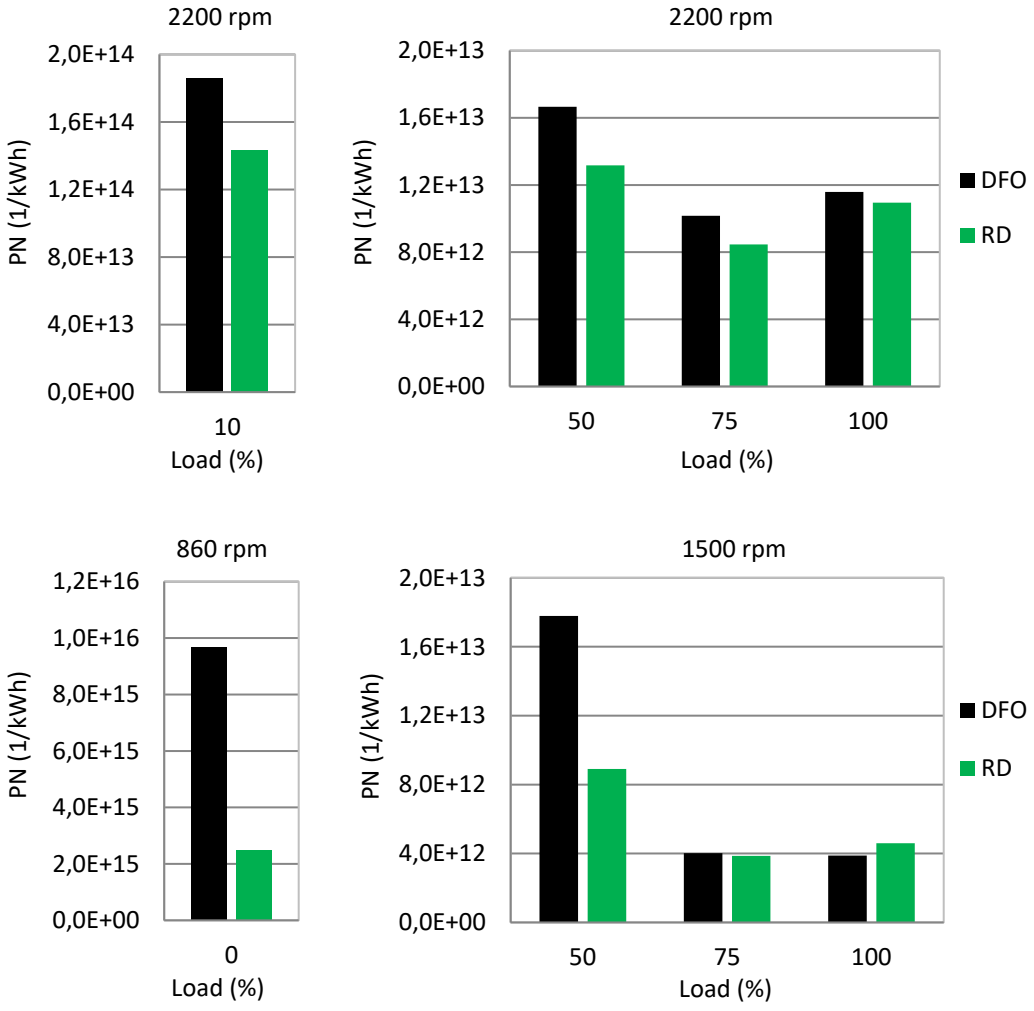

Figure 19. Particulate number emission within the particle size range of 5.6 to 560 nm at different speed and load configurations. CTO-derived renewable diesel after four years of ageing, DFO as a reference fuel

To conclude, four years of storage did not cause usability challenges for the CTO-derived renewable diesel. Its quality remained high, and the fuel delivered clear emission advantages compared with regular market diesel.

4 DISCUSSION

All sectors of the economy need rapid decarbonisation in order to limit global warming to 1.5 degrees above pre-industrial levels, in line with the target of the Paris Climate Agreement. Although electrification and hybridisation are growing trends in light-duty transport, electrification of the heavy-duty sector – shipping, non-road mobile machinery and heavy long-distance road transport – is significantly more difficult. Fuel has a considerable impact on emissions, so transition to alternative fuels is one of the strategies under discussion.

In this chapter, the emission results obtained in this study are extensively discussed. Particular attention is paid to methane emissions. Other topics of discussion are fuel storage stability and the current status and future prospects of the availability of the studied fuels, together with recommendations for candidate measures to accelerate the uptake of sustainably produced biofuels. Finally, certain weaknesses in the current emission regulatory framework identified during the research are discussed.

4.1 Greenhouse gas emissions

The regulatory requirements regarding GHG emissions from shipping are taking shape in the IMO and the EU (DNV, 2022). The FuelEU Maritime proposal (EU, 2021/562), a part of the EU Fit for 55 package, aims to promote renewable and low-carbon fuels in maritime transport by introducing GHG intensity targets for the energy used onboard by ships visiting European ports. The targets are expressed in well-to-wake CO_2-equivalent emissions to account for the entire life cycle GHG emissions of different fuels. The European Parliament adopted the regulation in October 2022. The Parliament's targets for cutting the GHG intensity of fuels used in shipping are 2 % by 2025, 6 % by 2030, 20 % by 2035, 38 % by 2040, 64 % by 2045, and 80 % by 2050 compared to the base year 2020 (European Parliament, 2022). The regulation applies to all ships above 5,000 gross tonnages, regardless of their flag. In addition, the IMO is preparing concrete proposals to promote the uptake of alternative low- and zero-carbon fuels, including developing life cycle GHG/carbon intensity guidelines for marine fuels (IMO, 2022).

This study identified substantial life-cycle GHG emission savings associated with shifting from fossil fuels to liquefied biomethane. LBG produced from sustainable feedstocks could reduce life-cycle GHG emissions from shipping by 60–75 % compared with marine diesel oil. Thus, using biomethane as fuel for ships could significantly contribute to achieving the EU's GHG emission reduction targets described above. In the base case (60 % GHG savings), a methane slip of 2 % from

fuel combustion was assumed. Eliminating all CH_4 slip from combustion increased the GHG savings to 75 %. Indeed, the GHG emission benefits of methane-based fuels are highly sensitive to the level of fugitive CH_4 leakages throughout the fuel supply chain and methane slip from combustion. The contribution analysis showed that CH_4 emissions represented 69 % of the total life-cycle GWP100 for LBG. This underlines the importance of controlling CH_4 emissions across the biomethane value chain.

In the literature, substantial CH_4 emissions from methane-fuelled ships have been reported. For example, Ushakov et al. (2019) presented comprehensive measurement data for low-pressure, dual-fuel engines. The measurement data pool consists of both onboard and test-bed measurements. At higher loads (>50 %), the mean CH_4 slip varied between 4.9 and 6.5 g/kWh. At 25 % load, the mean CH_4 slip reached 16 g/kWh. The IMO's Fourth GHG study (IMO, 2021) applies a CH_4 emission factor of 5.5 g/kWh, based on Pavlenko et al. (2020). However, considering recent improvements in dual-fuel engine technology, Paper I used a considerably lower methane slip rate of 2 %, corresponding to 3.2 g/kWh, for the new, modern dual-fuel engine. For example, Wärtsilä reports that by optimising engines and leakages, it has reduced CH_4 slip from new engines to 2–3 g/kWh (Wärtsilä, 2020).

Still, eliminating methane slip will be an important development topic this decade, in particular the effective control of CH_4 slip at low engine loads. The main technological methods to minimise methane emissions from low-pressure, dual-fuel engines are improved combustion chamber design and improved combustion process control (Zarrinkolah, & Hosseini, 2023; Peng et al., 2020; Ushakov et al., 2019). A promising future alternative to tackle CH_4 slip from lean-burn gas engines is catalytic oxidation of methane. Lehtoranta et al. (2021) have already demonstrated 70–80 % methane conversion with a methane oxidation catalyst at the exhaust temperature of 550 °C. However, further catalyst development is needed regarding the methane oxidation efficiency on different engine loadings and to resolve the long-term performance of onboard CH_4 catalyst systems (Lehtoranta et al., 2021; Aakko-Saksa et al., 2023). Methane emissions from dual-fuel engines can also be curtailed by operational measures, i.e., by switching to marine diesel oil at low load situations.

Effective mitigation of CH_4 emissions throughout the fuel supply chain is one of the most effective and fastest ways to slow the rate of global warming in the near term. This is based on the fact that, in the first two decades after it is emitted, methane has more than 80 times the warming power of CO_2 (Mar et al., 2022). Hence, regulatory measures to reduce methane emissions may be required in international shipping in the coming years. Continuing reductions in emissions of

CO_2, which remains the largest contributor to global warming, are also necessary to achieve the long-term climate goals (EEA, 2023b).

After publishing Paper I, the Intergovernmental Panel on Climate Change IPPC announced its sixth assessment report (AR6). Compared to AR5, the climate-carbon feedback for non-CO_2 gases is lower, but there is high confidence in the need for its inclusion. Therefore, AR6 now routinely includes the carbon cycle response for non-CO_2 gases. For the first time, AR6 also defines GWP values separately for fossil and non-fossil CH_4. The updated GWP100 factor for fossil CH_4 is 29.8, and for non-fossil CH_4, 27.0 (Forster et al., 2021). To provide the latest information, the global warming potentials of fuels studied in Paper I were recalculated using these updated GWP100 values. In the recalculation, LBG's potential to reduce life-cycle GHG emission compared with MDO was 65–78 % and compared with LNG, 63–72 %, depending on the methane slip (0–2 %).

Paper II focused on emissions from heavy-duty vehicles, using an urban bus as an example. Heavy-duty vehicles are responsible for around a quarter of EU road transport emissions (EEA, 2022a). Therefore, meeting the EU's climate neutrality target by 2050 will also require large-scale changes in the heavy transport sector. In addition to the improved efficiency of individual vehicles, the broader adoption of bio-based fuels could play a role in this development. In Paper II, even with a poorly functioning catalyst, 80 % life-cycle GHG emission savings were identified by switching from fossil diesel to compressed biomethane. Stricter CH_4 emission control during the tank-to-wheels stage would yield even higher GHG benefits. It would be worthwhile repeating both Paper II´s measurement campaigns with a new catalyst on the bus in future. This also would allow the weather-related comparison of emissions, filling the research gap of the impacts of low ambient temperatures on real-world exhaust emissions of gas-fuelled vehicles.

As a new material in this dissertation, the life-cycle GHG emissions of crude tall oil-derived renewable diesel were calculated. Paper III identified substantial (86 %) life-cycle GHG emission savings associated with use of waste/residual feedstock-based renewable diesel instead of fossil diesel, in line with (Bezergianni & Chrysikou, 2015; Neste, 2020; Thompson, 2022). GHG emissions of renewable diesel were practically entirely formed in the well-to-tank stage. The most critical parameter affecting the life-cycle GHG emission performance appeared to be the hydrogen needed for production of this renewable fuel, representing 55 % of its life-cycle GHG emissions. In Paper III, hydrogen was assumed to be produced from natural gas via steam reforming. Even higher emission benefits could be attributed to hydrogenation-derived renewable diesel if hydrogen was generated in a more environment-friendly manner.

During the finalisation of this dissertation, renewable diesel's potential to reduce maritime GHG emissions was also evaluated. The annual CO_2-equivalent emissions for RD100 were calculated using the case ship presented in Paper I as a basis. The results showed an 86 % GHG saving potential compared to MDO. Compared to Diesel B7 fuel (Paper II), RD100 showed GHG saving potential of 85 %.

4.2 Local air emissions

Although the global environmental discussion is increasingly focused on climate change, tackling local air pollution remains an important issue. Papers I, III, and IV showed that both investigated fuels – biomethane and renewable diesel – also reduced local air pollutants. In addition to reduced emissions of acidifying and eutrophying pollutants into the ecosystem, particulate emissions also decreased. Particulates are especially associated with adverse health effects.

Air pollution is the single most significant environmental health risk in Europe, according to the European Environment Agency (EEA, 2022b). Consequently, reducing local emissions is particularly important in cities and other densely populated areas. Local authorities can utilise the results of this study in designing strategies for transitioning to lower-emission urban traffic and cleaner cities.

4.3 Fuel storage stability

In addition to achieving acceptable emission performance, fuels are expected to remain stable during their storage. Fuel stability is particularly important, for example, for fuelling machinery with seasonal use or for emergency generator sets. Fuel storage stability is also a prerequisite for large-scale fuel production. Paper IV showed that hydrotreated renewable diesel could be stored under controlled conditions for several years without compromising fuel quality and without engine operability issues.

The situation is different for biomethane, as most storage technologies are designed for short-term requirements (Budzianowski & Brodacka, 2017). In particular, liquefied methane is not suitable for long-term storage. Heat entering the cryogenic tank during storage causes gradual evaporation of some of the liquefied methane, creating so-called boil-off gas, which needs to be removed from the tank to control its pressure and temperature. Over time, this thermal evaporation changes the gas composition and quality (Dobrota et al., 2013). Turning to compressed biomethane, storage issues are generally associated with its low energy density, necessitating large – and hence more costly – storage facilities. As

far as the author is aware, there are no studies in the existing literature investigating storage stability of compressed biomethane. Therefore, further research is recommended to fill the knowledge gap on the long-term storage stability of CBG.

4.4 Fuel availability

The primary concern facing biomethane and renewable diesel today is their limited availability. European biomethane production was 130 PJ in 2021 (EBA, 2022), and renewable diesel production approximately 120 PJ (IEA, 2022). To put those figures into perspective, Eurostat data show that the energy consumption of road transport in the EU in 2021 was 10,800 PJ. In shipping, the share of international maritime bunkers in EU ports in 2021 was 1,700 PJ (Eurostat, 2022). The EU's projected fuel demand for road transport in 2030 is 10,000 PJ, and the energy demand forecast for inland navigation and other off-road applications is 540 PJ (Yugo et al., 2021). As mentioned in the introduction, the EU RED II regulation requires the share of advanced biofuels and biogas in the transport sector to be at least 3.5 % by 2030. In international maritime transport, the European Commission wants renewable and low-carbon fuels to account for 6–9 % by 2030. This means that demand for biomethane and advanced liquid biofuels in the EU may reach 500 PJ in 2030. The target for European biomethane production in 2030 is 1,300 PJ (EBA, 2022). Production of renewable diesel is projected to increase to 170 PJ/year by 2030 (Yugo et al., 2021).

Looking at the numbers above, we see that the predicted production volume of renewable diesel is not enough to cover the EU's target for sustainably produced biofuels in 2030. The situation for biomethane seems to be more favourable as forecasted production exceeds projected demand. However, competing demand for biomethane from other sectors, such as industry and the built environment (Nelissen et al., 2020) complicates the situation. Furthermore, the supply of liquefied biomethane in particular must be increased considerably to make biomethane a realistic option for shipping and long-haul heavy transport. In addition, it must be borne in mind that demand for low-carbon fuels in shipping will accelerate significantly after 2030.

There is no doubt that the transport sector needs a wider selection of low- and zero-carbon fuels and new technologies on the way towards 2050. Governments and policymakers must define clear priorities for research and development and related infrastructure plans in order to accelerate the structural change and to secure the necessary investments. Another candidate measures to accelerate the

uptake of sustainably produced biofuels are stricter blending obligations for these fuels and fiscal measures to improve the price competitiveness of sustainably produced biofuels. These may entail carbon taxation or eliminating subsidies for fossil fuels, or tax reductions and carbon credits for sustainable biofuels.

4.5 Regulations

Certain shortcomings in the current legislation regarding the testing procedure were identified when processing the real-driving emission data. First, in the current legislation, the "emissions durability" period for, e.g., category M3 buses, is 300,000 km or six years, whichever is the sooner. For large trucks, the durability requirement is 700,000 km/seven years (EU, 2009/595). This period is the minimum distance or time during which the engine is expected to comply with applicable emission limits. However, the average age of bus fleets in EU member states is 12.7 years, and for trucks it is 14.2 years (Acea, 2023). Therefore, to ensure emission compliance throughout the vehicles' lifetime, the emission durability requirements should be revised to reflect actual vehicle lifetimes in the EU. Second, the regulatory in-service conformity test of Euro VI vehicles applies a minimum power threshold of 20 % or 10 %, depending on the registration date. Paper II indicated that approximately 30 % of emissions would be excluded if the 20 % power threshold was applied. Paper II also showed that a significant proportion of emissions were omitted if cold-start emissions, currently excluded in the legislation for Euro VI-C buses, were ignored. Based on these findings, it is clear that the real-driving emission testing procedure needs updating to reflect real-world driving conditions to a greater degree. This also was pointed out by the European Federation for Transport and Environment (T&E, 2020).

The studies conducted in this dissertation provide a strong environmental argument for biomethane and renewable diesel use. However, the CO_2 reduction potential of these fuels is not recognised in the current EU CO_2 standards for heavy-duty vehicles, which only follow the tank-to-wheels approach. For example, in February 2023, the European Commission proposed new CO_2 standards for trucks, trailers, and buses (EU COM, 2023/88). According to the proposal, new city buses in the EU will all have to be zero-emissions vehicles as of 2030. The mandate for zero-emission trucks is 90 % from 2040 onwards. Addressing only the tailpipe CO_2 emissions of regulated vehicle groups means that only battery-electric and hydrogen-powered vehicles are currently considered zero-emission vehicles. However, from the life-cycle CO_2 perspective, electric vehicles are not zero-emission vehicles. Total emissions depend highly on CO_2 emissions from manufacturing batteries and the type of electricity the vehicles are charged with.

Adopting a sustainability assessment based on the life-cycle approach would enable a proper evaluation of GHG emissions of future vehicle technology and fuel combinations, leaving room for alternative fuel systems in the heavy-duty sector, including sustainably produced liquid biofuels and biomethane. The same is valid for maritime transport and off-road machinery. The well-to-propeller and well-to-wheels approaches are also necessary when assessing the life-cycle GHG emissions of these sectors.

5 CONCLUSIONS

The results obtained in this dissertation allow the following conclusions to be drawn:

1. Using liquefied biomethane derived from sustainable biomass sources can reduce life-cycle GHG emissions from short sea shipping by 65–78 % compared with fossil marine diesel oil. Liquefied biomethane´s potential to reduce life-cycle GHG emission compared with liquefied natural gas is also significant, at 63–72 %.

2. The GHG emission benefits of methane-based fuels are highly sensitive to the level of fugitive CH_4 leakages throughout the fuel supply chain and to methane slip from combustion. For example, CH_4 emissions represented 69 % of LBG´s total life-cycle GWP100.

3. Eliminating methane slip from gas-powered engines will be an essential technology development topic this decade, with the biggest challenge being effective control of methane slip at low engine-loads.

4. Fuelling a city bus with compressed biomethane showed an 80 % GHG emission benefit over conventional diesel fuel, even with a poorly functioning catalyst. Catalyst replacement and strict lambda control would curtail methane emission more effectively, so GHG savings would advance towards 90 %.

5. Deterioration of exhaust aftertreatment systems over time should be monitored because they are exposed to different aging processes that elevate real-world emissions. Our results indicated the need to replace the three-way catalytic converter after 375,000 km of service life at the latest.

6. Crude tall oil-derived renewable diesel showed substantial (86 %) life-cycle GHG emission savings compared with fossil diesel.

7. Fuelling a ferry with liquefied biomethane showed clear advantages in terms of local environmental impacts. Acidifying emissions were reduced by 48 %, eutrophying emissions by 29 % and PM_{10} by 80 %, compared with marine diesel combined with selective catalytic reduction. Human health damage in terms of disability-adjusted life years decreased by 49 % compared with fossil diesel.

8. Renewable diesel resulted in lower brake-specific emissions than fossil diesel, for all emission species examined. The particulate number reduced by up to 26 %. NO_x, HC and CO decreased by 3–10 %.

9. Fuel analyses and engine experiments with hydrotreated renewable diesel stored for four years confirmed that this fuel could be stored under controlled conditions for several years without compromising fuel quality and without engine operability problems.

This dissertation has demonstrated that using biomethane and renewable diesel are effective ways to decarbonise transport in the short to medium term in hard-to-abate sectors. In addition to substantial greenhouse gas savings, local air pollutants are reduced, which immediately improves local air quality.

The primary concern facing biomethane and renewable diesel today is their limited availability. Furthermore, increasingly strict emission regulations mean demand for advanced biofuels and renewable gases in the transport sector will continue to grow towards 2030 and beyond. Guaranteed long-term policy is needed to scale up supply of sustainably produced biofuels. Increased blending obligations, targeted support for research and development activities, elimination of fossil fuel subsidies and carbon credits for sustainable biofuels all could increase the supply of these fuels and accelerate the necessary investments.

This book presents the first publicly available endeavour to quantify the life-cycle GHG emissions of crude tall oil-based renewable diesel fuel. Another merit of this thesis was the examination of emissions of a six-year-old bus fuelled with compressed biomethane, supplementing the insufficient emission data closer to the actual service life of gas-powered heavy-duty vehicles. Fleet owners and operators can utilise the results, e.g., in scheduling catalyst maintenance or replacement activities.

During the studies, further questions emerged as potential topics for future work. Soon, it would be worthwhile to repeat the emission measurements of the biomethane-fuelled city bus, but fitted with a new catalyst. This also would enable a weather-related comparison of emissions, filling the data gap on the effects of low ambient temperatures on real-world exhaust emissions from gas-powered vehicles. Further research is also recommended on the long-term storage stability of CBG. And methane's strong climate-warming effect prompts the need for additional studies and measures to further reduce methane emissions from all sizes of gas engines.

6 SUMMARY

The main goal of this dissertation was to demonstrate the emission reduction potential of sustainably produced renewable fuels in the transport sector. One gaseous and one liquid fuel were examined. The gaseous fuel was biomethane, produced from organic municipal waste; the liquid fuel was renewable diesel, produced by hydrotreatment of wood-based crude tall oil. The study paid particular attention to greenhouse gas emissions, in line with the global environmental agenda´s increasing focus on climate change. The life-cycle approach was used to assess the total carbon intensity of the studied fuels. In addition, local air pollutants, such as particulate matter and nitrous oxides, were examined. Current and forthcoming regulations on reducing carbon emissions in road and non-road transport were also reviewed.

The dissertation is based on four publications. Biomethane was studied in two ways. Liquefied biomethane was investigated through a case study on a RoPax vessel operating in the Baltic Sea. Compressed biomethane was studied by measuring real-driving emissions from a biomethane-powered city bus. In addition, a comprehensive well-to-wheels analysis was made to determine the carbon intensity of compressed biomethane. Renewable diesel was investigated with engine experiments with an off-road diesel engine in laboratory conditions. The investigation of life-cycle greenhouse gas emissions of crude tall oil-derived renewable diesel provides new material in this dissertation.

The results showed that using renewable fuels derived from sustainable biomass sources can reduce life-cycle GHG emissions by 65–90 % compared with fossil fuels. In addition to massive greenhouse gas savings, biomethane and renewable diesel also reduce local emissions, yielding an immediate improvement for local air quality. Burning liquefied biomethane reduced particulate matter by 80 % compared with marine diesel oil. Sulphur dioxide emissions were negligible, and nitrogen oxide emissions were also low. Renewable diesel reduced all regulated gaseous emissions (NO_x, CO, HC) by 3–10 %. The particulate number decreased by up to 26 %, the beneficial trend being most evident at low engine-loads.

In addition to emissions, the influence of long-term storage on renewable diesel properties was investigated. The fuel analyses and engine experiments with fuel stored for four years showed that hydrotreated renewable diesel could be stored under controlled conditions for several years without compromising fuel quality and without engine operability issues.

Biomethane and renewable diesel proved to be effective ways to decarbonise transport in the short to medium term in hard-to-abate sectors with no immediate

alternatives. The primary concern today is the limited availability of these fuels. Policy actions could increase the supply of these fuels and accelerate the necessary investments. Examples of such actions include separate blending obligations for sustainably produced biofuels; targeted support for research and development activities; elimination of fossil fuel subsidies; and carbon credits for sustainable biofuels. Moreover, the sustainability evaluation should be based on a life-cycle approach, instead of tailpipe measurements. This would enable a proper evaluation of greenhouse gas emissions of future technology and fuel combinations, leaving room for alternative fuel systems.

The study provides information to policymakers at both local and national levels. For example, regulatory measures to reduce methane emissions may be required in international shipping in the coming years. Equally, local authorities can utilise the results in designing strategies for transitioning to lower-emission urban traffic and cleaner cities. In addition, fleet owners and operators can apply the real-world emission results of the ageing biogas-fuelled city bus, for example, in scheduling catalyst maintenance or replacement.

References

Aakko-Saksa, P.T., Lehtoranta, K., Kuittinen, N., Järvinen, A., Jalkanen, J-P., Johnson, K., Jung, H., Ntziachristos, L., Gagné, S., Takahashi, C., Karjalainen, P., Rönkkö, T., & Timonen, H. (2023). Reduction in greenhouse gas and other emissions from ship engines: Current trends and future options. *Progress in Energy and Combustion Science*, 94, 101055. https://doi.org/10.1016/j.pecs.2022.101055

Acea. (2023, May 2). Facts and Figures. Average age of the EU Vehicle Fleet, by Country. The European Automobile Manufacturers' Association. Retrieved 19 June, 2023, from: https://www.acea.auto/figure/average-age-of-eu-vehicle-fleet-by-country/

Auvinen, P., Nevalainen, P., Suvanto, M., Oliva, F., Llamas, X., Barciela, B., Sippula, O., & Kinnunen, N.M. (2021). A detailed study on regeneration of SO_2 poisoned exhaust gas after-treatment catalysts: In pursuance of high durability and low methane, NH_3 and N_2O emissions of heavy-duty vehicles. *Fuel*, 291, 120223. https://doi.org/10.1016/j.fuel.2021.120223

Bezergianni, S. & Chrysikou, L. (2015). Life Cycle Assessment of Renewable Biodiesel Produced via Waste Cooking Oil Hydrotreatment. *10th International Colloquium Fuels – Conventional and Future Energy for Automobiles. Esslingen, Germany*. https://www.researchgate.net/publication/272162374_Life_Cycle_Assessment_of_Renewable_Biodiesel_Produced_via_Waste_Cooking_Oil_Hydrotreatment#fullTextFileContent

Budzianowski, W.M. & Brodacka, M. (2017). Biomethane storage: Evaluation of technologies, end uses, business models, and sustainability. *Energy Conversion and Management*, 141, 254–273. https://doi.org/10.1016/j.enconman.2016.08.071

Cashman, S.A., Moran, K.M. & Gaglione, A.G. (2015). Greenhouse Gas and Energy Life Cycle Assessment of Pine Chemicals Derived from Crude Tall Oil and Their Substitutes. *Journal of Industrial Ecology*, 20, 1108–1121. https://doi.org/10.1111/jiec.12370

Climate Watch (2022). *Historical GHG Emissions*. Climate Watch. Retrieved 18 October, 2022, from: https://www.climatewatchdata.org/ghg-emissions?breakBy=regions&end_year=2019&regions=EUU&sectors=transportation&source=CAIT&start_year=1990

DIN EN 590. (2017). *Automotive Fuels - Diesel - Requirements and Test Methods* (includes Amendment 2017). DIN German Institute for Standardization, Standard DIN EN 590, Rev. Oct. 2017.

DNV. (2022). *Maritime Forecast to 2050. Energy Transition Outlook 2022*. https://www.dnv.com/maritime/publications/maritime-forecast-2022/index.html

Dobrota, D., Lalić, B., & Komar, I. (2013). Problem of Boil - off in LNG Supply Chain. *Transactions on Maritime Science*, 2(2), 91–100. https://doi.org/10.7225/toms.v02.n02.001

EBA. (2020). *The contribution of the biogas and biomethane industries to medium-term greenhouse gas reduction targets and climate neutrality by 2050*. Background paper, April 2020. European Biogas Association. https://www.europeanbiogas.eu/wp-content/uploads/2020/04/20200419-Background-paper_final.pdf

EBA. (2022). *EBA Statistical Report 2022*. European Biogas Association. Retrieved 16 December, 2022, from: https://www.europeanbiogas.eu/SR-2022/EBA/

EEA. (2022a, December 7). *Reducing greenhouse gas emissions from heavy-duty vehicles in Europe*. European Environment Agency. Publications. Retrieved 12 December, 2022, from: https://www.eea.europa.eu/publications/co2-emissions-of-new-heavy

EEA. (2022b, October 5). *Air pollution: how it affects our health*. European Environment Agency. Retrieved 25 January, 2023, from: https://www.eea.europa.eu/themes/air/health-impacts-of-air-pollution

EEA. (2023a, February 25). *Impacts of air pollution on ecosystems*. European Environment Agency. Retrieved 11 June, 2023, from: https://www.eea.europa.eu/publications/air-quality-in-europe-2022/impacts-of-air-pollution-on-ecosystems

EEA. (2023b, April 26). *Methane emissions in the EU: the key to immediate action on climate change*. European Environment Agency. Retrieved 13 June, 2023, from: https://www.eea.europa.eu/publications/methane-emissions-in-the-eu

ERTRAC. (2016). *Future Light and Heavy Duty ICE Powertrain Technologies*. ERTRAC Working Group Energy and Environment. Edited version 05.04.2016. https://www.ertrac.org/uploads/documentsearch/id40/2016-04-05_ICE_roadmap_edited%20version.pdf

EU (2009/595). Regulation No 595/2009 of the European Parliament and of the Council of 18 June 2009 on Type-Approval of Motor Vehicles and Engines with Respect to Emissions from Heavy Duty Vehicles (Euro VI) and Amending Regulation (EC) No 715/2007 and Directive 2007/46/EC and Repealing Directives 80/1269/EEC, 2005/55/EC and 2005/78/EC. EC 595/2009. https://eur-lex.europa.eu/legal-content/EN/TXT/PDF/?uri=CELEX:02009R0595-20200901&from=EN

EU (2018/2001). Directive (EU) 2018/2001 of the European Parliament and of the Council of 11 December 2018 on the promotion of the use of energy from renewable sources. https://eur-lex.europa.eu/legal-content/EN/TXT/HTML/?uri=CELEX:32018L2001&from=EN#d1e32-204-1

EU (2021/562). Proposal for a Regulation of the European Parliament and of the Council on the use of renewable and low-carbon fuels in maritime transport and

amending Directive 2009/16/EC. Brussels, 14.7.2021. https://eur-lex.europa.eu/resource.html?uri=cellar:078fb779-e577-11eb-a1a5-01aa75ed71a1.0001.02/DOC_1&format=PDF

EU COM (2011/582). Commission Regulation (EU) No 582/2011 of 25 May 2011 implementing and amending Regulation (EC) No 595/2009 of the European Parliament and of the Council with respect to emissions from heavy duty vehicles (Euro VI) and amending Annexes I and III to Directive 2007/46/EC of the European Parliament and of the Council. https://eur-lex.europa.eu/legal-content/EN/TXT/HTML/?uri=CELEX:32011R0582&from=EN#ntr4-L_2011167FI.01008101-E0004

EU COM (2020/562). Communication from the Commission to the European Parliament, the Council, the European Economic and Social Committee and the Committee of the Regions. Stepping up Europe's 2030 Climate Ambition. Investing in a Climate-Neutral Future for the Benefit of Our People. Brussels, 17.9.2020. https://eur-lex.europa.eu/legal-content/EN/TXT/PDF/?uri=CELEX:52020DC0562&from=EN

EU COM (2023/88). Proposal for a Regulation of the European Parliament and of the Council amending Regulation (EU) 2019/1242 as regards strengthening the CO_2 emission performance standards for new heavy-duty vehicles and integrating reporting obligations, and repealing Regulation (EU) 2018/956. COM/2023/88 final. https://eur-lex.europa.eu/legal-content/EN/TXT/HTML/?uri=CELEX:52023PC0088

European Parliament. (2022). Amendments adopted by the European Parliament on 19 October 2022 on the proposal for a regulation of the European Parliament and of the Council on the use of renewable and low-carbon fuels in maritime transport and amending Directive 2009/16/EC. https://www.europarl.europa.eu/doceo/document/TA-9-2022-0367_EN.html

Eurostat. (2022, December 15). *Simplified energy balances*. The statistical office of the European Union. Retrieved 16 December, 2022, from: https://ec.europa.eu/eurostat/databrowser/view/NRG_BAL_S/default/table?lang=en&category=nrg.nrg_quant.nrg_quanta.nrg_bal

Forster, P., Storelvmo, T., Armour, K., Collins, W., Dufresne, J.-L., Frame, D., Lunt, D.J., Mauritsen, T., Palmer, M.D., et al. (2021). The Earth's Energy Budget, Climate Feedbacks, and Climate Sensitivity. In V. Masson-Delmotte, P. Zhai, A. Pirani, S.L. Connors, C. Péan, S. Berger, N. Caud, Y. Chen, L. Goldfarb, et al. (Eds.), *Climate Change 2021: The Physical Science Basis. Contribution of Working Group I to the Sixth Assessment Report of the Intergovernmental Panel on Climate Change* (pp. 923–1054). Cambridge University Press, Cambridge, United Kingdom and New York, NY, USA.

Gasser, T., Peterrs, G.P., Fuglestvedt, J.S., Collins, W.J., Shindell, D.T., & Ciais, P. (2017). Accounting for the climate–carbon feedback in emission metrics. *Earth System Dynamics*, 8, 235–253. https://doi.org/10.5194/esd-8-235-2017

Gillet, N.P. & Matthews, H.D. (2010). Accounting for carbon cycle feedbacks in a comparison of the global warming effects of greenhouse gases. *Environmental Research Letters,* 5, 034011. https://doi.org/10.1088/1748-9326/5/3/034011

Glaude, P., Fournet, R., Bounaceur, R., & Molière, M. (2010). Adiabatic flame temperature from biofuels and fossil fuels and derived effect on NOx emissions. *Fuel Processing Technology*, 91(2), 229–235. https://doi.org/10.1016/j.fuproc.2009.10.002

Gray, N., McDonagh, S., O'Shea, R., Smyth, B., & Murphy, J.D. (2021). Decarbonising ships, planes and trucks: An analysis of suitable low-carbon fuels for the maritime, aviation and haulage sectors. *Advances in Applied Energy*, 1, 100008. https://doi.org/10.1016/j.adapen.2021.100008

Heuser, B., Vauhkonen, V., Mannonen, S., Rohs, H., & Kolbeck, A. (2013). Crude Tall Oil-Based Renewable Diesel as a Blending Component in Passenger Car Diesel Engines. *SAE International Journal of Fuels and Lubricants*, 6(3), 817–825. https://doi.org/10.4271/2013-01-2685

IEA. (2022). *Renewables 2021. Biofuels*. International Energy Agency. Retrieved 16 December, 2022, from: https://www.iea.org/reports/renewables-2021/biofuels?mode=transport&region=Europe&publication=2021&flow=Production&product=Renewable+Diesel

IEA-AMF. (2020). *The Role of Renewable Transport Fuels in Decarbonizing Road Transport. Summary Report. November 2020*. Advanced Motor Fuels, Technology Collaboration Programme by International Energy Agency IEA. https://www.ieabioenergy.com/wp-content/uploads/2020/11/Summary-Report.pdf

IMO. (2018). *Initial IMO Strategy on Reduction of GHG Emissions from Ships*. International Maritime Organization. Marine Environment Protection Committee. MEPC 72/17/Add.1, Annex 11, Resolution MEPC.304(72), 13.4.2018. https://wwwcdn.imo.org/localresources/en/OurWork/Environment/Documents/ResolutionMEPC.304(72)_E.pdf

IMO. (2019). *IMO's work to cut GHG emissions from ships*. International Maritime Organization. Media Centre. Retrieved 17 October, 2022, from: https://www.imo.org/en/MediaCentre/HotTopics/Pages/Cutting-GHG-emissions.aspx

IMO. (2021). *Fourth IMO GHG Study 2020*. Published in 2021 by the International Maritime Organization, 4 Albert Embankment, London SE1 7SR. https://wwwcdn.imo.org/localresources/en/OurWork/Environment/Documents/Fourth%20IMO%20GHG%20Study%202020%20-%20Full%20report%20and%20annexes.pdf

IMO. (2022, June 13). *Cutting ships' GHG emissions - working towards revised strategy*. International Maritime Organization. Retrieved 8 December, 2022, from: https://www.imo.org/en/MediaCentre/PressBriefings/pages/MEPC-78-.aspx

IPCC. (2022). *Headline Statements from the Summary for Policymakers*. Intergovernmental Panel on Climate Change. Sixth Assessment Report. Working Group III: Climate Mitigation. April 4, 2022. https://report.ipcc.ch/ar6wg3/pdf/IPCC_AR6_WGIII_HeadlineStatements.pdf

ISO 8178-1. (2020). *Reciprocating Internal Combustion Engines - Exhaust Emission Measurement - Part 1: Test-bed Measurement Systems of Gaseous and Particulate Emissions* (ISO Standard No. 8178-1:2020). International Organization for Standardization.

ISO 8178-4. (2020). *Reciprocating Internal Combustion Engines - Exhaust Emission Measurement - Part 4: Steady-state and Transient Test Cycles for Different Engine Applications* (ISO Standard No. 8178-4:2020). International Organization for Standardization.

JRC. (2014). Joint Research Centre. Institute for Energy and Transport. Hamje, H., Weindorf, W., Edwards, R., et al. *Well-to-wheels report version 4.a. JEC well-to-wheels analysis: well-to-wheels analysis of future automotive fuels and powertrains in the European context*. R. Nelson, S. Godwin, A. Reid, H. Maas, K. Rose, L. Lonza, H. Hass, A. Krasenbrink, A. (Eds.). Publications Office of the European Union, Luxembourg. https://data.europa.eu/doi/10.2790/95629

Jutterström, S., Moldan, F., Moldanová, J., Karl, M., Matthias, V., & Posch, M. (2021). The impact of nitrogen and sulfur emissions from shipping on the exceedance of critical loads in the Baltic Sea region. *Atmospheric Chemistry and Physics,* 21, 15827–15845. https://doi.org/10.5194/acp-21-15827-2021

Kalghatgi, G. (2018). Is it Really the End of Internal Combustion Engines and Petroleum in Transport? *Applied Energy*, 225, 965–974. https://doi.org/10.1016/j.apenergy.2018.05.076

Keoleian, G.A. & Spitzley, D.V. (2006). Life Cycle Based Sustainability Metrics. In M.A. Abraham (Ed.), *Sustainability Science and Engineering – Defining Principles* (127–160). Elsevier B.V., Amsterdam, The Netherlands. ISBN 978-0444517128.

Kollamthodi, S., Norris, J., Dun, C., Brannigan, C., Twisse, F., Biedka, M., & Bates, J. (2016). *The Role of Natural Gas and Biomethane in the Transport Sector: Final Report*. Ricardo Energy & Environment. Harwell, UK. https://www.transportenvironment.org/wp-content/uploads/2021/07/2016_02_TE_Natural_Gas_Biomethane_Study_FINAL.pdf

Labeckas, G., Slavinskas, S., & Kanapkienė, I. (2017). The individual effects of cetane number, oxygen content or fuel properties on performance efficiency, exhaust smoke and emissions of a turbocharged CRDI diesel engine – Part 2. *Energy Conversion and Management*, 149, 442–466. https://doi.org/10.1016/j.enconman.2017.07.017

Lassi, U. (2003). Deactivation Correlations of Pd/Rh Three-way Catalysts Designed for Euro IV Emission Limits. Effect of Ageing Atmosphere, Temperature and Time. [Doctoral Dissertation, University of Oulu]. PQDT Open. http://jultika.oulu.fi/files/isbn9514269543.pdf

Lehtoranta, K., Koponen, P., Vesala, H., Kallinen, K., & Maunula, T. (2021). Performance and Regeneration of Methane Oxidation Catalyst for LNG Ships. *Journal of Marine Science and Engineering*, 9, 111. https://doi.org/10.3390/jmse9020111

Mar, K.A., Unger, C., Walderdorff, L., & Butler, T. (2022). Beyond CO_2 equivalence: The impacts of methane on climate, ecosystems, and health. *Environmental Science & Policy*, 134, 127–136. https://doi.org/10.1016/j.envsci.2022.03.027

McCaffery, C., Zhu, H., Sabbir Ahmed, C.M., Canchola, A., Chen, J.Y., Li, C., Johnson, K.C., Durbin, T.D., Lin, Y-H., & Karavalakis, G. (2022). Effects of hydrogenated vegetable oil (HVO) and HVO/biodiesel blends on the physicochemical and toxicological properties of emissions from an off-road heavy-duty diesel engine. *Fuel*, 323, 124283, https://doi.org/10.1016/j.fuel.2022.124283.

Myhre, G., Shindell, D., Bréon, F.-M., Collins, W., Fuglestvedt, J., Huang, J., Koch, D., Lamarque, J.-F., Lee, D., Mendoza, B., Nakajima, T., Robock, A., Stephens, G., Takemura, T., & Zhang, H. (2013). Anthropogenic and Natural Radiative Forcing. In T.F., Stocker, D., Qin, G.-K., Plattner, M. Tignor, S.K. Allen, J. Boschung, A. Nauels, Y. Xia, V. Bex, & P.M. Midgley (Eds.), *Climate Change 2013: The Physical Science Basis. Contribution of Working Group I to the Fifth Assessment Report of the Intergovernmental Panel on Climate Change* (pp. 659–740). Cambridge University Press, Cambridge, United Kingdom and New York, NY, USA.

Nelissen, D., Faber, J., van der Veen, R., van Grinsven, A., Shanthi, H., & van den Toorn, E. (2020). *Availability and costs of liquefied bio- and synthetic methane. The maritime shipping perspective*. Delft, CE Delft, March 2020. https://cedelft.eu/wp-content/uploads/sites/2/2021/03/CE_Delft_190236_Availability_and_costs_of_liquefied_bio-_and_synthetic_methane_Def.pdf

Neste. (2020). *Neste Renewable Diesel Handbook*. Neste Proprietary publication, Neste Corporation, Espoo, October 2020. https://www.neste.com/sites/default/files/attachments/neste_renewable_diesel_handbook.pdf

Niemi, S., Hissa, M., Ovaska, T., Sirviö, K., & Vauhkonen, V. (2019). Performance and Emissions of a Non-Road Diesel Engine Driven with a Blend of Renewable Naphtha and Diesel Fuel Oil. In N. Schubert (Ed.), *Fuels: Conventional and Future Energy for Automobiles: 12th International Colloquium Fuels - Conventional and Future Energy for Automobiles (2019), Ostfildern, Deutschland, 25.06.2019 - 26.06.2019*. Technische Akademie Esslingen.

Panoutsou, C., Germer, S., Karka, P., Papadokostantakis, S., Kroyan, Y., Wojcieszyk, M., Maniatis, K., Marchand, P., & Landalv, I. (2021). Advanced biofuels to decarbonise European transport by 2030: Markets, challenges, and policies that impact their successful market uptake. *Energy Strategy Reviews,* 34, 100633. https://doi.org/10.1016/j.esr.2021.100633

Pavlenko, N., Comer, B., Zhou, Y., Clark, N., & Rutherford, D. (2020). *The climate implications of using LNG as a marine fuel*. January 2020. ICCT, International Council of Clean Transportation. https://theicct.org/publications/climate-impacts-LNG-marine-fuel-2020

Peng, W., Yang, J., Corbin, J., Trivanovic, U., Lobo, P., Kirchen, P., Rogak, S., Gagné, S., Miller, J.W., & Cocker, D. (2020). Comprehensive analysis of the air quality impacts of switching a marine vessel from diesel fuel to natural gas. *Environmental Pollution*, 266(3), 115404. https://doi.org/10.1016/j.envpol.2020.115404

Pérez-Camacho, M.N., Curry, R., & Cromie, T. (2019). Life cycle environmental impacts of biogas production and utilisation substituting for grid electricity, natural gas grid and transport fuels. *Waste Management*, 95, 90–101. https://doi.org/10.1016/j.wasman.2019.05.045.

Peters, D. & Stojcheva, V. (2017). *Crude tall oil low ILUC risk assessment – Comparing global supply and demand*. Ecofys Netherlands B.V., 24 April 2017. https://www.upmbiofuels.com/siteassets/documents/other-publications/ecofys-crude-tall-oil-low-iluc-risk-assessment-report.pdf

Prussi, M., Yugo, M., De Prada, L., Padella, M., Edwards, R., & Lonza, L. (2020). *JEC Well-to-Tank report v5, EUR 30269 EN*. Publications Office of the European Union, Luxembourg. ISBN 978-92-76-19926-7, doi:10.2760/959137, JRC119036. https://publications.jrc.ec.europa.eu/repository/handle/JRC119036

Santos, N.D.S.A., Roso, V.E., Malaquias, A.C.T., & Baêta, J.G.C. (2021). Internal combustion engines and biofuels: Examining why this robust combination should not be ignored for future sustainable transportation. *Renewable and Sustainable Energy Reviews,* 148, 111292. https://doi.org/10.1016/j.rser.2021.111292

Scarlat, N., Dallemand, J.F., & Fahl, F. (2018). Biogas: Developments and perspectives in Europe. *Renewable Energy*, 129, Part A, 457–472. https://doi.org/10.1016/j.renene.2018.03.006

Schwinger, J. & Tjiputra, J. (2018). Ocean Carbon Cycle Feedbacks Under Negative Emissions. *Geophysical Research Letters*, 45, 5062–5070. https://doi.org/10.1029/2018GL077790

Sitra. (2022). *Biogenic Carbon Dioxide*. The Finnish Innovation Fund Sitra. Retrieved 18 October, 2022, from: https://www.sitra.fi/en/dictionary/biogenic-carbon-dioxide/

Smith, T.W.P., Jalkanen, J.P., Anderson, B.A., Corbett, J.J., Faber, J., Hanayama, S., O'Keeffe, E., Parker, S., Johansson, L., Aldous, L., Raucci, C., Traut, M., Ettinger, S., Nelissen, D., Lee, D.S., Ng, S., Agrawal, A., Winebrake, J.J., Hoen, M., et al. (2015). *Third IMO GHG Study 2014*. International Maritime Organization (IMO). London, UK.
https://wwwcdn.imo.org/localresources/en/OurWork/Environment/Documents/Third%20Greenhouse%20Gas%20Study/GHG3%20Executive%20Summary%20and%20Report.pdf

StatFin. (2021). *Fuel Classification*. Statistics Finland. Retrieved 3 May, 2022 from https://www.stat.fi/tup/khkinv/khkaasut_ polttoaineluokitus.html

Strauch, S., Krassowski, J., & Singhal, A. (2013). *Biomethane Guide for Decision Makers — Policy Guide on Biogas Injection into the Natural Gas Grid*. Project Green Gas Grids WP 2/D 2.3, April 2013.
https://www.dena.de/fileadmin/dena/Dokumente/Themen_und_Projekte/Erneuerbare_Energien/GreenGasGrids/Policy_Guide_for_Decision_Makers.pdf

Söderena, P., Nylund, N.-O., & Mäkinen, R. (2019). *City Bus Performance Evaluation*. VTT Technical Research Centre of Finland. VTT Customer Report No. VTT-CR-00544-19.
https://cris.vtt.fi/ws/portalfiles/portal/26400446/City_bus_performance_evaluation.pdf

T&E. (2020). *Road to Zero: the last EU emission standard for cars, vans, buses and trucks. T&E blueprint for post-Euro 6/VI regulations*. European Federation for Transport and Environment. April 2020.
https://www.transportenvironment.org/wp-content/uploads/2021/06/2020_04_Road_to_Zero_last_EU_emission_standard_cars_vans_buses_trucks.pdf

Thompson, T.N. (2020). The market for biofuels: sustainable prospects for international shipping and the advances of the Port of Rotterdam. *Maritime Economics & Logistics*. https://doi.org/10.1057/s41278-022-00250-w

Ushakov, S., Stenersen, D., & Einang, P.M. Methane slip from gas fuelled ships: a comprehensive summary based on measurement data. J*ournal of Marine Science and Engineering,* 24, 1308–1325. https://doi.org/10.1007/s00773-018-00622-z

Van Zelm, R., Huijbregts, M.A.J., den Hollander, H.A., van Jaarsveld, H.A., Sauter, F.J., Struijs, J., van Wijnen, H.J., & van de Meent, D. (2008). European characterization factors for human health damage of PM10 and ozone in life cycle impact assessment. *Atmospheric Environment*, 42(3), 441–453.
https://doi.org/10.1016/j.atmosenv.2007.09.072

WHO (2023). *Air pollution is responsible for 6.7 million premature deaths every year*. World Health Organization. Retrieved 11 June, 2023, from: https://www.who.int/teams/environment-climate-change-and-health/air-quality-and-health/health-impacts/types-of-pollutants

Wärtsilä (2020, October 30). *Mind the methane gap*. Retrieved 8 December, 2022, from https://www.wartsila.com/insights/article/mind-the-methane-gap

Yugo, M., Shafiei, E., Ager-Wick Ellingsen, L., & Rogerson, J. (2021). *Concawe's Transport and Fuel Outlook towards EU 2030 Climate Targets*. Concawe Report no. 2/21. https://www.concawe.eu/wp-content/uploads/Rpt_21-2.pdf

Zarrinkolah, M.T. & Hosseini, V. (2023). Methane slip reduction of conventional dual-fuel natural gas diesel engine using direct fuel injection management and alternative combustion modes. *Fuel*, 331(2), 125775. https://doi.org/10.1016/j.fuel.2022.125775

Publications

This doctoral dissertation summarises the following four original research articles, referred to in the text by their Roman numerals:

I. Spoof-Tuomi, K. & Niemi, S. (2020). Environmental and Economic Evaluation of Fuel Choices for Short Sea Shipping. *Clean Technologies,* 2(1), 34–52. https://doi.org/10.3390/cleantechnol2010004

II. Spoof-Tuomi, K., Arvidsson, H., Nilsson, O., Niemi, S. (2022). Real-Driving Emissions of an Aging Biogas-Fueled City Bus. *Clean Technologies*, 4(4), 954–971. https://doi.org/10.3390/cleantechnol4040059

III. Spoof-Tuomi, K., Vauhkonen, V., Niemi, S., Ovaska, T., Lehtonen, V., Heikkilä, S. & Nilsson O. (2021). Effects of Crude Tall Oil Based Renewable Diesel on the Performance and Emissions of a Non-Road Diesel Engine. *SAE Technical Paper* 2021-01-1197. https://doi.org/10.4271/2021-01-1197

IV. Spoof-Tuomi, K., Vauhkonen, V., Niemi, S., Ovaska, T., Lehtonen, V., Heikkilä, S. & Nilsson, O. (2021). Crude Tall Oil based Renewable Diesel: Performance, Emission Characteristics and Storage Stability. *SAE Technical Paper* 2021-01-1208, 2021. https://doi.org/10.4271/2021-01-1208

Author's contribution

Paper I: Spoof-Tuomi is the lead author. As the corresponding author, Spoof-Tuomi designed the study, collected and analysed the data, visualised the results and wrote the article. Niemi provided valuable comments on the paper and supervised the study.

Paper II: Spoof-Tuomi is the lead author and the corresponding author who designed the study and organised the experiments. Arvidsson and Nilsson performed the emission measurements. Arvidsson preprocessed the data: Spoof-Tuomi analysed the data, visualised the results and wrote the article. Niemi provided valuable comments and supervised the study.

Paper III: Spoof-Tuomi is the main author. Vauhkonen and Niemi designed the study. Spoof-Tuomi implemented the engine experiment with Nilsson, Ovaska, and Heikkilä. Spoof-Tuomi, Ovaska and Lehtonen analysed the data and visualised the results. Spoof-Tuomi wrote the paper, together with Vauhkonen and Ovaska. Niemi contributed to the discussions and provided valuable comments on the paper.

Paper IV: Spoof-Tuomi is the main author. Vauhkonen and Niemi designed the study. Spoof-Tuomi implemented the engine experiment with Nilsson, Ovaska, and Heikkilä. Spoof-Tuomi, Ovaska, and Lehtonen analysed the data and visualised the results. Spoof-Tuomi wrote the paper, together with Vauhkonen and Ovaska. Niemi contributed to the discussions and provided valuable comments on the paper.

clean technologies

MDPI

Article

Environmental and Economic Evaluation of Fuel Choices for Short Sea Shipping †

Kirsi Spoof-Tuomi * and Seppo Niemi

School of Technology and Innovations, University of Vaasa, P.O. Box 700, 65101 Vaasa, Finland; seppo.niemi@univaasa.fi

* Correspondence: kirsi.spoof-tuomi@univaasa.fi

† This paper is an extended version of our paper "Emission reduction by biogas use in short sea shipping" published in *Integrated Energy Solutions to Smart and Green Shipping*, Proceedings of the INTENS public project seminar, Espoo, Finland, 13 March 2019; Zou, G., Ed.; VTT Technical Research Centre of Finland, 2019, pp. 102–106.

Received: 19 December 2019; Accepted: 20 January 2020; Published: 22 January 2020

Abstract: The shipping industry is looking for strategies to comply with increasingly stringent emission regulations. Fuel has a significant impact on emissions, so a switch to alternative fuels needs to be evaluated. This study investigated the emission performances of liquefied natural gas (LNG) and liquefied biogas (LBG) in shipping and compared them to conventional marine diesel oil (MDO) combined with selective catalytic reduction (SCR). For assessing the complete global warming potential of these fuels, the life-cycle approach was used. In addition, the study evaluated the local environmental impacts of combustion of these fuels, which is of particular importance for short sea shipping operations near coastal marine environment and residential areas. All three options examined are in compliance with the most stringent emission control area (ECA) regulations currently in force or entering into force from 2021. In terms of local environmental impacts, the two gaseous fuels had clear advantages over the MDO + SCR combination. However, the use of LNG as marine fuel achieved no significant CO_2-equivalent reduction, thus making little progress towards the International Maritime Organization's (IMO's) visions of decarbonizing shipping. Major life cycle GHG emission benefits were identified by replacing fossil fuels with LBG. The most significant challenge facing LBG today is fuel availability in volumes needed for shipping. Without taxation or subsidies, LBG may also find it difficult to compete with the prices of fossil fuels.

Keywords: marine fuels; short sea shipping; LBG; LNG; MDO; global warming potential; life cycle assessment

1. Introduction

Reducing ship emissions and developing the sector in an environmentally friendly manner has been the subject of the regulatory framework for years. The International Maritime Organization (IMO) regulates both the maximum sulfur content of fuel and emissions of NO_x in Annex VI of MARPOL (International Convention for the Prevention of Pollution from Ships). Particularly strict regulations apply in some sensitive areas, known as emission control areas (ECAs). The Baltic Sea was designated a Sulphur Emission Control Area (SECA) in 1998, and the current fuel sulfur content limit of 0.1% came into force in 2015 [1]. In July 2017, the IMO'S Marine Environment Protection Committee (MEPC) also designated the Baltic Sea a NO_x Emission Control Area (NECA), effective from 1 January, 2021 onwards [2]. NECA regulation (Tier III) applies to all vessels built after 2021 and demands an 80% cut in NO_x emissions compared to the present emission level. Practically, this means new-builds either will have to be equipped with a proper exhaust after-treatment system for NO_x reduction, or use

liquefied natural gas (LNG) as fuel to comply with the regulation. There are also concerns about health risks associated with particle emissions from shipping, so regulations focused on particulates may be expected in the future [3].

In addition, greenhouse gas (GHG) emissions from shipping have received increased attention lately. This stems from the fact that shipping is one of the fastest-growing sectors in terms of GHG emissions [4]. In April 2018, MEPC adopted the Initial IMO Strategy on Reduction of GHG Emissions from Ships. According to the decision, international maritime transportation will reduce annual absolute GHG emissions by at least 50% by 2050 (compared to 2008 levels), despite rising volumes of traffic, and after that to continue the process of completely phasing out CO_2 emissions in line with the Paris Climate Agreement temperature target [5]. These restrictions apply to all maritime traffic, not just to new vessels.

The maritime sector is now looking for strategies to achieve these future emissions targets. Fuel has a significant impact on emissions, so switching to alternative fuels is one of the strategies being discussed. The environmental impact of fuel, however, is not only linked to combustion in the engine, but also the entire fuel life cycle [3]. Fuels always emit pollutants at various stages of their life cycle, like refining and distribution, or during the cultivation if they are of biological origin [6].

Natural gas has become an increasingly attractive alternative to conventional marine fuels. A large number of existing studies have examined the impact of the use of natural gas on NO_x, SO_x and particulate emissions in marine engines. The literature review shows that switching to LNG instead of traditional bunker fuels would significantly improve the overall environmental performance. NO_x emissions are reduced by approximately 80–85% compared to the use of heavy fuel oil (HFO)/marine diesel oil (MDO) [7–9] as a result of reduced peak combustion temperatures in the engine [10]. SO_x emissions are almost eliminated [11,12], and particulate matter (PM) production is very low. A recent study by Lehtoranta et al. [13] showed that dual-fuel operation, with LNG as the main fuel, resulted in PM levels 72–75% lower than MDO. Li et al. [14] reported similar results with a maximum drop percentage of 78% in dual fuel mode compared to pure diesel mode. Reduction of these local pollutants is particularly important for short sea vessels with regional operations near coasts and populated areas [15].

In LNG operation, CO_2 emissions are reduced by 25% compared to HFO or MDO, thanks to high hydrogen content in methane molecules [7]. However, LNG's advantage in terms of total GHG emissions is less clear-cut. This is because its main constituent, methane (CH_4), is a potent greenhouse gas with a global warming potential (GWP) 28–34 times greater than that of CO_2 over a 100-year timescale [16]. Consequently, LNG's real-world GHG benefits are highly dependent on the rates of methane leakage within the LNG supply chain (fuel production, storage, transportation, bunkering) and "methane slip", i.e., unburned methane from an engine's combustion process released during vessel operation [17]. The benefits of using LNG are reduced if methane slip is not adequately controlled, in which case LNG may give only marginal GHG emissions benefits over conventional bunker fuels [18]. The findings by Lowell et al. [19] indicated that relatively modest CO_2-equivalent emission benefits, in a range of 5–10 percent, should be applied when assessing the use of LNG by ships. Previously quoted higher values tended to underplay or ignore some of the upstream emissions.

In contrast, the combustion of liquefied bio-methane (LBG) exhibits a neutral recirculation loop for CO_2, which has been identified as the major reason for global warming. The literature review shows that the use of methane produced from biomass has the potential to cut life-cycle GHG emissions significantly [6,15,20,21]. Therefore, LBG could be an attractive low carbon alternative to LNG.

For GHG emissions studies, usually the global warming potential factor for 100 years of 25 (IPCC AR4) or 28 (IPCC AR5) is used. These values, however, does not include the climate-carbon feedback for methane. Gasser et al. [22] define climate-carbon feedback as "the effect that a changing climate has on the carbon cycle". In concrete: global warming slows down the capture of atmospheric CO_2 by land and ocean sinks, thereby increasing the fraction of CO_2 that remains in the atmosphere [22,23], and the warming climate is warmed further. Excluding the climate-carbon feedback may underestimate

the relative impacts of non-CO_2 gases [16,24]. For example, Gillet and Matthews [25] found that climate-carbon feedbacks inflate the GWPs of methane and nitrous oxide by approximately 20%.

One of the main purposes of the present study was to evaluate the emissions performance of fuel choices for short-sea shipping. The fuels investigated are LNG, LBG, and conventional marine diesel oil. For assessing the complete global warming potential of these fuels, the life-cycle approach was used. In addition, the study evaluated the local environmental impacts of combustion of these fuels in terms of acidification and eutrophication potential and impacts on human health. The preliminary results of the emission inventory have been previously presented in a conference paper [26], prepared by the authors. However, assessing the potential of an alternative fuel to become a viable option, in terms of large-scale deployment, requires a thorough analysis that also covers economic aspects and verification of fuel availability.

The present study provides an updated life-cycle GHG analysis for MDO, LNG and LBG as a marine fuel. In the investigation, the carbon-climate feedback effect was included to avoid underestimating the impacts of non-CO_2 greenhouse gases. Furthermore, the study made an economic analysis for operating on LNG, LBG, and on MDO combined with selective catalytic reduction (SCR), thus addressing the need for an economic evaluation of LBG as a marine fuel, so far lacking in the literature. Finally, the study assessed current and future prospects of fuel availability, which is of particular relevance to LBG. The study used a Ro-Ro/passenger vessel, equipped with a dual-fuel (DF) engine, in the Baltic Sea ECA as a case ship.

2. Investigated Fuels and the Case Ship

Three different fuels were selected for detailed analysis and comparison: MDO, LNG and LBG.

2.1. MDO 0.1% S

Marine diesel oil is a blend of middle distillates derived from the crude oil refining process. Its international trading names are DMA (marine gas oil/MGO) and DMB (marine diesel oil/MDO). The main difference between DMA and DMB is that DMB may contain traces of residual fuel. In terms of CO_2 and NO_x emissions, these fuels are not significantly different from heavy fuel oil (HFO) [27]. The reduced sulfur level does, however, result in lower SO_x emissions, making them attractive for shipping in ECA.

2.2. LNG

LNG is the liquid form of natural gas, a mixture of hydrocarbon compounds found deep in underground reservoirs near other solid and liquid hydrocarbons beds like crude oil and coal. The main constituent of natural gas is methane, along with smaller quantities of other hydrocarbons like ethane, propane, and butane. The production of LNG from natural gas includes the removal of these trace gases, carbon dioxide, hydrogen sulfide, water, and other components that freeze at low temperatures. Then the gas is cooled to −162 °C to change it into a liquid form. As a liquid, the volume of the methane is reduced to 1/600 its gaseous state. This makes the fuel easier and safer to store and transport.

2.3. LBG

Bio-methane is methane produced from organic matter. Like its fossil equivalent natural gas, bio-methane also can be converted into a liquid form. LNG and LBG are nearly identical as far as engine's fueling is concerned, so using LBG instead of LNG does not pose any additional challenges. It is in the upstream section of their life cycles that they differ, e.g., the raw material used and the production processes [28].

Biogas, the pre-stage of bio-methane, can be produced from a vast variety of raw materials. Wet organic matter with low lignocellulose content, such as organic waste or sewage sludge, is suitable for biogas production by anaerobic digestion [29]. This is the most common way to produce bio-methane

currently. It is also possible to produce bio-CH_4 from gasification of biomass [21]. Irrespective of production method, biogas then is cleaned of impurities and upgraded to increase its CH_4 content so that it matches natural gas specifications [28].

LBG has potential to be carbon-neutral because combustion of bio-methane releases biogenic CO_2, which does not add to the natural carbon cycle. However, although in principle bio-methane combustion offers climatic-neutral energy production, it still affects the atmosphere. As with LNG, burning bio-methane releases CH_4 and some particulate emissions. Some GHG emissions also occur during its processing, transport and distribution, and so these must be included when evaluating LBG's credentials over the entire life cycle.

2.4. The Case Ship

The environmental performance of the fuels described above is assessed by a case study on a Ro-Ro/passenger ship (RoPax) vessel operating one route across the Gulf of Bothnia. The 53-nautical-mile crossing between Vaasa (Finland) and Umeå (Sweden) takes 4 h and 30 min. A new ferry with a dual-fuel engine will be deployed by the beginning of the summer season 2021. Thus, the new vessel must meet both the NO_x and the SOx emission standards set by IMO. Characteristics of the vessel are presented in Table 1.

Table 1. RoPax vessel basic data.

Engine output (kW)	16,000
Engine type	Dual fuel (liquefied natural gas (LNG)/ liquefied biogas (LBG) + 1.4% marine diesel oil (MDO) as pilot fuel)
Engine speed (rpm)	750
Engine efficiency at maximum continuous rating (MCR) (%)	48
Hours per year (h)	4000

There are different strategies for dealing with ECA regulations. For sulfur oxides, the most apparent reduction strategy is to avoid the problem by using low-sulfur (below 0.1% S) marine fuels. For nitrogen oxides, the situation is somewhat different. The most significant contributor to these types of emissions is thermally produced NO_x, which is formed in the combustion process by high-temperature oxidation of the molecular nitrogen present in the combustion air. The formation of thermal NO_x is strongly dependent on combustion temperature, residence time, and the concentration of oxygen atoms. In other words, the formation of thermal NO_x is associated with high temperatures and fuel-lean environments. Different fuels give rise to different degrees of NO_x formation: LNG and LBG will give significant reductions compared to heavy fuel oil, while a switch to MGO/MDO gives a reduction of only a few percent [21]. It can be difficult to reach the most stringent NO_x standard, IMO Tier III, with MGO/MDO without using exhaust gas after-treatment.

3. Method and Data Collection

3.1. Life Cycle Assessment

Any activity or process during the lifetime of a product causes environmental impacts due to the consumption of resources, emissions of harmful substances into the natural environment, and through other environmental exchanges [30]. Life cycle assessment (LCA) is a standardized method for assessing the potential environmental impact of a product or service throughout its life cycle [31]. Environmental impacts commonly assessed include global warming, eutrophication, acidification, human toxicity, and the depletion of resources [32].

This study used the LCA method for evaluating the global warming potential of the selected fuels. Data on GHG emissions were collected for all processes in the life cycle chains of the fuels (Figure 1),

including extraction and pre-treatment of the raw materials, fuel production, storage and transport and distribution (termed well-to-tank, WTT), and finally, combustion in a dual-fuel marine engine (termed tank-to-propeller, TTP).

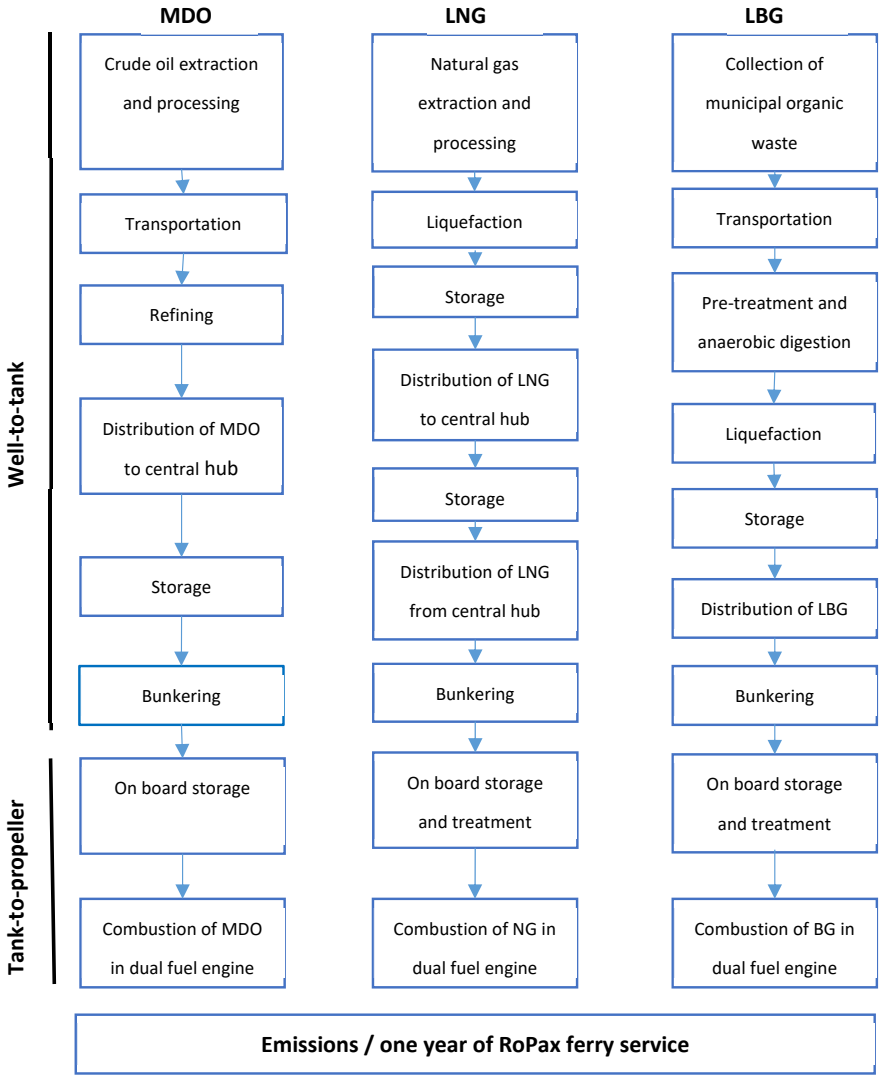

Figure 1. Flowchart of studied fuels and included processes.

The local environmental impacts evaluated in this study include acidification potential, eutrophication potential, formation of particulate matter and human health damage caused by PM_{10}. These impacts were analyzed only for the tank-to-propeller phase. Table 2 outlines the modelling choices made in this study.

Table 2. Modelling choices of the study. Reproduced from [26], VTT Technical Research Centre of Finland: 2019.

Functional unit	One year of RoPax ferry service to and from Vaasa and Umeå
Fuel chains	Marine diesel oil (MDO) 0.1% S Liquefied natural gas (LNG) Liquefied bio-methane (LBG)
Geographical boundaries	The sulfur emission control area (SECA) in the Baltic Sea The NO_x emission control area (NECA) in the Baltic Sea (from 2021)
System boundary	In terms of greenhouse gas (GHG) emissions, the study covers the entire fuel life cycle from the extraction of raw materials to production, distribution, and combustion in a dual-fuel marine engine. Local environmental impacts are evaluated from the termed tank-to-propeller (TTP) perspective, i.e., only the emissions released during vessel operation are taken into account.
Included primary pollutants	GHG • carbon dioxide (CO_2), • methane (CH_4), • nitrous oxide (N_2O)
	Local pollutants • nitrogen oxides (NOx), • sulfur dioxide (SO_2), • particulate matter (PM_{10}) and • ammonia (NH_3)
Impact categories	Global warming potential (GWP_{100})
	Local environmental impacts • acidification potential • eutrophication potential • formation of PM_{10} • human health

3.2. Functional Unit

The functional unit is the reference unit against which life-cycle inventory data is calculated. This reference value is necessary to ensure the comparability of the investigated alternatives [31,32]. The functional unit considered in this study is one year of RoPax ferry operation, including freight and passenger transportation. The average engine load was set to 45%. Engine efficiency at 45% load is 46%. Based on these values and vessel data in Table 1, the annual fuel consumption was calculated to correspond to the energy content of 225 TJ fuel.

3.3. Fuel Chains and Data Sources

3.3.1. MDO Route

The production steps of MDO include drilling and extracting crude oil, pre-treatment, and refining. After refining, MDO is transported on dedicated tankers to a distribution hub and stored prior further distribution. GHG emissions data during well-to-tank for MDO are from Kollamthodi et al. [18].

MDO is combusted in a medium-speed four-stroke engine equipped with SCR after-treatment system, which reduces NO_x emissions by 82% from 9.6 g/kWh (Tier II engine) to 1.73 g/kWh. Urea

dosing for target NO_x conversion was determined based on stoichiometric dosing, assuming 1:2 for urea:NH_3 stoichiometry and 1:1 for NO_x:NH_3 stoichiometry [33,34]:

$$\text{Urea consumption } = \frac{M_{urea}}{2 \cdot M_{NO_2}} \cdot \Delta NO_x \quad (1)$$

Using molar masses 46 g/mole for NO_x and 60 g/mole for urea, we can conclude that 5.1 g pure urea/kWh is needed. This corresponds to 12.8 kg UWS40/MWh (11.7 L/MWh).

For operational emission factors the 3rd IMO Greenhouse Gas Study [35] was used, augmented with data from Brynolf et al. [36]. Ammonia (NH_3) was included in the inventory since the use of urea in SCR may cause ammonia emissions, known as ammonia slip. Ammonia emission factor 0.005 g/MJ fuel was used, corresponding to NH_3 slip just below 10 ppm. Ammonia emissions were calculated by using the equation:

$$EP\left(\frac{\text{g}}{\text{kWh}}\right) = \frac{EV}{10^6} \cdot \frac{M_{NH_3}}{M_{Exh.}} \cdot \dot{m}_{Exh.}\left(\frac{\text{g}}{\text{kWh}}\right), \quad (2)$$

where EP = pollutant mass referenced to output power (g/kWh), EV = exhaust emission value in ppm, M_{NH3} = molecular mass of NH_3 (17.031 g/mole), $M_{Exh.}$ = molecular mass of wet exhaust (28.84 g/mole), and $\dot{m}_{Exh.}$ = exhaust mass flow in g/kWh. For exhaust gas mass flow, the rate 7 kg/kWh was applied.

3.3.2. LNG Route

In this study, natural gas was assumed to be extracted from North Sea and brought to the LNG plant in Norway by subsea pipeline. At the LNG plant the gas first passes through a cleansing process, separating CO_2 and water. Then the gas is cooled to approximately −162 °C to change it into a liquid form. The liquid gas is then transported cryogenically to the central hub in Finland and stored before distribution by road tankers.

GHG emissions data during the well-to-tank phase for LNG are from Edwards et al. [37], with the exception that the assumed shipping distance was reduced from 5500 nautical miles to 2000 nm, and the road transport distance was halved from 500 km to 250 km. The emission factors for the combustion of natural gas were collected from Gilbert et al. [6], Brynolf et al. [21] and Bengtsson et al. [20]. It was assumed an SCR system would not be needed. A methane slip rate of 2%, calculated from Gilbert et al. [6], and a pilot fuel (MDO) rate of 1.4% for ignition were applied.

3.3.3. LBG Route

An LCA study of biogas production systems can be complex. There is a large range of systems to consider, reflecting the great variety of available raw materials (feedstocks), digestion technologies and biogas applications [38]. This study assumed LBG to be produced from anaerobic digestion of locally collected municipal organic waste. Other biomass resources could lead in somewhat different emission profiles. Following anaerobic digestion, the biogas is purified and upgraded to around 97% methane. Then it is liquefied and stored before distribution via cryogenic road tanker to the customer.

Operation of the biogas plant is usually the most energy-intensive part of the process, accounting for 50–80% of the energy input embodied in these products [38]. However, the fossil energy share is moderate, as the biogas produced in the system can be used, for example, in heating processes. A significant source of GHG emissions is through methane leakages. Kollamthodi et al. [18] applied methane leakage of 1.2% for anaerobic digestion and 0.5% for upgrading the biogas to bio-methane, leading to total CO_2-equivalents 21.3 g CO_2-eq./MJ fuel. These values are also used in this study. It should be noted that higher leakage rates associated with, e.g., incomplete processing or inadequate storage would markedly increase total GHG emissions in CO_2-equivalents. For example, methane slippage of 3% from anaerobic digestion would increase CH_4 emissions from this step to 0.6 g CH_4/MJ, leading to total CO_2-equivalents 33.5 g CO_2-eq./MJ during well-to-tank. Therefore, it is extremely important that leakages during the gas processing are carefully prevented and monitored.

Tank-to-propeller emissions data are mainly from Bentgsson et al. [20] and Brynolf et al. [36]. Producing bio-methane from anaerobic digestion of organic waste results in fuels that contain only biogenic carbon. Hence, combustion of bio-derived methane releases only biogenic CO_2 emissions. Biogenic CO_2 emissions are related to the natural carbon cycle, and are not considered to contribute to global warming [18,37]. Dinitrogen oxide (N_2O) emissions were assumed to be the same as in the LNG case. No SCR system was expected to be needed. Methane slip of 2% during the tank-to-propeller phase and a pilot fuel (MDO) rate 1.4% for ignition were applied, also identical to the rates used for LNG.

Table 3 summarizes the emissions to air, divided into well-to-tank and tank-to-propeller phases.

Table 3. Summary of emissions to air from well-to-tank and tank-to-propeller.

	MDO 0.1% S	**LNG**	**LBG**
Net calorific value (MJ/kg)	42.6	48.6	49.3
Well-to-tank GHG-emissions:	g/MJ fuel	g/MJ fuel	g/MJ fuel
CO_2 (fossil)	14.6	10.5	9.7
CH_4	0.021	0.18	0.34
N_2O	<0.001	<0.001	<0.001
Total in CO_2-eq.	15.3	16.6	21.3
	MDO 0.1% S + SCR	LNG	LBG
Emissions to air from the fuel combustion (tank-to-propeller):	g/MJ fuel	g/MJ fuel	g/MJ fuel
CO_2 (fossil)	75	56	1
CO_2 (biogenic)	0	0	54
CH_4	0.0014	0.41	0.41
N_2O	0.0038	0.0022	0.0022
NO_x	0.22	0.17	0.17
SO_2	0.047	0.00056	0.00058
PM_{10}	0.022	0.0043	0.0043
NMVOC	0.059	-	-
NH_3	0.005	-	-

3.4. Impact Categories and Included Primary Pollutants

This study addressed both local pollutants and GHG emissions. Global warming potential (GWP) is used to determine a substance's climate impact. "This is a measure of the effect on radiation of a particular quantity of the substance over time, relative to that of the same quantity of CO_2" [39]. Therefore, GWP depends on the gas's time in the atmosphere and on its capacity to affect radiation [39]. The main GHG from shipping are CO_2, CH_4 and N_2O. All three species are evaluated in this study and total GHG emissions are presented in terms of CO_2-equivalents, using 100-years global warming potential factors of 34 for CH4 and 298 for N_2O [16].

Examples of regional environmental impacts categories include acidification and eutrophication. The primary contributors to acidification are oxides of sulfur (SO_x), nitrogen oxides (NO_x) and ammonia. "In order to describe the acidifying effect of substances, their acid formation potential (ability to form H+ ions) is calculated and set against a reference substance, SO_2" [39]. This produces a measure of their acidification potential, expressed as an SO_2-equivalent (SO_2-eq.) [40]. This study applies SO_2-eq. factors of 0.5 for NOx and 1.6 for NH_3. These values are based on Huijbregts et al. [41], where acidification and terrestrial eutrophication potentials for a number of European regions were determined, taking into account background depositions and ecosystem sensitivities.

Eutrophication refers to the enrichment of nutrients in the ecosystem that cause excessive biomass growth in water or soil, leading to numerous adverse effects such as oxygen depletion in the sea. Eutrophication in marine and terrestrial ecosystems mainly is linked to transformation of NO_x and NH_3 emissions into nitrogen [39]. In this study, NO_x-equivalent (NO_x-eq.) factor 3.7 for NH_3 was used, also based on Huijbregts et al. [41].

Important air pollutants causing human health damage include primary fine particles (PM_{10}), NH_3, NO_x and SO_2 producing inorganic secondary PM_{10} aerosols [42]. Two different evaluation methods were included in this study. First, primary PM_{10} emissions from combustion of selected fuels were calculated (in kg emissions/functional unit) as an indicator for impact on human health. Second, the disability-adjusted life year (DALY) concept was applied as a more specific method for assessing impacts on human life. DALY is a sum of years lost due to illness, disability or early death [40]. It is expressed as the number of years lost per kilogram emission. The characterization factors (Table 4) for health effects of PM, NH_3, NO_x and SO_x emissions are from van Zelm et al. [42].

Table 4. Characterization factors for health effects of PM, NH_3, NOx and SOx.

Emitted Substance	Characterization Factor (Years Lost Per Kg Emission)
NH_3	8.3×10^{-5}
NO_x	5.7×10^{-5}
SO_x	5.1×10^{-5}
PM_{10}	2.6×10^{-4}

4. Results

The main results of the analysis are presented in the following sections. More detailed calculations and complete numerical results are available as Supplementary Materials, Spreadsheet S1, accompanying the online article

4.1. Global Warming Potential

Total GHG emissions from all three species considered (CO_2, CH_4 and N_2O) are presented in terms of CO_2-equivalents, using 100-years global warming potential value 34 for CH_4 and 298 for N_2O.

The dominance analysis (Figure 2) shows where in the life cycle the largest GHG emissions occur. With fossil fuels, MDO and LNG, the TTP phase of the life cycle dominates the global warming impact. Approximately 80% of the total GHG emissions from the whole chain are released during this phase. The analysis for LBG is markedly different, showing very large TTP emissions benefits in the shift from fossil fuel to bio-methane. This difference is due to the biogenic nature of CO_2 emissions from the combustion of renewable fuels. As mentioned above, biogenic CO_2 emissions are not considered to contribute to global warming and are therefore reported as zero from an accounting perspective [18]. LBG's TTP phase GHG emissions mainly are caused by methane slip from the dual-fuel engine, and to a minor extent from fossil CO_2 emissions originating from the MDO pilot fuel. The WTT phase GHG emissions mainly originate from the use of electricity during biogas production and bio-methane liquefaction processes and from methane leakages during anaerobic digestion.

The contribution analysis (Figure 3) shows how the three different climate gases contribute to each fuel's global warming impact. CO_2 is the main contributor to the GWP_{100} for the two fossil fuels, MDO and LNG. The direct life cycle CO_2 emissions from combustion of natural gas are about 25% lower than with MDO. However, much of this benefit is negated due to higher CH_4 emissions when using LNG instead of MDO. Overall, the analysis shows that when assuming 2% methane slip from the dual-fuel engine used for natural gas combustion, the life-cycle climate impact of LNG is slightly lower (5%) than for MDO.

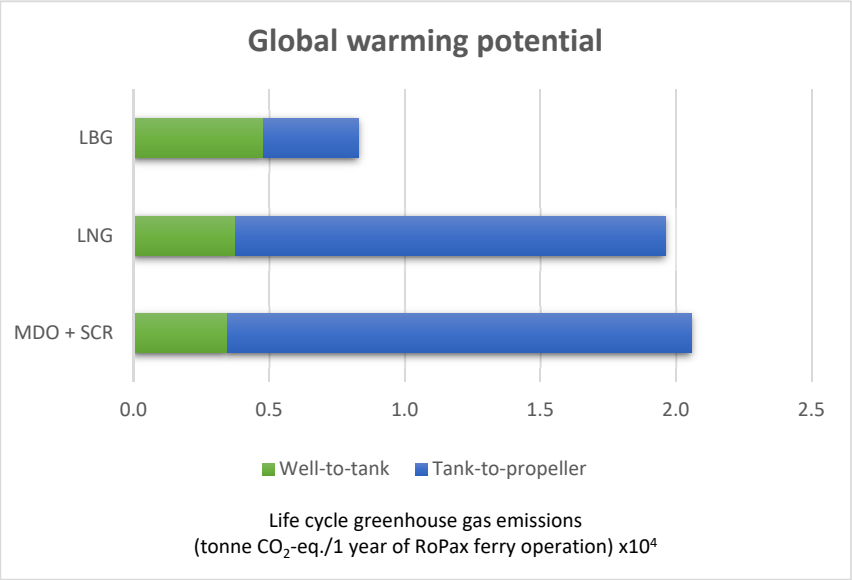

Figure 2. Life cycle GWP_{100} for the compared alternatives divided into well to tank (WTT) and termed tank to propeller (TTP) phases.

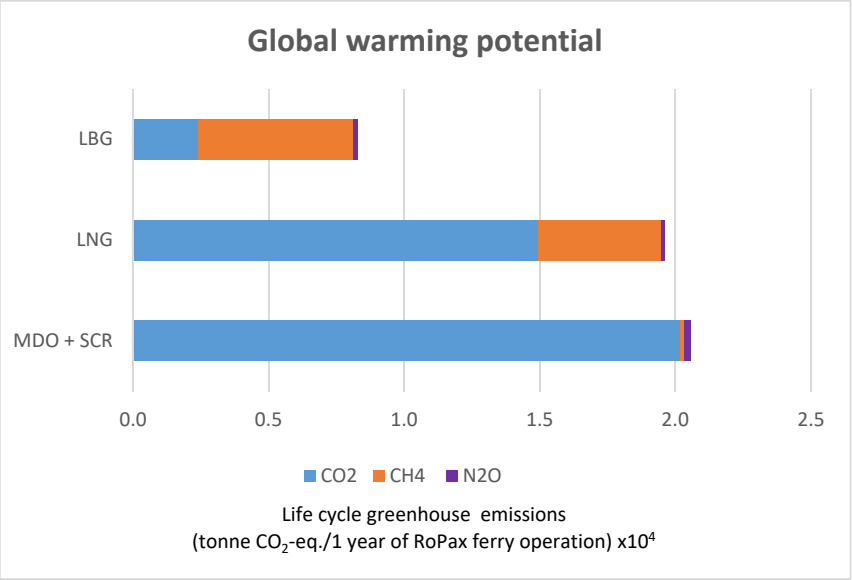

Figure 3. Life cycle GHG emissions for the compared alternatives divided into the different contributing emissions.

The climate impact contribution from CH_4 emissions is significant for both methane-based fuels, LNG and LBG. The methane stems from fugitive leakages in the fuel chain and methane slip from combustion. Well-to-propeller CH_4 emissions for LNG represent 23% of the total life cycle GWP_{100}, and for LBG the CH_4 emissions are 69% of the total life cycle GWP_{100}. Direct CO_2 emissions from LBG originate mainly from biogas production and liquefaction processes, and to a lesser extent from the MDO pilot fuel.

Emissions of N_2O account for less than 2% of the total GWP_{100} of all three fuels in this study, despite its potency as a GHG being assessed as 298 times greater than CO_2.

The contribution analysis indicates clearly that GHG emission impacts of methane-fueled vessels are highly sensitive to the level of methane slip. In Figure 4b, a comparison of life cycle GHG emissions from the three investigated fuel options is presented as a function of methane leakage from the dual-fuel engine.

It shows that with methane slip of approximately 2.5% (4 g CH_4/kWh engine out) during combustion, the life cycle GHG emissions of MDO and LNG use are equal. With zero CH_4 slip from combustion, LNG would give a 20% reduction in total life cycle GHG compared with MDO. This underscores the theoretical potential to decrease the GWP_{100} impact by a fuel switch from MDO to LNG. Conversely, poor control of combustion (CH_4 slip > 2.5%) would result in an increase in LNG GWP_{100} compared with the MDO alternative.

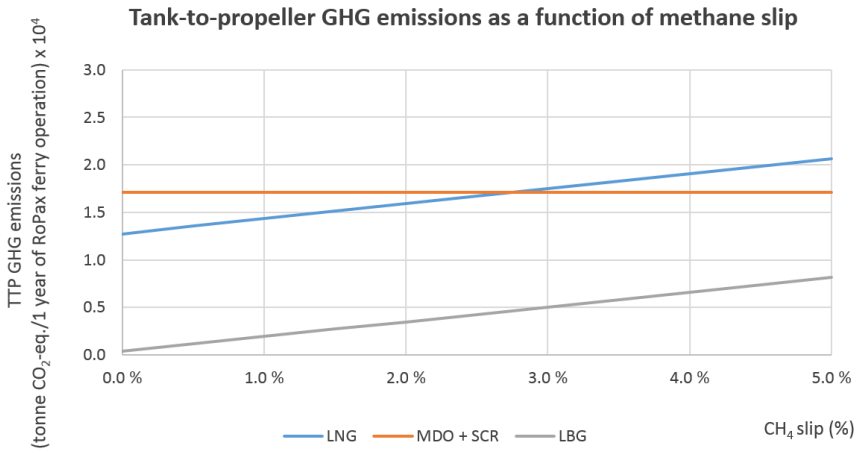

(**a**)

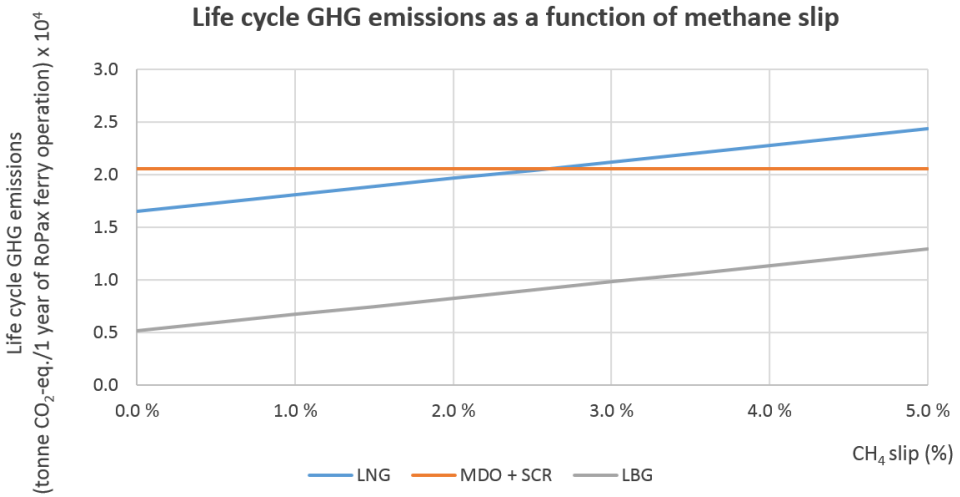

(**b**)

Figure 4. (**a**) Tank-to-propeller and (**b**) life cycle GHG emissions (in metric tons CO_2-eq./year) as a function of CH_4 slip from the dual-fuel engine.

In Figure 4a, only tank to propeller GHG emissions are considered. It shows that annual TTP GHG emissions from an LNG vessel with zero methane slip during combustion would be 26% lower than those from MDO-fueled vessels.

LBG significantly lowers GHG emissions on both life cycle and tank-to-propeller measures. With assumed zero CH_4 slip, LBG would cut life cycle GHG emissions by 75% and TTP GHG emissions by 98% compared to MDO.

4.2. Local Environmental Impacts

All emissions analyzed here result from fuel combustion. The results are presented in Figure 5. Two clear trends can be seen. First, MDO has a higher contribution than gaseous fuels across all four impact categories. Secondly, local environmental impacts are closely related to nitrogen oxide emissions. The two gaseous fuels, LNG and LBG, produce comparable NO_x emissions. Even with the benefit of SCR's proven NO_x reduction, MDO cannot match the two gaseous fuels. Potential ammonia slip from the SCR system's urea also adds a further small increase to human health damage and to acidification and eutrophication potentials in the case of MDO + SCR.

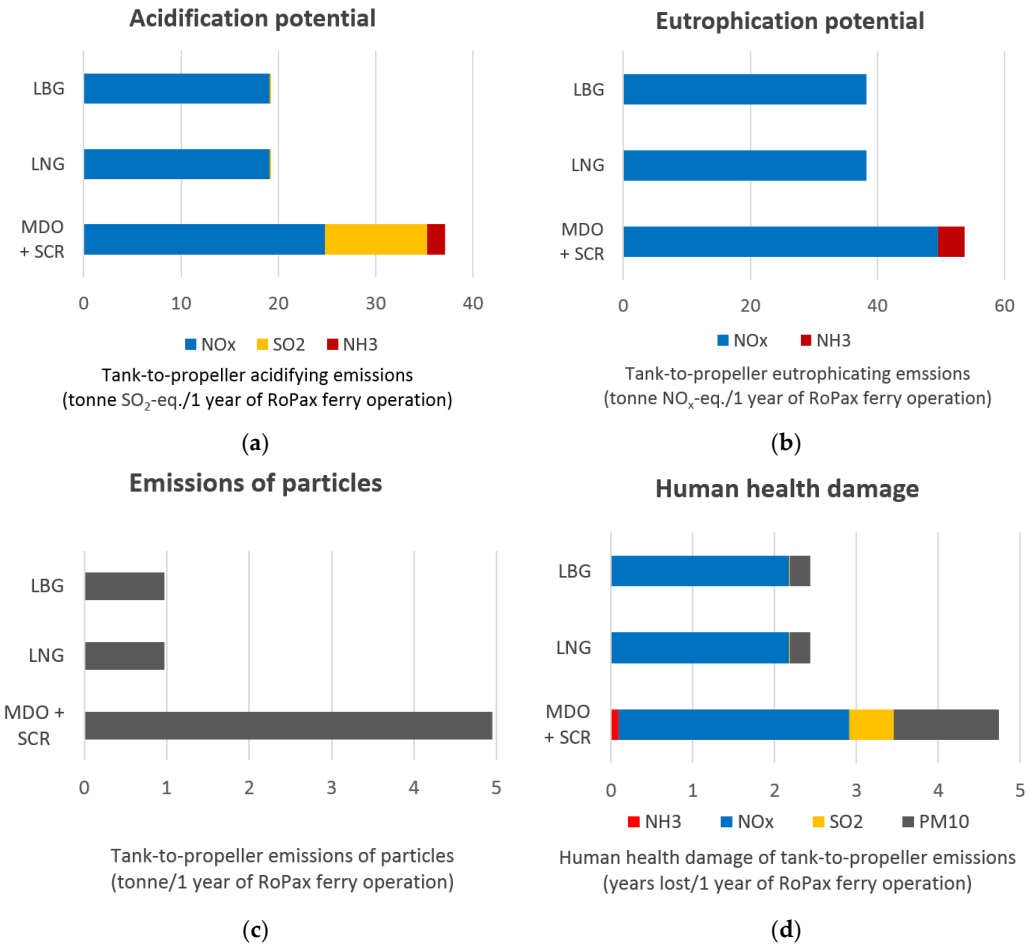

Figure 5. Tank-to-propeller (**a**) acidifying and (**b**) eutrophying emissions, (**c**) formation of primary particulate matter (in metric ton/year), and the impact of emissions on (**d**) human health.

MDO 0.1% S is a low-sulfur option to standard heavy fuel oil but the SO_2 produced in its combustion is still a major addition to this fuel's acidifying potential compared to LNG and LBG.

MDO's total acidifying emissions are almost double those of the other two fuels. MDO also produces the highest PM emissions: particulates from LNG and LBG are approximately 80% lower. This is due to the gaseous fuels' low sulfur content and simple fuel molecule, which burns with low soot and PM formation [43].

The impact category for human health damage identifies the relative contributions of NO_x, SO_2 and NH_3 emissions, plus directly emitted particles. Human health damage in terms of years lost due to illness, disability or early death for each year of RoPax ferry operation nearly doubles (from 2.4 to 4.7 years) with MDO compared to LNG or LBG.

4.3. Economic Aspects

Figure 6 deals with marine fuel prices, giving an overview of the price development for natural gas and low-sulfur MDO/MGO. The price data refers to lower heating values, so the gas prices are about 10% higher than the figures commonly used in the gas industry that relate to the upper heating value [44]. The gas price does not include liquefaction.

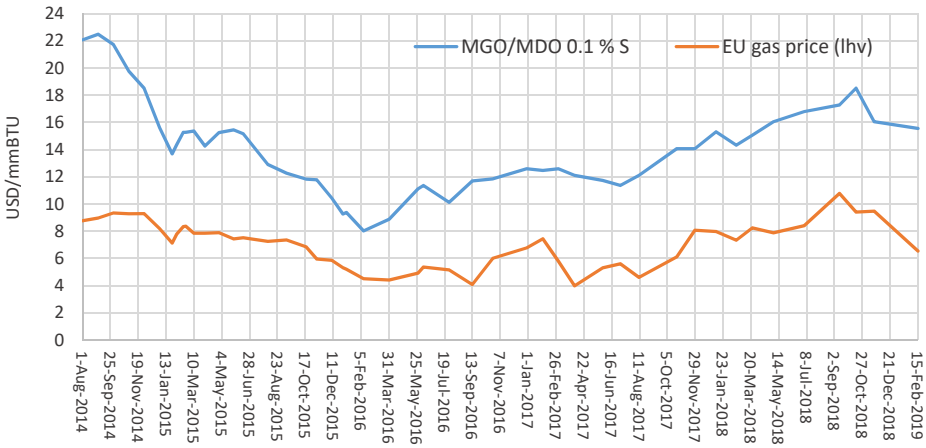

Figure 6. Price development for natural gas and ultra low sulfur MGO/MDO. The price data are retrieved from DNV GL [44]; 1 mmBTU energy equals 1055 MJ in energy; 10 USD/mmBTU is equivalent to approx. 30 EUR/MWh.

Unlike conventional marine fuel oil, LNG has no global bunker prices. LNG price is generally tied to European pipeline gas prices, supplemented by the additional costs of liquefaction and logistics [45]. This study uses \$3/mmBTU (2.50 €/GJ) as the cost for liquefaction [44]. Price statistics for LBG in maritime transportation were not found on literature. Information on LBG price was obtained from North European Oil Trade (NEOT); the current price of LBG is 80–90 €/MWh [46].

Based on the above information and fuel prices in February 2019, the prices used in this study were:

- MDO 0.1% S: 554 EUR/t (13.00 EUR/GJ)
- LNG: 389 EUR/t (8.00 EUR/GJ)
- LBG: 1080 EUR/t (22.00 EUR/GJ)

In the case of MDO, the SCR after-treatment system incurs additional operating costs. This study assumes SCR operation and maintenance cost to be 5.55 EUR/MWh, as indicated by Campling et al. [47]. The major operating cost is that of the reducing agent, UWS40. The SCR maintenance procedures include regular cleaning by compressed air to reduce fouling of the catalyst surfaces and gas passages. The urea handling system's filters and injection nozzles also need regular cleaning. The catalyst has a finite life, so the maintenance regime should include periodic analysis of catalyst activity. Typical lifespans for catalyst

blocks are between two and five years, with replacement undertaken by SCR suppliers or authorized contractors [48]. The cost of replacement catalysts can be considered an operating cost.

An SCR after-treatment system can increase exhaust backpressure, typically by around 12–15 mbar at 100% engine load [49]. Any fuel penalties that may arise due to this slight increase in backpressure were not included in this study.

Operational costs per functional unit (1 year of RoPax ferry operation) are presented in Table 5. Only fuel costs and SCR operation and maintenance costs are included. Fuel costs do not include the cost of final delivery to the ship.

Table 5. Operational costs/one year of RoPax ferry service.

Cost	MDO 0.1% S	LNG	LBG
Fuel	2,925,000 €	1,800,000 €	4,950,000 €
SCR O&M	159,563 €	-	-
Total	3,084,563 €	1,800,000 €	4,950,000 €

The SCR system's capital cost is not included in the cost matrix. An SCR system, including installation, costs between 50 and 65 EUR/kW [49,50].

Based on above, there is a strong economic argument for LNG in shipping compared to the other two investigated alternatives. Without taxation or subsidies, LBG will find it difficult to compete with the prices of fossil fuels.

5. Discussion

5.1. Environmental Performance

All three options studied are in compliance with the most stringent ECA regulations currently in force or entering into force from 2021. Still, in terms of local environmental impacts, the two gaseous fuels had clear advantages over the MDO + SCR combination. In addition to reduced emissions of acidifying and eutrophying pollutants into the ecosystem, clear health benefits were found associated, e.g., with substantially reduced PM emissions. Reducing particulate emissions can also have short-term climate benefits. For example, Kandlikar et al. [51] found that black carbon—one of the components in PM—could be responsible for about 15 percent of current global warming. Lower PM emissions also facilitate compliance with possible future PM regulations. PM emissions for international shipping currently are regulated only indirectly, by means of limiting sulfur level in fuels. However, quantitative emissions standards for PM already have been incorporated in Euro standards for inland waterway vessels [52] and other non-road machinery. Therefore, new regulations for PM emissions in international shipping may be expected. In this case, specific PM abatement technology would be required for engines running on MDO.

Moreover, concerns about climate change and security of supply of fossil fuels are driving interest in alternative ship fuels. A shift from marine diesel oil to LNG leads to significantly reduced particulate matter, SO_2 and NO_x emissions, so it is unsurprising that these local environmental benefits are generating substantial interest in LNG as a marine fuel. However, progress towards decarbonization and cutting GHG emissions appears more difficult. Life cycle CO_2 emissions of LNG are about 25% lower than with marine diesel oil, but the case for LNG as a marine fuel is less persuasive in terms of total emissions of CO_2-equivalents. The overall greenhouse gas impact of LNG depends to a large extent on the amount of methane leaks in LNG production and distribution, and in particular, on the methane slip from fuel combustion. Already, 2.5% methane slip from LNG combustion negates the benefit of reduced CO_2 emissions, leading to global warming potential equal to diesel fuel. It, therefore, appears that natural gas currently does not provide the significant reduction in CO_2-equivalents needed to achieve the IMO's ambitious GHG reduction target. This conclusion is consistent with previous studies [3,6,36,53,54]. This underlines the importance of controlling methane emissions from engines.

If a methane slip could be minimized to near-zero level, by emissions regulations and technology development, life cycle GHG savings of 20% versus MDO would be possible.

To meet IMO's goal on decarbonization of shipping is a huge challenge. The active uptake of alternative low-carbon and zero-carbon fuels is needed to meet this target [27,53]. This study demonstrates significant life-cycle GHG emission benefits by replacing fossil fuels with bio-methane; in terms of CO_2-equivalent, the reduction is 58% compared to LNG, and 60% compared to MDO.

5.2. Fuel Availability

Availability of LNG in Finland is good. For example, the most effective way today for the forthcoming RoPax vessel in the case study would be to deliver LNG to the ship while in port in Vaasa by tanker truck from Pori LNG terminal. There is also a new LNG terminal in Tornio. Estimated LNG consumption for the Vaasa-Umeå route is 4600 tons/year, equating to four to five tanker truckloads per week, 20 tons/delivery. The truck-to-ship bunkering (Figure 7) time is less than two hours for each delivery [45].

Figure 7. Truck-to-ship bunkering in the Port of Helsinki.

Availability of LBG is limited at present, but growing. For example, during 2019 Gasum (Espoo, Finland) is expanding its biogas production in Turku and also adding a bio-methane liquefaction plant on the site. In Sweden, Gasum delivers LBG from the company's Lidköping biogas facility. The first supply of LBG to a marine customer was in 2018, delivered to Swedish shipping line Furetank's chemical tanker M/T Fure Vinga. Furthermore, in October 2018 Gasum announced it is cooperating with Stora Enso in the construction of a biogas plant, including upgrading and liquefaction, at Stora Enso's Nymölla paper mill in Sweden. The Nymölla plant is scheduled to start operations in 2020, with LBG production projected to be 220 MWh per day [55]. Gasum and other industry players are also working on LBG projects not yet in the public domain [45]. All this activity confirms that LBG will available to a greater extent by 2021 when the new Vaasa-Umeå vessel comes into service.

Today, the greatest challenge facing LBG is fuel availability in the volumes needed for shipping [27, 56]. The adoption of biofuels on the market is, however, also possible by blending biofuels with fossil-based fuels [4]. LBG is perfectly suitable for blending with LNG and can be mixed with LNG with any desired ratio [45]. So far, LNG provides a bridge technology to a lower carbon shipping. Having infrastructure already in place enables a smooth transition to LBG in the long term.

5.3. Recommendations

The main barriers to the deployment of bio-methane in short sea shipping identified in this study are (1) the limited availability of the fuel and (2) the large price gap between bio-methane and fossil

fuels. A major policy push is needed to address these barriers. Eliminating fossil fuel subsidies and implementing carbon pricing could be important measures to increase the competitiveness of low-carbon renewable fuels [57]. The two basic ways to implement carbon pricing are via a carbon tax or an emission-trading scheme [58]. Moreover, specific blending mandates could guarantee the demand for renewable fuels and secure the necessary investments [57]. Despite the global nature of the shipping industry and the need for global regulation, there is also room for national regulations and initiatives to promote carbon-free shipping [58]. Many innovations depend on favorable national and local conditions and policies. Regulatory actions may also be required to reduce methane slip emissions in the coming years.

This study covers the environmental impacts of fuel choices for short sea shipping from local to global impacts, economic aspects, and prospects for fuel availability. The study provides important information for decision-makers and local authorities to support and promote the shift to more sustainable energy sources in short sea shipping. The research also provides relevant information for ship-owners, who play an important role here. The economic part of the study could be further developed by including various fuel price scenarios.

Adopting LBG into business is not simple or risk-free: it requires not only significant investments but also changes in existing practices and business models and the establishment of business relationships with new players. These factors raise many questions and create uncertainty. Further research is needed to identify which market dialogue mechanisms would support the deployment of bio-methane in short sea shipping. Local actors would also benefit from feasibility studies related to the establishment of new regional biogas/LBG infrastructure. Thorough investigations of market sizes and market development, investment costs, risks, and profitability margins play a crucial role in investment decisions.

6. Conclusions

Environmental concerns and new emissions regulations for shipping are the main drivers behind the introduction of alternative marine fuels. Today, the global environmental agenda is increasingly shifting to focus on climate change. In addition, tackling local air pollutants remains an important issue, especially for short sea shipping operations near coastal marine environment and residential areas.

This paper has given a detailed emission analysis for three marine fuel alternatives. The study also addressed economic aspects and prospects for fuel availability. The main findings were:

- In terms of local environmental impacts, both gaseous fuels had clear advantages over the MDO + SCR combination, but LNG is not the solution for decarbonizing shipping.
- Achieving IMO's ambitious GHG reduction target seems possible only with the transition towards low-carbon and zero-carbon fuels.
- Replacing fossil fuels with bio-methane produced from organic municipal waste showed 60% life cycle GHG benefits compared with marine diesel oil.
- The most significant challenge facing LBG today is fuel availability in volumes needed for shipping.
- LNG can provide a bridge technology to a lower carbon shipping. Having infrastructure already in place enables a smooth transition to LBG in the long term.
- For now, there is also a strong economic argument for LNG in shipping. Without taxation or subsidies, LBG will find it difficult to compete with the prices of fossil fuels.
- Eliminating fugitive methane emissions and methane slip will be an important technology development topic for the coming decade.

Supplementary Materials: The following is available online at http://www.mdpi.com/2571-8797/2/1/4/s1. Spreadsheet S1: Calculations and complete numerical results.

Author Contributions: Conceptualization, K.S.-T.; funding acquisition, S.N.; investigation, K.S.-T.; project administration, S.N.; supervision, S.N.; writing–original draft, K.S.-T.; writing—review and editing, K.S.-T. and S.N. All authors have read and agree to the published version of the manuscript.

Funding: This work is part of the INTENS (Integrated Energy Solutions to Smart and Green Shipping) project, Task 3.3.5 'Emission reduction by biogas use'. The authors would like to express their gratitude to Business Finland for funding support, grant number 7889/31/2017.

Acknowledgments: We acknowledge Wasaline for allowing use of its ferry traffic for the case study. The authors would also like to express their gratitude to Tommy Mattila from Gasum for his assistance in determining LNG and LBG availability.

Conflicts of Interest: The authors have no conflicts of interest to declare.

References

1. HELCOM; Baltic Marine Environment Protection Commission. Cleaner Exhaust Gases from Baltic Shipping—The New NECA Regulations. HELCOM 2017. Available online: http://www.helcom.fi/Lists/Publications/Baltic%20Sea%20NECA%20-%20Cleaner%20Exhaust%20Gases%20from%20Baltic%20Shipping.pdf (accessed on 28 February 2019).
2. International Maritime Organization; Marine Environment Protection Committee. *Designation of the Baltic Sea and the North Sea Emission Control Areas for NOx Tier III Control*; MEPC 71/17/Add.1, Annex 1, Resolution MEPC.286(71); International Maritime Organization: London, UK, 2017.
3. Bengtsson, S.; Andersson, K.; Fridell, E. A comparative life cycle assessment of marine fuels: Liquefied natural gas and three other fossil fuels. *J. Eng. Marit. Environ.* **2011**, *225*, 97–110. [CrossRef]
4. Winnes, H.; Styhre, L.; Fridell, E. Reducing GHG emissions from ships in port areas. *Res. Transp. Bus. Manag.* **2015**, *17*, 73–82. [CrossRef]
5. International Maritime Organization; Marine Environment Protection Committee. *Initial IMO Strategy on Reduction of GHG Emissions from Ships*; MEPC 72/17/Add.1, Annex 11, Resolution MEPC.304(72); International Maritime Organization: London, UK, 2018.
6. Gilbert, P.; Walsh, C.; Traut, M.; Kesieme, U.; Pazouki, K.; Murphy, A. Assessment of full life-cycle air emissions of alternative shipping fuels. *J. Clean. Prod.* **2018**, *172*, 855–866. [CrossRef]
7. Burel, F.; Taccani, R.; Zuliani, N. Improving sustainability of maritime transport through utilization of Liquefied Natural Gas (LNG) for propulsion. *Energy* **2013**, *57*, 412–420. [CrossRef]
8. Seddiek, I.B.; Elgohary, M.M. Eco-friendly selection of ship emissions reduction strategies with emphasis on SOx and NOx emissions. *Int. J. Nav. Archit. Ocean Eng.* **2014**, *6*, 737–748. [CrossRef]
9. Verbeek, R.; Kadijk, G.; Menscli, P.V.; Wulffers, C.; Beemt, B.; Fraga, F. *Environmental and Economic Aspects of Using LNG as a Fuel for Shipping in The Netherlands*; Report No. 2011-00166; The Netherlands Organisation for Applied Scientific Research: The Hague, The Netherlands, 2011.
10. Woodyard, D. *Pounder's Marine Diesel Engines and Gas Turbines*, 9th ed.; Butterworth-Heinemann: Oxford, UK, 2009; ISBN 978-0-7506-8984-7.
11. Aakko-Saksa, P.; Lehtoranta, K. *Ship Emissions in the Future—Review*; VTT Research Report; No. VTT-R-00335-19; VTT Technical Research Centre of Finland: Espoo, Finland, 2019.
12. Anderson, M.; Salo, K.; Fridell, E. Particle-and Gaseous Emissions from an LNG Powered Ship. *Environ. Sci. Technol.* **2015**, *49*, 12568–12575. [CrossRef] [PubMed]
13. Lehtoranta, K.; Aakko-Saksa, P.; Murtonen, T.; Vesala, H.; Ntziachristos, L.; Rönkkö, T.; Karjalainen, P.; Kuittinen, N.; Timonen, H. Particulate Mass and Nonvolatile Particle Number Emissions from Marine Engines Using Low-Sulfur Fuels, Natural Gas, or Scrubbers. *Environ. Sci. Technol.* **2019**, *53*, 3315–3322. [CrossRef] [PubMed]
14. Li, J.; Wu, B.; Mao, G. Research on the Performance and Emission Characteristics of the LNG-Diesel Marine Engine. *J. Nat. Gas Sci. Eng.* **2015**, *27*, 945–954. [CrossRef]
15. Bengtsson, S.; Fridell, E.; Andersson, K. Fuels for short sea shipping: A comparative assessment with focus on environmental impact. *J. Eng. Marit. Environ.* **2014**, *228*, 44–54. [CrossRef]
16. Myhre, G.; Shindell, D.; Bréon, F.-M.; Collins, W.; Fuglestvedt, J.; Huang, J.; Koch, D.; Lamarque, J.-F.; Lee, D.; Mendoza, B.; et al. Anthropogenic and Natural Radiative Forcing. In *Climate Change 2013: The Physical Science Basis. Contribution of Working Group I to the Fifth Assessment Report of the Intergovernmental Panel on Climate Change*; Stocker, T.F., Qin, D., Plattner, G.-K., Tignor, M., Allen, S.K., Boschung, J., Nauels, A., Xia, Y., Bex, V., Midgley, P.M., Eds.; Cambridge University Press: Cambridge, UK; New York, NY, USA, 2013; pp. 659–740.

17. Corbett, J.J.; Thomson, H.; Winebrake, J.J. *Methane Emissions from Natural Gas Bunkering Operations in the Marine Sector: A Total Fuel Cycle Approach*; U.S. Department of Transportation, Maritime Administration: Washington, DC, USA, 2015.
18. Kollamthodi, S.; Norris, J.; Dun, C.; Brannigan, C.; Twisse, F.; Biedka, M.; Bates, J. *The Role of Natural Gas and Biomethane in the Transport Sector: Final Report*; Ricardo Energy & Environment: Harwell, UK, 2016.
19. Lowell, D.; Wang, H.; Lutsey, N. *Assessment of the Fuel Cycle Impact of Liquefied Natural Gas as Used in International Shipping*; ICCT White Paper; The International Council on Clean Transportation: Washington, DC, USA, 2013.
20. Bengtsson, S.; Fridell, E.; Andersson, K. Environmental assessment of two pathways the use of biofuels in shipping. *Energy Policy* **2012**, *44*, 451–463. [CrossRef]
21. Brynolf, S.; Fridell, E.; Andersson, K. Environmental assessment of marine fuels: Liquefied natural gas, liquefied biogas, methanol and bio-methanol. *J. Clean. Prod.* **2014**, *74*, 86–95. [CrossRef]
22. Gasser, T.; Peters, G.P.; Fuglestvedt, J.S.; Collins, W.J.; Shindell, D.T.; Ciais, P. Accounting for the climate—Carbon feedback in emission metrics. *Earth Syst. Dyn.* **2017**, *8*, 235–253. [CrossRef]
23. IPCC. *Climate Change 2007: The Physical Science Basis. Working Group I Contribution to the Fourth Assessment Report of the Intergovernmental Panel on Climate Change*; Solomon, S., Qin, D., Manning, M., Chen, Z., Marquis, M., Averyt, K.B., Tignor, M., Miller, H.L., Eds.; Cambridge University Press: Cambridge, UK, 2007; p. 996.
24. Levasseur, A.; Cavalett, O.; Fuglestvedt, J.S.; Gasser, T.; Johansson, D.J.A.; Jørgensen, S.V.; Raugei, M.; Reisinger, A.; Schivley, G.; Strømman, A.; et al. Enhancing life cycle impact assessment from climate science: Review of recent findings and recommendations for application to LCA. *Ecol. Indic.* **2016**, *71*, 163–174. [CrossRef]
25. Gillet, N.P.; Matthews, H.D. Accounting for carbon cycle feedbacks in a comparison of the global warming effects of greenhouse gases. *Environ. Res. Lett.* **2010**, *5*. [CrossRef]
26. Spoof-Tuomi, K.; Niemi, S. Emission reduction by biogas use in short sea shipping. In *Integrated Energy Solutions to Smart and Green Shipping, Proceedings of the INTENS Public Project Seminar, Espoo, Finland, 13 March 2019*; Zou, G., Ed.; VTT Technical Research Centre of Finland: Espoo, Finland, 2019; pp. 18102–18106.
27. DNV, GL. *Assessment of Selected Alternative Fuels and Technologies*; DNV GL: Oslo, Norway, 2019.
28. Dominguez, J. *LNG Blue Corridors—Liquefied Biomethane Experiences*; The Seventh Framework Programme; Deliverable No. D3.6; European Commission: Brussels, Belgium, 2014.
29. Strauch, S.; Krassowski, J.; Singhal, A. *Biomethane Guide for Decision Makers—Policy Guide on Biogas Injection into the Natural Gas Grid*; Project Green Gas Grids WP 2/D 2.3; Fraunhofer UMSICHT: Oberhausen, Germany, 2013.
30. Life Cycle Assessment (LCA). European Commission, LIFE Programme. EU LIFE04 ENV/GR/110. Available online: http://www.ecoil.tuc.gr/LCA-2.pdf (accessed on 1 March 2019).
31. International Organization for Standardization. *Environmental Management—Life Cycle Assessment—Principles and Framework*; ISO: Geneva, Switzerland, 2006.
32. Rebitzer, G.; Ekvall, T.; Frischknecht, R.; Hunkeler, D.; Norris, G.; Rydberg, T.; Schmidt, W.-P.; Suh, S.; Weidema, B.P.; Pennington, D.W. Life cycle assessment Part 1: Framework, goal and scope definition, inventory analysis, and applications. *Environ. Int.* **2004**, *30*, 701–720. [CrossRef] [PubMed]
33. Prieto, G.; Iitsuka, Y.; Yamauchi, H.; Mizuno, A.; Prieto, O.; Gay, C.R. Urea in Water-in-Oil Emulsions for Ammonia Production. *Int. J. Plasma Environ. Sci. Technol.* **2009**, *3*, 54–60.
34. Willems, F. *Modeling & Control of Diesel Aftertreatment Systems*; TNO-TU/e-LiU Course; Linköping University: Linköping, Sweden, 2015.
35. Smith, T.W.P.; Jalkanen, J.P.; Anderson, B.A.; Corbett, J.J.; Faber, J.; Hanayama, S.; O'Keeffe, E.; Parker, S.; Johansson, L.; Aldous, L.; et al. *Third IMO GHG Study 2014*; International Maritime Organization (IMO): London, UK, 2015.
36. Brynolf, S.; Magnusson, M.; Fridell, E.; Andersson, K. Compliance possibilities for the future ECA regulations through the use of abatement technologies or change of fuels. *Transp. Res.* **2014**, *28*, 6–18. [CrossRef]
37. Edwards, R.; Larivé, J.F.; Rickeard, D.; Weindorf, W. *JEC Well-to-Wheels Analysis: Well-to-Wheels Analysis of Future Automotive Fuels and Powertrains in the European Context*; Well-to-Tank Report Version 4.0; JRC Technical Reports; Publications Office of the European Union: Brussels, Belgium, 2013. [CrossRef]

38. Berglund, M.; Börjesson, P. Assessment of energy performance in the life-cycle of biogas production. *Biomass Bioenergy* **2006**, *30*, 254–266. [CrossRef]
39. Environmental Impacts Analysed and Characterisation Factors. A Study to Examine the Costs and Benefits of the ELV Directive—Final Report Annexes, Annex 5. GHK in Association with Bio Intelligence Service 2006. Available online: https://ec.europa.eu/environment/waste/pdf/study/annex5.pdf (accessed on 5 March 2019).
40. Keoleian, G.A.; Spitzley, D.V. Life Cycle Based Sustainability Metrics. In *Sustainability Science and Engineering—Defining Principles*; Abraham, M.A., Ed.; Elsevier B.V.: Amsterdam, The Netherlands, 2006; pp. 127–160. ISBN 978-0444517128.
41. Huijbregts, M.A.J.; Schöpp, W.; Verkuijlen, E.; Heijungs, R.; Reijnders, L. Spatially explicit characterization of acidifying and eutrophying air pollution in life-cycle assessment. *J. Ind. Ecol.* **2000**, *4*, 75–92. [CrossRef]
42. Van Zelm, R.; Huijbregts, M.A.J.; den Hollander, H.A.; van Jaarsveld, H.A.; Sauter, F.J.; Struijs, J.; van Wijnen, H.J.; van de Meent, D. European characterization factors for human health damage of PM10 and ozone in life cycle impact assessment. *Atmos. Environ.* **2008**, *42*, 441–453. [CrossRef]
43. Stenersen, D.; Thonstad, O. *GHG and NOx Emissions from Gas Fueled Engines—Mapping, Verification, Reduction Technologies*; SINTEF Report No. OC2017 F-108, Version 3.0; SINTEF Ocean AS: Trondheim, Norway, 2017.
44. DNV, GL. LNG as Ship Fuel. Current Price Development Oil and Gas. Available online: https://www.dnvgl.com/maritime/lng/current-price-development-oil-and-gas.html (accessed on 1 March 2019).
45. Mattila, T.; (Skangas, Göteborg, Sweden). Personal communication, 2018.
46. Hellman, R.; (North European Oil Trade Oy NEOT, Helsinki, Finland). Personal communication, 2019.
47. Campling, P.; Janssen, L.; Vanherle, K.; Cofala, J.; Heyes, C.; Sander, R. *Final Report: Specific Evaluation of Emissions from Shipping including Assessment for the Establishment of Possible New Emission Control Areas in European Seas*; VITO Vision on Technology: Mol, Belgium, 2013.
48. Lloyd's Register. *Your Options for Emissions Compliance. Guidance for Shipowners and Operators on the Annex VI SOx and NOx Regulations*; Lloyd's Register: London, UK, 2015.
49. Fathom. *The Ship Operator's Guide to NOx Reduction*; Macdonald, F., Rojon, I., Austin, C., Eds.; Fathom Maritime Intelligence: Windsor, UK, 2015; ISBN 978-0-9932678-8-8.
50. Bachér, H.; Albrecht, P. *Evaluating the Costs Arising from New Maritime Environmental Regulations*; Transport Safety Agency Trafi: Helsinki, Finland, 2013; ISBN 978-952-5893-89-2.
51. Kandlikar, M.; Reynolds, C.C.O.; Grieshop, A.P. *A Perspective Paper on Black Carbon Mitigation as a Response to Climate Change*; Copenhagen Consensus Center Report; Copenhagen Consensus Center: Copenhagen, Denmark, 2009.
52. European Union. *Regulation (EU) 2016/1628 of the European Parliament and of the Council of 14 September 2016 on Requirements Relating to Gaseous and Particulate Pollutant Emission Limits and Type-Approval for Internal Combustion Engines for Non-Road Mobile Machinery, Amending Regulations (EU) No 1024/2012 and (EU) No 167/2013, and Amending and Repealing Directive 97/68/EC*; EU: Brussels, Belgium, 2016.
53. Baresic, D.; Smith, T.; Raucci, K.; Rehmatulla, C.; Narula, N.; Rojon, I. *LNG as a Marine Fuel in the EU: Market, Bunkering Infrastructure Investments and Risks in the Context of GHG Reductions*; UMAS: London, UK, 2018.
54. Verbeek, R.; Verbeek, M. *LNG for Trucks and Ships: Fact Analysis. Review of Pollutant and GHG Emissions*; TNO Report 2014 R11668; The Netherlands Organisation for Applied Scientific Research: The Hague, Netherlands, 2015.
55. Gasum. About Gasum. For the Media. News. Available online: https://www.gasum.com/en/About-gasum/for-the-media/News/2018/circular-economy-cooperation-with-stora-enso-gasum-to-produce-biogas-from-waste-waters-at-nymolla-mill/ (accessed on 15 December 2018).
56. Florentinus, A.; Hamelinck, C.; van der Bos, A.; Winkel, R.; Cuijpers, M. *Potential of Biofuels for Shipping—Final Report*; European Maritime Safety Agency (EMSA): Lisbon, Portugal, 2011.
57. IRENA; IEA; REN21. *Renewable Energy Policies in a Time of Transition*; IRENA: Abu Dhabi, United Arab Emirates; OECD/IEA: Paris, France; REN21: Paris, France, 2018; ISBN 978-92-9260-061-7.
58. International Transport Forum. *Decarbonising Maritime Transport. Pathways to Zero-Carbon Shipping by 2035*; Case-Specific Policy Analysis; OECD: Paris, France, 2018.

clean technologies

MDPI

Article

Real-Driving Emissions of an Aging Biogas-Fueled City Bus

Kirsi Spoof-Tuomi [1,*], Hans Arvidsson [2], Olav Nilsson [1] and Seppo Niemi [1]

[1] School of Technology and Innovations, University of Vaasa, Box 700, FI-65101 Vaasa, Finland
[2] RISE Research Institutes of Sweden, Box 5053, SE-90403 Umeå, Sweden
* Correspondence: kirsi.spoof-tuomi@uwasa.fi

Abstract: Transition to low emission transportation and cleaner cities requires a broad introduction of low- and zero-carbon alternatives to conventional petrol- and diesel-powered vehicles. New-generation gas buses are a cost-effective way to reduce local air pollutants from urban transportation. Moreover, major greenhouse gas (GHG) savings may be achieved using biogas as the power source. The main objective of this research was to investigate CH_4 and other gaseous emissions of a biogas-fueled urban bus equipped with a three-way catalyst (TWC) in real-world conditions. The study focused on emissions from a six-year-old gas-powered city bus, supplementing emission data from aging bus fleets. Impaired CH_4 oxidation and NO_x reduction were observed in the catalyst after its service life of 375,000 km–400,000 km. The main reason for low CH_4 and NO_x conversion over the TWC was concluded to be the partial deactivation of the catalyst. Another critical issue was the fluctuating air-to-fuel ratio. The results show that the efficiency of exhaust after-treatment systems should be closely monitored over time, as they are exposed to various aging processes under transient driving conditions, leading to increased real-world emissions. However, the well-to-wheels (WTW) analysis showed that an 80% GHG emission benefit could be achieved by switching from diesel to biomethane, giving a strong environmental argument for biogas use.

Keywords: real-driving emission; portable emission measurement system; Euro VI; urban bus; catalyst deactivation; compressed biogas; well-to-wheels analysis

Citation: Spoof-Tuomi, K.; Arvidsson, H.; Nilsson, O.; Niemi, S. Real-Driving Emissions of an Aging Biogas-Fueled City Bus. *Clean Technol.* **2022**, *4*, 954–971. https://doi.org/10.3390/cleantechnol4040059

Academic Editors: Dong Li, Fuqiang Wang, Zhonghao Rao and Chao Shen

Received: 27 July 2022
Accepted: 22 September 2022
Published: 2 October 2022

1. Introduction

There is a worldwide consensus that significant reductions in greenhouse gas (GHG) emissions are needed to avoid the worst impacts of climate change, and various laws and regulations have already been implemented to combat and respond to global warming. In July 2021, the European Commission adopted an extensive legislative package, Fit for 55, with the goal of reducing the economy-wide GHG emissions by at least 55% by 2030 compared to 1990 levels [1]. This is a substantial increase from the previous 40% target. Achieving the 55% reduction in GHG emissions over the next decade is crucial for Europe to achieve climate neutrality by 2050. Moreover, Finland has set itself the goal of becoming carbon neutral by 2035 [2]. This is one of the most ambitious targets of any country in the industrialized world.

In 2019, GHG emissions from domestic transportation accounted for 21 percent of Finland's total greenhouse gas emissions and about 30 percent of the energy sector's GHG emissions [3]. Road transportation is likely to remain a significant contributor to air pollution in the coming decades, especially in urban areas [4]. Transition to low emission transportation and cleaner cities will undoubtedly require a broad introduction of low- and zero-carbon alternatives to conventional petrol- and diesel-powered vehicles.

New generation gas buses are a cost-effective way to reduce CO_2 and local pollutants from urban transportation. Fueling with gas reduces pollutant emissions, including carbon monoxide (CO), nitrogen oxides (NO_x), and particulate matter (PM), as shown, e.g., by Biernat et al. [5]. Moreover, major GHG savings can be achieved by using biogas as the power source. This is based on the fact that producing biomethane from organic waste

material results in fuel that contains only biogenic carbon, and combustion of such fuel releases only biogenic CO_2, which is, unlike CO_2 from fossil fuels, not considered to contribute the climate change [6].

Buses running on biogas are becoming more common in Finland as cities and transportation companies invest in greener alternatives. For example, in the western coastal city of Vaasa, biogas buses have been touring since 2017. Life cycle GHG emissions from biogas vehicles largely depend on the extent of methane (CH_4) leakage throughout the fuel life cycle, and unintended CH_4 emissions from different stages of the fuel chain can narrow their potential climate benefits. Methane is a powerful greenhouse gas with a global warming potential (GWP) 28–34 times that of CO_2 over a 100-year timescale [7]. In addition, due to the strong C–H bonds of methane, it is one of the most difficult hydrocarbons to treat catalytically [8], and insufficient removal rates of exhaust after-treatment systems at low loads and low exhaust temperatures may lead to increased real-world CH_4 emissions [9].

Besides exhaust gas temperature, another critical issue is the effect of rapid changes in exhaust gas composition—typical in real-world driving conditions—on after-treatment devices. This phenomenon is particularly evident when dealing with stoichiometric gas engines using three-way catalytic converters (TWC), requiring a very precise control of air-to-fuel ratio (AFR), as some deviations from the stoichiometric lambda value can interfere with the catalyst efficiency [10]. For example, Rodman Opršnik et al. [11] reported instantaneous, local rises of THC emissions as a result of occasional inadequate lambda control of a CNG bus during transient regime and, consequently, increased cumulative emissions.

The main objective of this research was to investigate CH_4 and other gaseous emissions plus fuel consumption of a biogas-fueled urban bus in real-world operation. The actual driving emissions were recorded using a portable emissions measurement system (PEMS). The key advantage of on-board measurements is that they can truly demonstrate the emission characteristics of vehicles under various traffic conditions, operating cycles, and ambient conditions, including those that are challenging to replicate in the laboratory, such as varying road gradients [4]. The load on the lines that buses serve and the number of passengers may also affect exhaust emissions under actual traffic conditions [12].

Exhaust emissions under real-world conditions were examined by Lv et al. [13]. The authors showed an underestimation of road emissions of gas- and diesel-powered heavy vehicles; emission factors under real-driving conditions were significantly higher than in previous chassis dynamometer studies, likely caused by frequent accelerations, decelerations, and start-stop operation. In a recent study, Rosero et al. [14] investigated the effects of passenger load, road grade, and congestion level on real-world emissions and fuel consumption of urban Euro VI CNG and Euro V diesel buses. As the road grade and congestion level increased, both buses' fuel consumption and CO_2 emissions increased by 6–55%. Gallus et al. [15] studied the impact of driving style and road grade on gaseous exhaust emissions of Euro V and Euro VI diesel vehicles. CO_2 and NO_x emissions, measured with PEMS, showed a linear increase with road grade. Chen et al. [16] investigated the impact of speed and acceleration on emissions of heavy-duty (HD) vehicles in Shanghai. They found that congestion conditions with low speed and frequent deceleration and acceleration increased THC and CO emissions. Ozener & Ozkan [17] reported that the acceleration effect on both fuel consumption and emission values was significant. They concluded that the real-driving emission data could be effectively used in developing cleaner engine calibrations and more economical operations.

In addition, gaseous emissions are strongly affected by starting conditions. The cold-start emissions challenge has been highlighted, e.g., in [18,19]. During the first minutes of operation, emissions are high because the after-treatment equipment has not reached the appropriate temperature required to efficiently remove gaseous pollutants. Faria et al. [20] also showed a substantial increase in energy consumption for cold-start, leading to increased CO_2 emissions during the cold-start period. The problem of cold-starts is

considered more pronounced at low ambient temperatures, as lower ambient temperature increases the cold-start running duration [20,21].

One crucial topic rarely addressed in real-driving emissions (RDE) studies is the catalyst deactivation and deterioration over time. Indeed, the presence of catalyst poisons and other impurities in the feed, the fluctuating exhaust gas composition and flow rate in the converter, as well as high temperatures and temperature gradients, all increase the possibility of catalyst deactivation [22]. Therefore, to ensure a significant reduction of emission levels throughout the vehicle's useful life, EU regulation has adopted dedicated "emission durability" periods, i.e., the minimum mileage or time after which the engine is still expected to comply with applicable emission limits. For example, for category M3 buses, the required emission durability period is six years or 300,000 km, whichever comes first [23]. However, the useful life of urban buses is usually much longer; e.g., the Finnish bus fleet's average age is 12.5 years [24]. Therefore, emission levels after the emission durability period and closer to the service life of the vehicles need to be investigated.

This study focused on emissions from a six years old gas-powered city bus, supplementing emission data from aging bus fleets. PEMS measurements were performed in real-traffic conditions on a regular bus line in Vaasa in collaboration with the University of Vaasa and RISE Research Institutes of Sweden. In addition to methane emissions, gaseous emissions of NO_x, CO, and CO_2 were measured. Both cold-start and warm-engine emissions were recorded. We conducted two measurement campaigns, the first in March 2022 and the second in June 2022. In addition, the total carbon footprint of compressed biogas (CBG) is discussed in terms of its GHG reduction potential, defined as the percentage reduction in life cycle GHG emissions relative to its fossil counterpart natural gas and traditional diesel fuel.

2. Materials and Methods

2.1. Test Vehicle

Exhaust emission tests in real-driving conditions were carried out on a Scania Euro VI bus owned by the City of Vaasa and operated by Wasa Citybus. The CBG-fueled bus was equipped with a spark ignition engine with a displacement of 9.3 dm^3 and a power of 206 kW. The vehicle was equipped with exhaust gas recirculation (EGR) and a three-way catalytic converter. Table 1 presents the characteristics of the test vehicle and Table 2 summarizes the engine technical specifications.

Table 1. Vehicle technical specifications.

Parameter	Value
Model name	Scania Citywide LE
Model year	2016
Gross vehicle weight (kg)	19,100
Curb weight (kg)	12,960
Max passenger number	75
Axle configuration	4 × 2
Gearbox	6-speed automatic transmission
Accumulated mileage (km)	375,000 (Test 1), 400,000 (Test 2)
After-treatment system	TWC
Other systems	EGR
Exhaust emission norm	Euro VI-C

Table 2. Engine technical specifications.

Parameter	Value
Model	Scania OC09 101
Engine type	Spark ignition engine
Fuel	CNG/CBG

Table 2. *Cont.*

Parameter	Value
Number of cylinders	5
Compression ratio	12.6:1
Total displacement (L)	9.3
Maximum power (kW@rpm)	206 kW@1900 rpm
Engine peak torque (Nm@rpm)	1350 Nm@1000–1400 rpm

2.2. Portable Emissions Measurement System

The real-driving gaseous emissions of CH_4, CO, CO_2, NO, and NO_2 from the tested city bus were measured and recorded using an on-board VARIOplus Industrial device manufactured by MRU Messgeräte für Rauchgase und Umweltschutz GmbH. VARIOplus measures CH_4, CO, and CO_2 concentrations using a non-dispersive infrared (NDIR) sensor, and NO_x concentrations are measured using electrochemical cells. Table 3 shows the technical characteristics of the measurement apparatus used in this work.

Table 3. Technical characteristics of VARIOplus Industrial.

Parameter	Measurement Method	Accuracy
CH_4	NDIR—Non-dispersive infrared, range 0–10,000 ppm	±2%
CO	NDIR—Non-dispersive infrared, range 0–10%	±0.03% or * ±3% reading
CO_2	NDIR—Non-dispersive infrared, range 0–30%	±0.05% or * ±3% reading
NO	electrochemical, range 0–1000 ppm	±5 ppm or * 5% reading
NO_2	electrochemical, range 0–200 ppm	±5 ppm or * 5% reading
O_2	electrochemical, range 0–10%	±0.2 Vol-% abs.
Sampling	1 Hz	

* = whichever is larger.

The engine speed, torque, coolant temperature, air flow, lambda, and the vehicle speed were recorded from the vehicle engine control unit (ECU) via an on-board diagnostics (OBD) system using Scania Diagnosis & Programmer (SDP3) software version 2.50.3 (in Test 1) and version 2.52.1 (in Test 2), copyright Scania CV AB, Scania Suomi Oy, Vaasa, Finland. The vehicle's position in terms of latitude, longitude, and altitude, and the vehicle speed data were registered using an external global positioning system (GPS). A dedicated weather station was used to register the ambient temperature, pressure, and relative humidity. The real-world emission data obtained with PEMS and the GPS and the weather data were collected and stored with the DEWESoft data acquisition system. All data were recorded with a frequency of 1 Hz. Prior to the data processing, the SDP3 and DEWESoft data were synchronized based on the vehicle speed from the ECU and the GPS.

An external power unit supplied the electrical power to the PEMS system. Figure 1 depicts the system set-up.

2.3. Test Route

Emission tests were performed in real-driving conditions on an urban route in Vaasa, i.e., in normal traffic and with normal driving patterns and typical passenger loads. The selected test route was the same route the bus usually travels daily. The measurements started in the morning at the same time and the same driver from Wasa Citybus was used in both measurement campaigns. Figure 2 shows the driving circuit chosen for the tests. The length of one circuit was 25.5 km, and the same circuit was run three times. The total test duration was approx. 3 h. The route included both urban and rural driving. The speed profile of the driving circuit is presented in Figure 3. Table 4 shows the percentages and mean velocities for three different driving speed ranges. The passenger load varied between 5 and 30 percent during the tests.

Figure 1. Measurement system set-up.

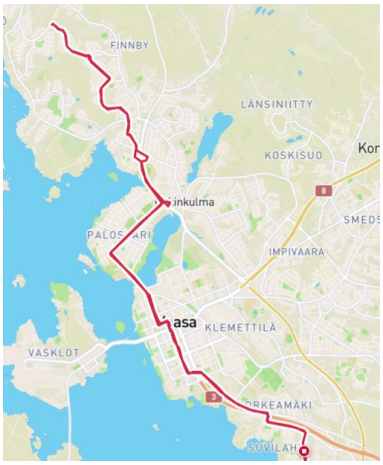

Figure 2. Driving circuit.

The first measurement campaign was performed in March 2022, and the second in June 2022. In June, only warm engine measurements were recorded, while in March, both cold-start and hot-start emissions were investigated.

2.4. Fuel

The fuel used in the test was CBG from a commercial filling station. The methane content of the fuel was 97% by volume. The other main components of the fuel were CO_2 (2.2 vol.-%), nitrogen (0.5 vol.-%), and oxygen (0.3 vol.-%), so the energy content of the fuel was solely related to the methane concentration. The calculated lower heating value (LHV) of the gas was 46.4 MJ/kg.

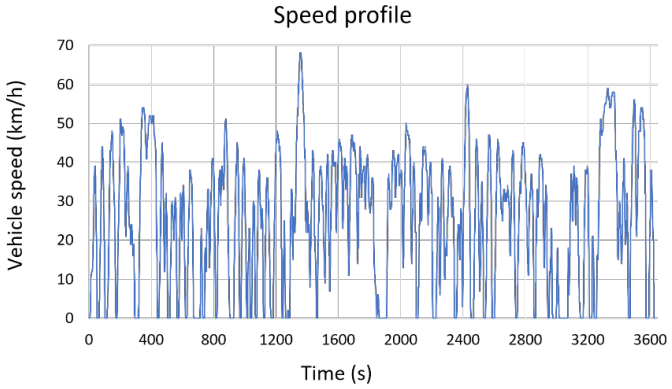

Figure 3. Speed profile of the driving circuit.

Table 4. Shares of driving speed ranges.

	Speed Range	Time (min)	%	Mean Velocity
Urban driving	0–30 km/h	102	56	12
Urban driving	30–50 km/h	65	36	38
Rural driving	50–75 km/h	16	9	57
Total		182		25

2.5. Calculation Procedure

2.5.1. Calculation of Fuel Mass Flow

The instantaneous fuel flow ($\dot{m}_{fuel}$) in kg/s was calculated based on the recorded instantaneous air flow ($\dot{m}_{air}$) and lambda (λ) values and the stoichiometric air-to-fuel ratio (AFR_{stoich}), according to Equation (1).

$$\dot{m}_{fuel} = \frac{\dot{m}_{air}}{AFR_{stoich} \times \lambda} \quad (1)$$

To determine AFR_{stoich}, the stoichiometric oxygen demand ($n_{O2,stoich}$) in moles per kg of fuel was calculated first, based on the chemical composition of the fuel (Equation (2)). In the equation, w_c, w_{H2} and w_{O2} are the fuel mass fractions of carbon, hydrogen and oxygen in the fuel.

$$n_{O2,\ stoich} = \frac{w_c}{0.012011} + \frac{1}{2} \times \frac{w_{H2}}{0.002016} - \frac{w_{O2}}{0.031999} \quad (2)$$

As air contains 20.95% of oxygen, the stoichiometric air demand ($n_{air,stoich}$) in moles per kg fuel could be determined by Equation (3):

$$n_{air,stoich} = \frac{n_{O2,stoich}}{0.2095} \quad (3)$$

Finally, the stoichiometric air demand in kg of air per kg of fuel was calculated by multiplying $n_{air,stoich}$ by the molar mass of air (M_{air}), see Equation (4):

$$AFR_{stoich} = n_{air,stoich} \times M_{air} \quad (4)$$

2.5.2. Calculation of Fuel Consumption

The total fuel mass (ΣFC_i) over the test cycle was calculated based on the instantaneous (second-by-second) fuel mass flows according to Equation (5).

$$\Sigma FC_i = \left(\frac{1}{2}\dot{m}_{fuel,0} + \dot{m}_{fuel,1} + \dot{m}_{fuel,2} + \ldots + \dot{m}_{fuel,n-1} + \frac{1}{2}\dot{m}_{fuel,n}\right) \quad (5)$$

2.5.3. Calculation of Exhaust Mass Flow

The instantaneous exhaust gas mass flow ($\dot{m}_{exh.,i}$) (wet basis) in kg/s was determined based on the recorded air flow and the calculated fuel flow values (Equation (6)):

$$\dot{m}_{exh.,i} = \dot{m}_{air,i} + \dot{m}_{fuel,i} \quad (6)$$

2.5.4. Emissions Dry–Wet Correction

The emission concentrations were measured on a dry basis. Dry concentration (c_{dry}) was converted to a wet basis with the dry–wet conversion factor (K_{d-w}):

$$c_{wet} = K_{d-w} \times c_{dry} \quad (7)$$

K_{d-w} was calculated according to the UN/ECE Regulation 49 [25], Equation (8):

$$K_{d-w} = \left(\frac{1}{1 + a \times 0.005 \times (c_{CO2} + c_{CO})} - k_{w1} \right) \times 1.008 \quad (8)$$

where a is the molar hydrogen to carbon ratio of the fuel, and

$$k_{w1} = \frac{1.608 \times H_a}{1000 + (1.608 \times H_a)} \quad (9)$$

where H_a is the intake air humidity in g water per kg dry air.

2.5.5. Calculation of Mass Emissions

Second-by-second mass flow of the pollutant ($\dot{m}_{gas}$) in g/s was calculated using Equation (10):

$$\dot{m}_{gas} = u_{gas} \times c_{gas} \times \dot{m}_{exh.} \quad (10)$$

where u_{gas} is the ratio between the density of pollutant and the density of exhaust gas, and c_{gas} is the instantaneous concentration of the pollutant in raw exhaust in ppm (wet basis). The instantaneous u values were calculated following the UN/ECE Regulation No 49 [25], according to Equations (11)–(14):

$$u_{gas,i} = \frac{\rho_{gas}}{(\rho_{exh.,i} \times 1000)} \quad (11)$$

$$\rho_{gas} = \frac{M_{gas}}{22.414} \quad (12)$$

where M_{gas} is the molar mass of the gas component in g/mol, ρ_{gas} is the density of the gas component in kg/m^3, and $\rho_{exh.,i}$ the instantaneous density of the exhaust gas in kg/m^3, derived from Equation (13):

$$\rho_{exh.,i} = \frac{1000 + H_a + 1000 \times \left(\frac{\dot{m}_{fuel,i}}{\dot{m}_{dry\ air,i}} \right)}{773.4 + 1.2434 \times H_a + k_{fw} \times 1000 \times \left(\frac{\dot{m}_{fuel,i}}{\dot{m}_{dry\ air,i}} \right)} \quad (13)$$

where k_{fw} is the fuel specific factor of wet exhaust, obtained from Equation (14):

$$k_{fw} = 0.055594 \times W_\alpha + 0.0080021 \times W_\Delta + 0.0070046 \times W_\varepsilon \quad (14)$$

where W_α is the hydrogen content (wt%) of the fuel, W_Δ the nitrogen content (wt%), and W_ε the oxygen content (wt%) of the fuel.

The mass of gaseous emissions (m_{gas}) in grams per test cycle was calculated using Equation (15).

$$m_{gas} = \sum_{i=1}^{i=n} u_{gas,i} \times c_{gas,i} \times \dot{m}_{exh.,i} \times \frac{1}{f} \quad (15)$$

where f is the data sampling rate in Hz.

The final results are expressed in g/kWh and in g/km, i.e., the total mass of each pollutant over the test cycle was divided by the engine cycle work or by the distance covered in km.

2.5.6. Calculation of Cycle Work

The engine work (W_i) in kWh over the test cycle was calculated based on the instantaneous (second-by-second) engine power values (P_e), according to Equation (16):

$$W_i = \frac{\left(\frac{1}{2}P_{e,0} + P_{e,1} + P_{e,2} + \ldots + P_{e,n-2} + P_{e,n-1} + \frac{1}{2}P_{e,n}\right)}{3600} \quad (16)$$

2.5.7. Calculation of Effective Power of the Engine

The instantaneous engine power in kW was calculated by using each pair of recorded engine speed and torque values (Equation (17)):

$$P_e = \frac{2 \times \pi \times N \times \tau}{60 \times 1000} \quad (17)$$

where N is the engine speed in rpm and τ is the engine torque in Nm.

3. Results and Discussion

3.1. Ambient Conditions

Table 5 summarizes the average ambient conditions during the tests.

Table 5. Ambient conditions during the tests.

Ambient Condition	Test 1	Test 2
	March 2022	**June 2022**
Temperature (°C)	−5 °C	+18 °C
Pressure (kPa)	102.5	100.5
Humidity (%)	65.5	54.7

3.2. Gaseous Emissions

In the current legislation, the regulatory in-service conformity (ISC) emission test applies the 20% power threshold as a boundary condition for Euro VI-C bus engines. However, Mendoza Villafuerte et al. [26] showed that a large fraction of urban operation is not considered if the current power threshold boundary for post-processing the PEMS data is applied, and up to 80% of the data may be excluded from the emission analysis. They also showed that cold-start emissions, which are currently also excluded from the analysis, could account for a significant proportion of total emissions. To give a more accurate depiction of real-driving emissions, no power threshold boundaries were applied in this study. In addition, in Test 1, both cold-start and hot-start emissions were recorded. In Test 2, unfortunately, only hot-start emissions were successfully recorded.

3.2.1. Hot-Start Emissions

A test was considered a hot-start once the coolant temperature had reached 70 °C for the first time or stabilized within ±2 °C over a period of 5 min, whichever came first [27]. Specific emissions were calculated in both g/kWh and g/km, and the results are presented separately for the total trip and for urban and rural sections of the circuit (Figure 4). Although the tests performed did not fully reflect the ISC tests in the type-approval procedure regarding boundary conditions and route requirements, the Euro VI standard limits (ISC limit) are also presented for comparative purposes.

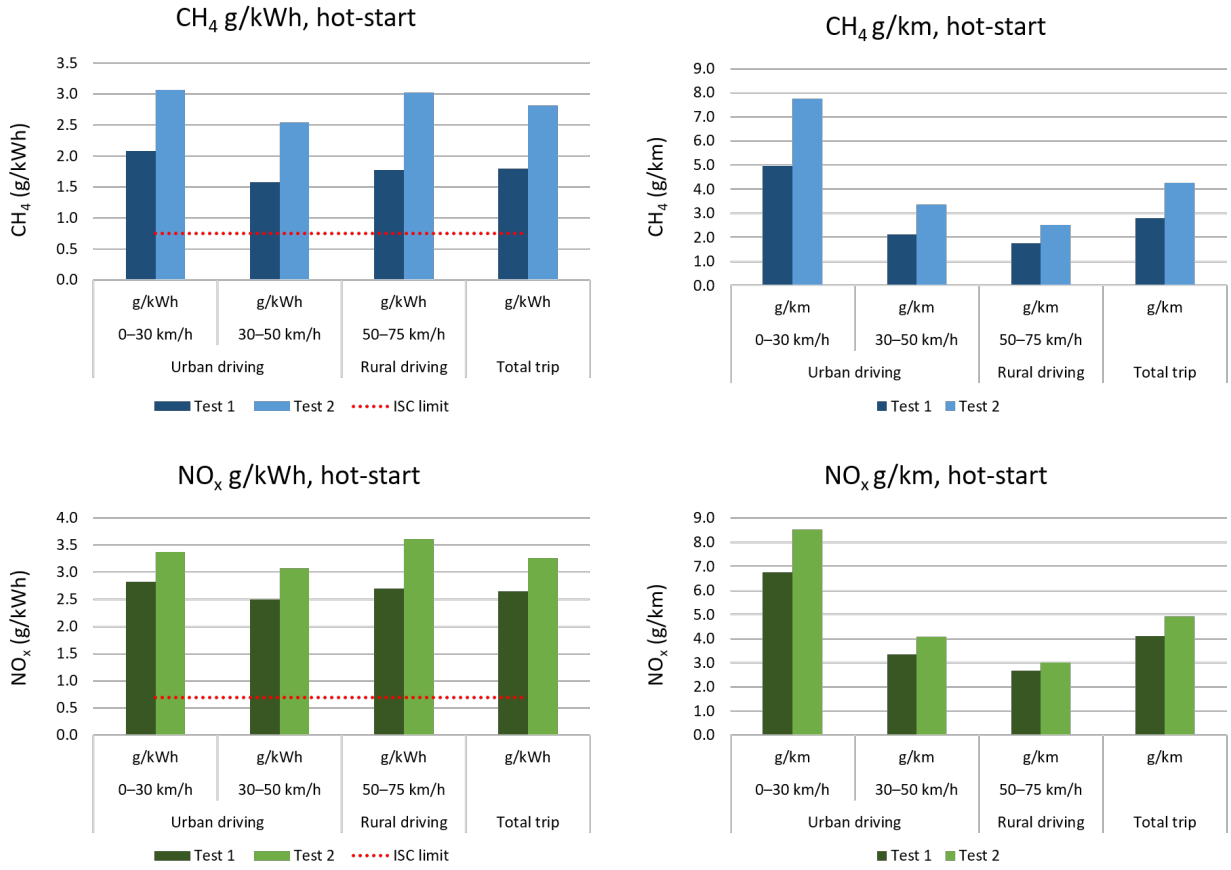

Figure 4. Specific CH_4 and NO_x emissions in g/kWh and g/km in hot-start tests.

CO emission values were low and well below the ISC limit of 6 g/kWh in both tests, indicating efficient oxidation of CO in the catalyst. In contrast, relatively high values were observed for CH_4 and NO_x, indicating impaired CH_4 oxidation and NO_x reduction in the catalyst after its service life of 375,000 km (Test 1). After 400,000 km (Test 2), the catalyst efficiency had further deteriorated. Here, it should be noted that according to EU Regulation EC 595/2009 [23], the minimum mileage or time after which the engine is still expected to comply with applicable emission limits for category M3 buses, is 300,000 km or six years, whichever comes first. Hence, the required "emission durability" period had already been exceeded in our case. Nevertheless, the bus has passed the regular technical inspections valid in Finland, including CO_2 and HC measurements.

The primary reason for relatively high CH_4 and NO_x emissions after the TWC was assumed to be the low CH_4 reactivity due to a partial deactivation of the catalyst. In addition to the low CH_4 oxidation rate, low CH_4 reactivity also means that methane-based reducing agents for NO_x reduction do not work, leading to substantial NO_x breakthrough from the catalyst, also concluded by Van den Brink & McDonald [28].

One of the most important reasons for the deactivation of the TWC in automotive applications is chemical deactivation [29], mainly caused by lubricating oil additives and other impurities in the exhaust gases. For example, Winkler et al. [30] observed a significant increase in hydrocarbon emissions during CNG operation over a relatively short TWC lifetime of 35,000 km. Contaminants originating from the lubricating oil, such as calcium, phosphorus, and magnesium, detected on the catalyst's surface, appeared to affect especially CH_4 oxidation. In addition to lubricating oil, another source of catalyst poisons is the impurities in the fuel. The CBG used in this study contained small traces of commonly

encountered catalyst poison sulfur (<2.3 mg/Nm^3) and siloxanes (0.7 mg/Nm^3). Although the amounts of these compounds were very low, they could have had a deactivating effect on the emissions control system.

Furthermore, the light-off of a TWC in gas-fueled engine exhaust typically occurs at higher temperatures compared to gasoline engines [31]. Indeed, methane is the most difficult hydrocarbon to oxidize due to its high stability [8]. A typical light-off temperature for methane is 400 °C [8], but in a deactivated catalyst, significantly higher temperatures, up to 500–600 °C [32], may be required to break the strong C–H bonds in methane. At low loads (Figure 5), common in a city bus's driving profile, the exhaust gas temperature was too low to allow the deactivated catalyst to work effectively.

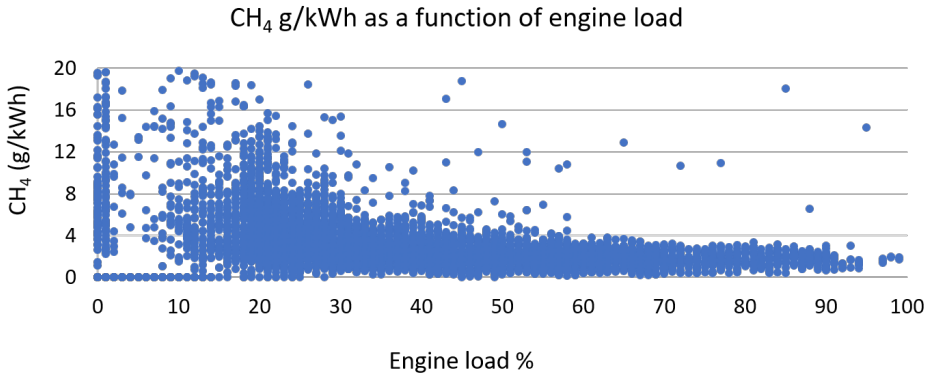

Figure 5. Specific CH_4 emissions as a function of engine load%.

Thus, restoring the catalytic activity of a deactivated TWC is a critical consideration. In some cases, depending on the adsorbed poison, the activity of the poisoned catalyst can be at least partially restored by regeneration [22]. For example, SO_2 can be removed from the catalyst under elevated temperatures and anoxic or very rich conditions, as shown by Auvinen et al. [32]. Careful control of the exhaust gas composition during regeneration could provide significant benefits in terms of CH_4 emissions. However, under real-driving conditions, the rapidly and dramatically varying exhaust gas temperature and composition between oxidizing and reducing environment make the on-board regeneration difficult to control.

Another possible deactivation mechanism for the TWC is thermal degradation. Three-way catalysts are known to lose their activity when exposed to high temperature (>800 °C) oxidizing environments, typically occurring during fuel shut-off phases [33]. Switching off the fuel flow, e.g., during engine braking, is a strategy of the automotive industry to improve fuel economy. Thermal degradation is critical to the catalyst's performance since these changes are typically irreversible.

In addition to the partial deactivation of the catalyst, another probable reason for the relatively high emissions was the fluctuating lambda value. Indeed, close control of the exhaust gas composition is essential for high emission conversion as the composition of the gas entering the TWC significantly affects its catalytic efficiency [34]. For simultaneous conversion of HC, CO, and NO_x species in the TWC, the engine must be operated within a very narrow AFR window—near stoichiometric conditions—due to a rapid drop in NO_x conversion efficiency on the lean side and a non-complete conversion of hydrocarbons both in lean and rich stoichiometry [10]. For example, Lou et al. [34] detected the highest TWC conversion efficiency when AFR was controlled between 0.995 and 1. The narrow AFR range over which significant conversion of natural gas exhaust emissions is possible presents a challenging control problem. As seen in Figure 6, lambda was outside the optimal range for a significant part of the time in our experiments.

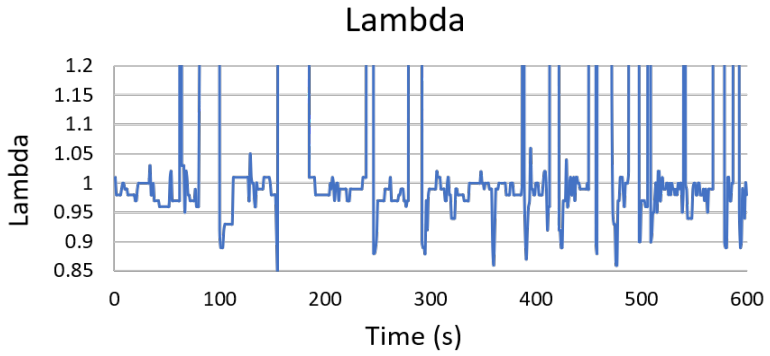

Figure 6. Fluctuating lambda values under real-driving conditions.

In sum, deterioration of the exhaust after-treatment systems over time should be monitored as they are exposed to different aging processes resulting in elevated real-world emissions. Our results indicate a catalyst replacement need after 375,000 km of service life. In addition, a precise lambda control is absolutely necessary to ensure high conversion rates throughout the vehicle's lifetime.

3.2.2. Cold-Start Emissions

Cold-start emissions were recorded from the moment the coolant temperature had reached 30 °C for the first time and continued until the coolant temperature was stabilized within ±2°C over 5 min [27]. In Test 1 (at −5 °C), the cold-start period lasted 14.5 min. The combined cold- and hot-start emissions were calculated according to EU Regulation 1718 [35]: the vehicle was driven over a cold-test cycle followed by nine hot-test cycles, identical to the cold one in a way that the work developed by the engine was the same as the one achieved in the cold cycle.

Figure 7 illustrates CH_4 and NO_x emissions during cold-start versus hot-start. During the cold-start, CH_4 emissions were 2.3 times higher and NO_x emissions 1.4 times higher than those during the hot-start. This highlights the temperature sensitivity of catalytic emission control systems, which is also evidenced in Figure 8.

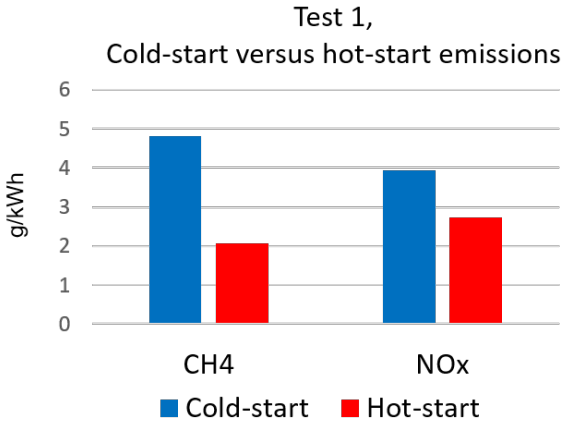

Figure 7. Cold-start versus hot-start emissions.

Over the combined cold- and hot-start cycles, CH_4 emissions increased by 30%, NO_x by 13%, and CO by 33% compared to hot-start-only measurements.

The cold-start emissions challenge is more pronounced at low ambient temperatures because it then takes longer for the TWC to reach effective operating temperature, leading to a prolonged period of high emission rates [18,20,21].

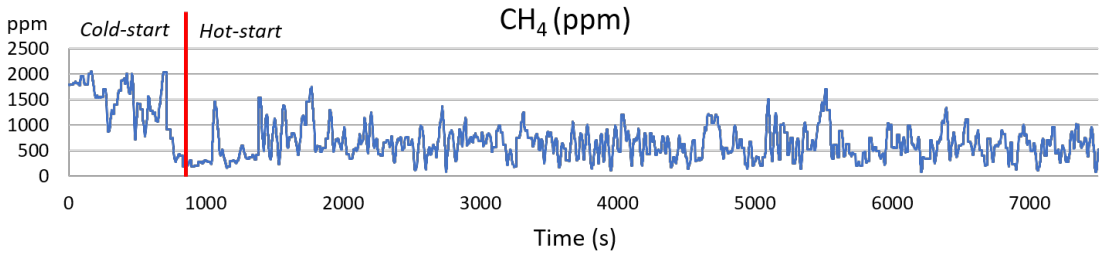

Figure 8. CH_4 emissions during combined cold- and hot-start test.

3.3. Well-to-Wheels Analysis

In the transport sector, well-to-wheels (WTW) analysis is a commonly used method for assessing the carbon intensity of a fuel. Carbon intensity refers to the amount of greenhouse gases—including CO_2, nitrous oxide, and methane—released during the production and consumption of a transportation fuel, measured in grams of carbon dioxide equivalent per megajoule of energy (g CO_2-eq./MJ).

3.3.1. Fuel Consumption

The total fuel consumption in the hot-start test at −5 °C was 21.9 MJ/km (6.1 kWh/km), corresponding to 0.306 kg/kWh and 47.1 kg/100 km. In June, at +18 °C, the vehicle showed better fuel economy with fuel consumption of 19.8 MJ/km (5.5 kWh/km), corresponding to 0.283 kg/kWh and 42.7 kg/100 km (Figure 9).

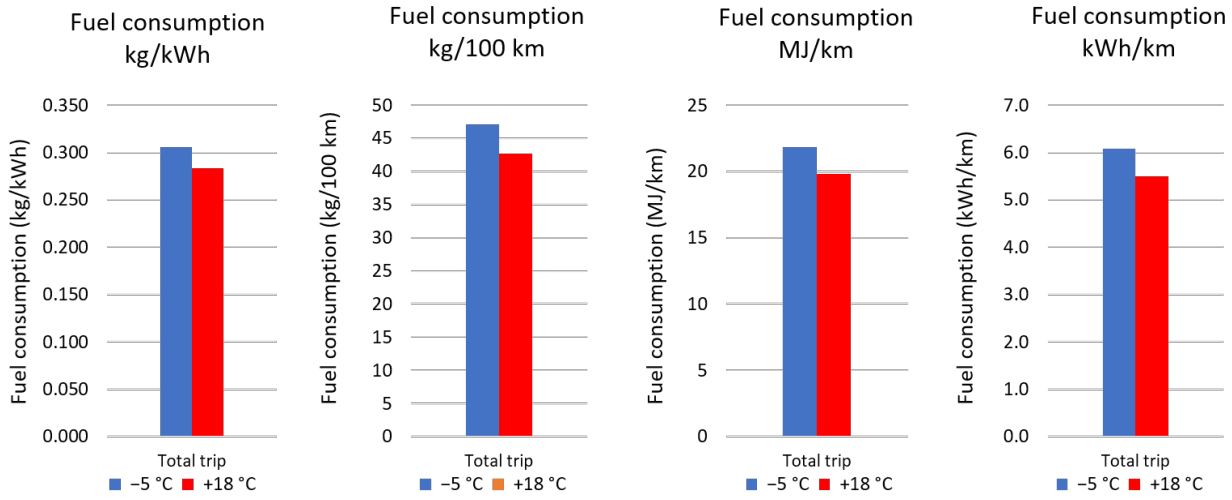

Figure 9. Fuel consumption in hot-start tests at −5 °C and +18 °C.

3.3.2. Biogas Production Process

The life cycle steps for CBG investigated in this study are feedstock collection and transportation, biogas production, biogas processing to biomethane, biomethane compression, and finally, combustion in an engine. The CBG was produced at Stormossen waste treatment plant near Vaasa. The anaerobic digestion process at Stormossen is divided into two separate process lines. Biogas reactor 1 is fed with wastewater sludge, and the raw material used in biogas reactor 2 is municipal biowaste, supplied within a radius of 40 km [36].

In 2020, raw biogas production at Stormossen was 2.7 million Nm^3, of which 52% was upgraded into biomethane, 32% was used for heat and electricity production, and the rest was flared [37]. The methane content of the raw biogas was 62%.

The biogas upgrading is executed by an amine scrubber. The main advantages of chemical absorption with amine solvents are a high methane recovery rate in the upgraded biogas and a low methane slip of <0.1% [38]. In addition, amine solvents are effective at near atmospheric pressure and thus consume a low quantity of electric energy [39]. On the other hand, chemical scrubbing liquids require substantial thermal energy during regeneration, which must be supplied as process heat [39]. After the refining stage, biogas contains 97–98% methane. Finally, the processed biomethane is piped to a gas filling station near the biogas plant. At the refueling station, the gas is pressurized to 300 bar and stored in gas cylinders.

Although the combustion of waste-based biomethane is considered carbon-neutral in Finland's national GHG inventories (CO_2 emissions from biogas combustion are reported as zero), the use of biomethane may still have climate impact from the above-mentioned earlier stages of the fuel chain. For CBG production, the major contributors of GHG emissions are energy consumption and fugitive losses of methane during digestion and upgrading processes [40]. In addition, some GHG emissions form during the collection of wastes and residues.

3.3.3. GHG Inventory

In this study, the calculation of GHG emissions begins with feedstock collection and transportation. GHG emissions from these steps are based on the following assumptions. Transportation distance 40 km and diesel B7 fuel consumption 20 l/100 km. The lower calorific value of diesel B7 fuel is 43 MJ/kg. The biocomponent of diesel fuel was assumed to be hydrotreated vegetable oil made from waste materials, so the calculated well-to-tank emission factor for diesel B7 was 14.7 g CO_2-eq./MJ fuel, based on the JRC [41] data. Tank-to-wheels CO_2 emission factor for diesel B7 was set at 68.4 g CO_2-eq./MJ fuel [42]. The heat and electricity needs of biogas production and upgrading processes are covered internally by the plant's own CHP biogas engine and were, therefore, ignored in the GHG inventory. Methane emissions were calculated assuming a methane loss of 1% during anaerobic digestion [43] and 0.1% during the upgrading process [39]. Methane emissions are converted to CO_2-equivalents using a 100-year time horizon global warming potential (GWP) factor of 28 [7]. The energy demand for biomethane compression to 300 bar is 0.25 kWh/m^3 (NTP) [44], and the electric energy for compression is taken from the public grid. The CO_2 emission factor for electricity generation in Finland in 2020 was 68.6 g CO_2-eq./kWh [45]. Table 6 summarizes the main assumptions and input data used in the calculation.

Table 6. CBG well-to-tank GHG emissions.

Parameter	Value	Unit	g CH_4/$MJ_{bio\text{-}CH4}$	g CO_2-Equivalent /$MJ_{bio\text{-}CH4}$	Source
Feedstock collection and transportation					
Diesel trucks, diesel fuel biocomponent 7%	40	km		1.95	[41,42]
Biogas production and refining					
Total biogas production	2,716,000	Nm^3			[37]
52% of raw gas for upgrading	1,412,320	Nm^3			[37]
Methane content (62%)	875,638	Nm^3			[37]
Total biomethane production	31,522,982	MJ			
Heat demand *					
- Anaerobic digestion	0.19	kWh/$Nm^3_{raw\ gas}$			[43]
- Upgrading	0.110	$kWh/kWh_{bio\text{-}CH4}$			
Electricity demand *					
- Anaerobic digestion	0.14	kWh/$Nm^3_{raw\ gas}$			[43]
- Upgrading	0.0136	$kWh/kWh_{bio\text{-}CH4}$			
Methane losses					
- Anaerobic digestion, 1%	6368	kg	0.202	5.66	[43]
- Upgrading, 0.1%	630	kg	0.020	0.56	[39]

Table 6. *Cont.*

Parameter	Value	Unit	g CH_4/$MJ_{bio-CH4}$	g CO_2-Equivalent /$MJ_{bio-CH4}$	Source
Compression					
Electricity demand	0.25	kWh/m^3 (NTP)		0.48	[44,45]
CBG well-to-tank GHG emissions				**8.65**	

* Covered internally by the plant's own CHP biogas engine.

After the anaerobic digestion, the digestate is dewatered and composted to be used as a soil improvement product or as landscaping soil. The digestate treatment is not included in the above table. Any fertilizer or sludge credits are also not considered in GHG calculations.

The GHG benefits associated with transition from fossil-based natural gas or diesel to biomethane were calculated by comparing well-to-wheels CO_2-Equivalent emissions, shown in Table 7. Well-to-tank GHG emission factors for compressed natural gas and diesel fuel were taken from the JRC report [41]. Tank-to-wheel GHG emissions for gas buses are based on the CO_2 and CH_4 emission results recorded in this study, but CO_2 emissions are considered only for fossil CNG. Tank-to-wheels CO_2 emission factor for diesel buses was taken from [42]. The average fuel consumption from Test 1 and 2 in this study was 20.8 MJ/km, and this value is applied to both CBG and CNG bus. It is well known that compression-ignition diesel engines have higher thermal efficiency compared to spark ignition gas engines. Therefore, the fuel consumption of a diesel bus was set at 80% of that of a gas bus, based on the VTT's (Technical Research Centre of Finland) comprehensive report on city bus emissions measurements [46].

Table 7. Well-to-wheels CO_2 Equivalent emissions for CBG, CNG, and diesel B7.

	CBG	CNG	Diesel B7
GHG emissions			
Well-to-tank (g/MJ_{fuel})	8.65	13.0	14.7
Tank-to-wheels			
• CO_2 (g/MJ_{fuel})		46.6	68.4
• CH_4 (g/MJ_{fuel})	0.1708	0.1708	
Total GHG (g CO_2-eq./MJ_{fuel})	13.4	64.4	83.1
Fuel consumption (MJ/km)	20.8	20.8	16.7
Specific GHG (g CO_2-eq./km)	**279**	**1342**	**1385**

Figure 10 shows the percentage changes in life cycle GHGs for the studied fuels. Shifting from conventional diesel to fossil natural gas does not show meaningful GHG benefits, bearing in mind the higher thermal efficiency of compression-ignition engines compared to spark-ignition gas engines. However, for biomethane, the situation is very different; 80% GHG emission benefit is achieved by switching from diesel to biomethane. With more precise methane emission control, GHG emission savings would advance towards 90%.

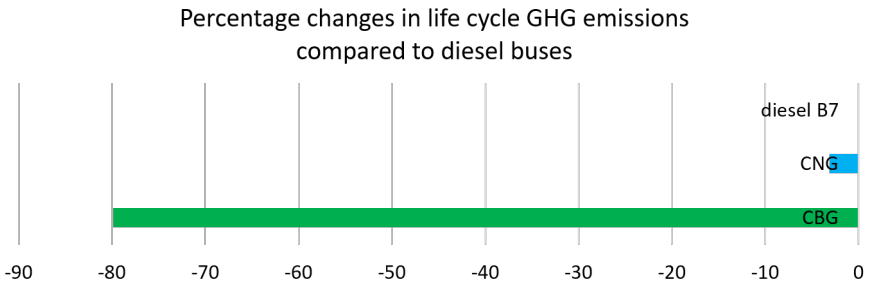

Figure 10. Percentage changes in life cycle GHGs.

This gives a strong environmental argument for biogas use. Increasing biogas use would be a quick and cost-effective way to reduce GHG emissions from urban traffic. Unfortunately, the potential of renewable gas is not acknowledged in the current EU emission standards, which only focus on tank-to-wheels emissions. Changing the measurement method to life cycle-based WTW instead of tailpipe measurement would enable a proper assessment of GHG emissions of future vehicle technology and fuel combinations. However, the results of this study can be utilized in designing strategies for transitioning to sustainable urban transport systems.

4. Conclusions

Transition to low-emission transportation and cleaner cities requires a broad introduction of low- and zero-carbon alternatives to conventional petrol- and diesel-powered vehicles. This paper presents the results of real-driving emission measurements from a Euro VI biogas-powered city bus equipped with a TWC. In addition, the lifetime carbon intensity of CBG was investigated and compared to its fossil counterpart CNG and traditional diesel fuel. The main findings were, first, for the bus:

- The rapid changes in exhaust gas temperature and composition under transient driving conditions seemed to be a critical challenge to an efficient operation of the TWC.
- Unimpressive CH_4 oxidation and NO_x reduction were observed in the catalyst after its service life of 375,000 km–400,000 km. In contrast, CO emissions were low, indicating efficient oxidation of CO in the catalyst.
- The primary reason for deficient CH_4 and NO_x conversion over the TWC was assumed to be the low CH_4 reactivity due to a partial deactivation of the catalyst. At low loads, common in a city bus's driving profile, the exhaust gas temperature was too low to allow efficient CH_4 oxidation. In addition to the low CH_4 oxidation rate, low CH_4 reactivity also means that methane-based reducing agents for NO_x reduction do not work, leading to substantial NO_x breakthrough from the catalyst.
- In addition, during the cold-start, CH_4 emissions were 2.3 times and NO_x emissions 1.4 times as high as those during the hot-start, highlighting the temperature sensitivity of catalytic emission control systems.
- Based on the above, deterioration of the exhaust after-treatment systems over time should be monitored as they are exposed to different aging processes resulting in elevated real-world emissions.
- Another critical issue was the fluctuating air-to-fuel ratio. Lambda was outside the optimal range for a significant part of the time, likely reducing the TWC efficiency. This highlights the need for precise lambda control to ensure high conversion rates throughout the vehicle's lifetime.

Additionally,

- The WTW analysis showed an 80% GHG emission benefit by switching from diesel to biomethane, giving a strong environmental argument for biogas use. With more precise methane emission control, GHG emission savings would advance towards 90%.

The presented real-driving emission results are of great importance in supplementing the emission data for aging gas-powered HD vehicles, filling the gap of data on emissions closer to the service life of the vehicles. After all, the average age of bus fleets in Finland, for example, is over 12 years. The results of this study can also be utilized in scheduling catalyst maintenance or replacement activities.

In the future, it would be worthwhile to repeat the weather-related comparison with a completely new bus or with a new catalyst on an old bus.

Author Contributions: Conceptualization, K.S.-T. and S.N.; data curation, K.S.-T.; formal analysis, K.S.-T. and H.A.; funding acquisition, K.S.-T. and S.N.; investigation, K.S.-T., H.A. and O.N.; methodology, K.S.-T. and H.A.; project administration, K.S.-T.; supervision, S.N.; validation, K.S.-T. and H.A.; visualization, K.S.-T.; writing—original draft, K.S.-T.; writing—review and editing, K.S.-T., H.A., O.N. and S.N. All authors have read and agreed to the published version of the manuscript.

Funding: This research was funded by The European Regional Development Fund (ERDF) through The Council of Tampere Region, under Sustainable Growth and Jobs 2014–2020—Structural Funds Programme of Finland, grant number A75906. The APC was funded by MDPI/Clean technologies (2020 Best Paper Award).

Data Availability Statement: Not applicable.

Acknowledgments: The authors would like to thank Tuomas Wentin from Scania, Mikko Lähdesmäki from Wasa Citybus, and the City of Vaasa for their support and collaboration. The main author would also like to thank Gasum Oy for awarding a personal grant to support the research.

Conflicts of Interest: The authors declare no conflict of interest.

Abbreviations

The following abbreviations are used in this manuscript:

AFR	air-to-fuel ratio
CAN	controller area network
CH_4	methane
CO	carbon monoxide
CO_2	carbon dioxide
CBG	compressed biogas
CNG	compressed natural gas
ECU	engine control unit
EGR	exhaust gas recirculation
GPS	global positioning system
HC	hydrocarbon
HD	heavy-duty
ISC	in-service conformity
NDIR	non-dispersive infrared
NO	nitrogen monoxide
NO_2	nitrogen dioxide
NO_x	nitrogen oxides
OBD	on-board diagnostics
PEMS	portable emissions measurement system
PM	particulate matter
RDE	real-driving emissions
THC	total hydrocarbons
TWC	three-way catalyst
WTW	well-to-wheels

References

1. Communication from the Commission to the European Parliament, the Council, the European Economic and Social Committee and the Committee of the Regions. Stepping up Europe's 2030 Climate Ambition. Investing in a Climate-Neutral Future for the Benefit of Our People. EU COM/2020/562 Final. Available online: https://eur-lex.europa.eu/legal-content/EN/TXT/?uri=CELEX%3A52020DC0562 (accessed on 14 May 2022).
2. Finnish Government; Marin's Government; Government Programme. Strategic Themes. 3.1 Carbon Neutral Finland that Protects Biodiversity. Available online: https://valtioneuvosto.fi/en/marin/government-programme/carbon-neutral-finland-that-protects-biodiversity (accessed on 2 May 2022).
3. Liikennefakta. Liikenteen Kasvihuonekaasupäästöt ja Energiankulutus. Finnish Transport and Communications Agency Traficom. Available online: https://liikennefakta.fi/fi/ymparisto/liikenteen-kasvihuonekaasupaastot-ja-energiankulutus (accessed on 2 May 2022).
4. Franco, V.; Kousoulidou, M.; Muntean, M.; Ntziachristos, L.; Hausberger, S.; Dilara, P. Road vehicle emission factors development: A review. *Atmos. Environ.* **2013**, *70*, 84–97. [CrossRef]
5. Biernat, K.; Samson-Bręk, I.; Chłopek, Z.; Owczuk, M.; Matuszewska, A. Assessment of the Environmental Impact of Using Methane Fuels to Supply Internal Combustion Engines. *Energies* **2021**, *14*, 3356. [CrossRef]
6. Biogenic Carbon Dioxide. The Finnish Innovation Fund Sitra. Available online: https://www.sitra.fi/en/dictionary/biogenic-carbon-dioxide/ (accessed on 2 May 2022).

7. Myhre, G.; Shindell, D.; Bréon, F.-M.; Collins, W.; Fuglestvedt, J.; Huang, J.; Koch, D.; Lamarque, J.-F.; Lee, D.; Mendoza, B.; et al. Anthropogenic and Natural Radiative Forcing. In *Climate Change 2013: The Physical Science Basis*; Contribution of Working Group I to the Fifth Assessment Report of the Intergovernmental Panel on Climate Change; Stocker, T.F., Qin, D., Plattner, G.-K., Tignor, M., Allen, S.K., Boschung, J., Nauels, A., Xia, Y., Bex, V., Midgley, P.M., Eds.; Cambridge University Press: Cambridge, UK; New York, NY, USA, 2013; pp. 659–740. Available online: https://www.ipcc.ch/site/assets/uploads/2018/02/WG1AR5_Chapter08_FINAL.pdf (accessed on 16 May 2022).
8. Stoian, M.; Rogé, V.; Lazar, L.; Maurer, T.; Védrine, J.C.; Marcu, I.C.; Fechete, I. Total Oxidation of Methane on Oxide and Mixed Oxide Ceria-Containing Catalysts. *Catalysts* **2021**, *11*, 427. [CrossRef]
9. Pan, D.; Tao, L.; Sun, K.; Golston, L.M.; Miller, D.J.; Zhu, T.; Qin, Y.; Zhang, Y.; Mauzerall, D.L.; Zondlo, M.A. Methane emissions from natural gas vehicles in China. *Nat. Commun.* **2020**, *11*, 4588. [CrossRef]
10. Di Maio, D.; Beatrice, C.; Fraioli, V.; Napolitano, P.; Golini, S.; Rutigliano, F.G. Modeling of Three-Way Catalyst Dynamics for a Compressed Natural Gas Engine during Lean–Rich Transitions. *Appl. Sci.* **2019**, *9*, 4610. [CrossRef]
11. Rodman Oprešnik, S.; Seljak, T.; Vihar, R.; Gerbec, M.; Katrašnik, T. Real-World Fuel Consumption, Fuel Cost and Exhaust Emissions of Different Bus Powertrain Technologies. *Energies* **2018**, *11*, 2160. [CrossRef]
12. Gis, M.; Pielecha, J.; Gis, W. Exhaust emissions of buses LNG and Diesel in RDE tests. *Open Eng.* **2021**, *11*, 356–364. [CrossRef]
13. Lv, L.; Ge, Y.; Ji, Z.; Tan, J.; Wang, X.; Hao, L.; Wang, Z.; Zhang, M.; Wang, C.; Liu, H. Regulated emission characteristics of in-use LNG and diesel semi-trailer towing vehicles under real driving conditions using PEMS. *J. Environ. Sci.* **2020**, *88*, 155–164. [CrossRef]
14. Rosero, F.; Fonseca, N.; López, J.M.; Casanova, J. Effects of passenger load, road grade, and congestion level on real-world fuel consumption and emissions from compressed natural gas and diesel urban buses. *Appl. Energy* **2021**, *282*, 116195. [CrossRef]
15. Gallus, J.; Kirchner, U.; Vogt, R.; Benter, T. Impact of driving style and road grade on gaseous exhaust emissions of passenger vehicles measured by a Portable Emission Measurement System (PEMS). *Transp. Res. D Transp. Environ.* **2017**, *52*, 215–226. [CrossRef]
16. Chen, C.; Huang, C.; Jing, Q.; Wang, H.; Pan, H.; Li, L.; Zhao, J.; Dai, Y.; Huang, H.; Schipper, L.; et al. On-road emission characteristics of heavy-duty diesel vehicles in Shanghai. *Atmos. Environ.* **2007**, *41*, 5334–5344. [CrossRef]
17. Ozener, O.; Ozkan, M. Assessment of real driving emissions of a bus operating on a dedicated route. *Therm. Sci.* **2020**, *24*, 66–73. [CrossRef]
18. Giechaskiel, B.; Valverde, V.; Kontses, A.; Suarez-Bertoa, R.; Selleri, T.; Melas, A.; Otura, M.; Ferrarese, C.; Martini, G.; Balazs, A.; et al. Effect of Extreme Temperatures and Driving Conditions on Gaseous Pollutants of a Euro 6d-Temp Gasoline Vehicle. *Atmosphere* **2021**, *12*, 1011. [CrossRef]
19. Reiter, M.S.; Kockelman, K.M. The problem of cold starts: A closer look at mobile source emissions levels. *Transp. Res. D Transp. Environ.* **2016**, *43*, 123–132. [CrossRef]
20. Faria, M.V.; Varella, R.A.; Duarte, G.O.; Farias, T.L.; Baptista, P.C. Engine Cold Start Analysis Using Naturalistic Driving Data: City Level Impacts on Local Pollutants Emissions and Energy Consumption. *Sci. Total Environ.* **2018**, *630*, 544–559. [CrossRef]
21. Yusuf, A.A.; Inambao, F.L. Effect of cold start emissions from gasoline-fueled engines of light-duty vehicles at low and high ambient temperatures: Recent trends. *Case Stud. Therm. Eng.* **2019**, *14*, 100417. [CrossRef]
22. Lassi, U. Deactivation Correlations of Pd/Rh Three-way Catalysts Designed for Euro IV Emission Limits. Effect of Ageing Atmosphere, Temperature and Time. Academic Dissertation, University of Oulu, Department of Process and Environmental Engineering, Oulu, Finland, 2003. Available online: http://jultika.oulu.fi/files/isbn9514269543.pdf (accessed on 8 June 2022).
23. Regulation No 595/2009 of the European Parliament and of the Council of 18 June 2009 on Type-Approval of Motor Vehicles and Engines with Respect to Emissions from Heavy Duty Vehicles (Euro VI) and Amending Regulation (EC) No 715/2007 and Directive 2007/46/EC and Repealing Directives 80/1269/EEC, 2005/55/EC and 2005/78/EC. EC 595/2009. Available online: https://eur-lex.europa.eu/legal-content/EN/TXT/PDF/?uri=CELEX:02009R0595-20200901&from=EN (accessed on 14 May 2022).
24. ACEA. Facts and Figures. Average age of the EU Vehicle Fleet, by Country. Available online: https://www.acea.auto/figure/average-age-of-eu-vehicle-fleet-by-country/ (accessed on 20 June 2022).
25. Regulation No 49 of the Economic Commission for Europe of the United Nations (UN/ECE)—Uniform Provisions Concerning the Measures to be Taken against the Emission of Gaseous and Particulate Pollutants from Compression-Ignition Engines and Positive Ignition Engines for Use in Vehicles. UN/ECE 49/2013. Available online: https://eur-lex.europa.eu/legal-content/EN/TXT/PDF/?uri=CELEX:42013X0624(01)&from=EN (accessed on 12 May 2022).
26. Mendoza Villafuerte, P.; Suarez Bertoa, R.; Giechaskiel, B.; Riccobono, F.; Bulgheroni, C.; Astorga, C.; Perujo, A. NO_x, NH_3, N_2O and PN real driving emissions from a Euro VI heavy-duty vehicle. Impact of regulatory on-road test conditions on emissions. *Sci. Total Environ.* **2017**, *609*, 546–555. [CrossRef]
27. Commission Regulation (EU) No 582/2011 of 25 May 2011, Implementing and Amending Regulation (EC) No 595/2009 of the European Parliament and of the Council with Respect to Emissions from Heavy Duty Vehicles (Euro VI) and Amending Annexes I and III to Directive 2007/46/EC of the European Parliament and of the Council. EU COM/582/2011. Available online: https://eur-lex.europa.eu/legal-content/EN/TXT/HTML/?uri=CELEX:32011R0582&from=EN#ntr4-L_2011167FI.01008101-E0004 (accessed on 6 May 2022).

28. Van den Brink, P.J.; McDonald, C.M. Influence of the fuel hydrocarbon composition on nitric oxide conversion in 3-way catalysts: The NO_x/aromatics effect. *Appl. Catal. B Environ.* **1995**, *6*, 97–103. [CrossRef]
29. Matam, S.K.; Otal, E.H.; Aguirre, M.H.; Winkler, A.; Ulrich, A.; Ulrich, A.; Rentsch, D.; Weidenkaff, A.; Ferri, D. Thermal and chemical aging of model three-way catalyst Pd/Al2O3 and its impact on the conversion of CNG vehicle exhaust. *Catal. Today* **2012**, *184*, 237–244. [CrossRef]
30. Winkler, A.; Dimopoulos, P.; Hauert, R.; Bach, C.; Aguirre, M. Catalytic activity and aging phenomena of three-way catalysts in a compressed natural gas/gasoline powered passenger car. *Appl. Catal. B Environ.* **2008**, *84*, 162–169. [CrossRef]
31. Jääskeläinen, H. Three Way Catalysts for Methane. DieselNet Technology Guide. Revision 2017.12. Available online: https://dieselnet.com/tech/catalyst_methane_three-way.php (accessed on 21 June 2022).
32. Auvinen, P.; Nevalainen, P.; Suvanto, M.; Oliva, F.; Llamas, X.; Barciela, B.; Sippula, O.; Kinnunen, N.M. A detailed study on regeneration of SO_2 poisoned exhaust gas after-treatment catalysts: In pursuance of high durability and low methane, NH_3 and N_2O emissions of heavy-duty vehicles. *Fuel* **2021**, *291*, 120223. [CrossRef]
33. Zheng, Q.; Farrauto, R.; Deeba, M.; Valsamakis, I. Part I: A Comparative Thermal Aging Study on the Regenerability of Rh/Al2O3 and Rh/CexOy-ZrO_2 as Model Catalysts for Automotive Three Way Catalysts. *Catalysts* **2015**, *5*, 1770–1796. [CrossRef]
34. Lou, D.; Ren, Y.; Li, X.; Zhang, Y.; Sun, X. Effect of Operating Conditions and TWC Parameters on Emissions Characteristics of a Stoichiometric Natural Gas Engine. *Energies* **2020**, *13*, 4905. [CrossRef]
35. Commission Regulation (EU) 2016/1718 of 20 September 2016 Amending Regulation (EU) No 582/2011 with Respect to Emissions from Heavy-Duty Vehicles as Regards the Provisions on Testing by Means of Portable Emission Measurement Systems (PEMS) and the Procedure for the Testing of the Durability of Replacement Pollution Control Devices. Available online: https://eur-lex.europa.eu/legal-content/EN/TXT/HTML/?uri=CELEX:32016R1718&from=EN (accessed on 12 May 2022).
36. Systemic. Stormossen Ab/Oy (Vaasa/Korsholm, Finland). *SYSTEMIC Circular Solutions for Biowaste.* Available online: https://systemicproject.eu/wp-content/uploads/Stormossen_fact-sheet-Associated-plants_20191003.pdf (accessed on 2 May 2022).
37. Stormossen. Annual Report 2020. Available online: https://ar2020.stormossen.fi/annual_report/vuosikertomus-2020/tulostus/ (accessed on 2 May 2022).
38. TUV. Biogas to Biomethane Technology Review. Contract Number: IEE/10/130, Deliverable Reference: Task 3.1. TUV—Vienna University of Technology. Institute of Chemical Engineering, Research Division Thermal Process Engineering and Simulation. 2012. Available online: https://www.membran.at/downloads/2012_BioRegions_BiogasUpgradingTechnologyReview_ENGLISH.pdf (accessed on 2 May 2022).
39. Ardolino, F.M.; Cardamone, G.F.; Parrillo, F.; Arena, U. Biogas-to-biomethane upgrading: A comparative review and assessment in a life cycle perspective. *Renew. Sustain. Energy Rev.* **2021**, *139*, 110588. [CrossRef]
40. Uusitalo, V.; Havukainen, J.; Manninen, K.; Höhn, J.; Lehtonen, E.; Rasi, S.; Soukka, R.; Horttanainen, M. Carbon footprint of selected biomass to biogas production chains and GHG reduction potential in transportation use. *Renew. Energy* **2014**, *66*, 90–98. [CrossRef]
41. JRC. *Well-to-Wheels Analysis of Future Automotive Fuels and Powertrains in the European Context, Well-to-Tank Report Version 4.a*; European Commission Joint Research Centre (JRC): Brussels, Belgium, January 2014. [CrossRef]
42. StatFin. Fuel Classification. Statistics Finland. 2021. Available online: https://www.stat.fi/tup/khkinv/khkaasut_polttoaineluokitus.html (accessed on 3 May 2022).
43. Majer, S.; Oehmichen, K.; Kircshmeyr, F.; Scheidl, S. *Calculation of GHG Emission Caused by Biomethane. Biosurf. Fuelling Biomethane. Deliverable 5.3*; European Union: Brussels, Belgium, 2016. [CrossRef]
44. Bauer, F.; Hulteberg, C.; Persson, T.; Tamm, D. Biogas Upgrading—Review of Commercial Technologies. Swedish Gas Technology Centre, SGC Report 2013:270. Available online: https://www.sgc.se/ckfinder/userfiles/files/SGC270.pdf (accessed on 20 May 2022).
45. EEA. Indicators. Greenhouse Gas Emission Intensity of Electricity Generation in Europe. European Environment Agency. 2021. Available online: https://www.eea.europa.eu/ims/greenhouse-gas-emission-intensity-of-1 (accessed on 2 May 2022).
46. Söderena, P.; Nylund, N.-O.; Mäkinen, R. City Bus Performance Evaluation. VTT Technical Research Centre of Finland. VTT Report No. VTT-CR-00544-19. 2019. Available online: https://cris.vtt.fi/ws/portalfiles/portal/26400446/City_bus_performance_evaluation.pdf (accessed on 10 June 2022).

2021-01-1197 Published 21 Sep 2021

Effects of Crude Tall Oil Based Renewable Diesel on the Performance and Emissions of a Non-Road Diesel Engine

Kirsi Spoof-Tuomi Univ Of Vaasa

Ville Vauhkonen UPM-Kymmene Corp

Seppo Niemi, Teemu Ovaska, Vilja Lehtonen, Sonja Heikkilä, and Olav Nilsson Univ Of Vaasa

Citation: Spoof-Tuomi, K., Vauhkonen, V., Niemi, S., Ovaska, T. et al., "Effects of Crude Tall Oil Based Renewable Diesel on the Performance and Emissions of a Non-Road Diesel Engine," SAE Technical Paper 2021-01-1197, 2021, doi:10.4271/2021-01-1197.

Abstract

Environmental concerns and government policies aiming to increase biofuel shares have led to the search for alternative fuels from a variety of renewable raw materials. The development of hydrotreated vegetable oil (HVO) type fuels has been strong in the Nordic countries, partly due to the early use of tall oil from the forest industry as feedstock. An innovative production process to convert crude tall oil (CTO) - a residue of pulp production - into high-quality renewable diesel fuel was developed by a Finnish forestry company UPM. Paraffinic, high cetane and low aromatic CTO renewable diesel allows efficient and clean combustion, resulting in reductions of local air pollution in addition to not releasing any new CO_2 into the atmosphere during their combustion. This research investigated the influence of CTO renewable diesel on the performance and exhaust emissions of a non-road diesel engine. The examined fuels were neat CTO renewable diesel (BVN) and a blend of BVN and fossil diesel fuel oil (DFO) (50/50% v/v). Neat DFO served as the reference fuel. During a thorough test bench campaign, the engine was driven with the loads of the ISO 8178-4 C1 test cycle. The test engine had no exhaust after-treatment system, and no engine modifications or parameter optimizations were made during the tests. CTO renewable diesel proved to be beneficial in terms of CO, HC and particle number (PN) emissions. With neat BVN, a reduction of 9 % for CO, 10 % for HC, and 10% for PN compared with DFO were observed. The beneficial trends were most evident at low loads. Renewable fuel also slightly reduced brake specific NO_x emissions. CTO renewable diesel proved to be a high-quality, sustainable alternative to fossil diesel and fully compatible with existing non-road diesel engines.

1. Introduction

Today, heavy-duty road transportation and non-road applications are almost entirely powered by internal combustion engines (ICE) in which the petroleum-derived liquid fuels are burned [1, 2]. Diesel engines are recognized as superior power sources among the ICE family due to their fuel efficiency, strength and durability [3]. Liquid fossil fuels have become the predominant transport fuel due to their high energy density and ease of distribution and storage, and a vast global infrastructure has been built over the past century to support this system [4].

At the same time, there is a global understanding of the need to reduce emissions of air pollutants and greenhouse gas (GHG) emissions, encouraging the development and adoption of alternative energy sources. In September 2020, the European Commission decided on increasingly stringent GHG emission reduction targets. The new goal is to reduce EU GHG emissions by at least 55% by 2030, compared to 1990 levels [5]. This is a substantial increase from the earlier target of 40%. This level of ambition for the next decade is expected to set Europe on a balanced pathway to becoming climate neutral by 2050 - an economy with net-zero GHG emissions.

Climate strategies will inevitably affect the design solution of non-road mobile machinery (NRMM) and heavy-duty vehicles (HDV). Although internal combustion engines are still undergoing continuous further improvements with, e.g., advances in combustion technologies [6], the sole increase of energy efficiency of the conventional technology will not be sufficient by itself to meet the current emissions target levels. Therefore, alternatives not relying exclusively on the combustion of fossil fuels will undoubtedly be required [7].

All solutions are needed to achieve climate targets. Indeed, powertrain electrification is a growing trend in light-duty vehicle applications [7]. Electrification of heavy equipment is, however, still in its infancy. This segment will also be the most difficult to electrify due to the high energy demand [8]. The energy density of today´s batteries is not even close to that of diesel fuel [7], and the expected large battery capacities would burden vehicle weight and reduce the payload capacity. In addition, the cost would be high and the charging time

long. For non-road machinery operating for extended periods far away from charging infrastructure, the issue of battery technology is even more complicated. There are also doubts whether the global lithium resources will be able to sustain the simultaneous mass electrification of both light and heavy segments [9]. Moreover, concerns of the human toxicity impacts associated with the extraction of metals needed for batteries are growing [2].

Based on the above arguments, robust and efficient diesel engines are expected to continue to power heavy machinery and HDV to a large extent for decades to come [2,4,6,8]. As the GHG reductions of the required magnitude cannot be achieved through energy efficiency measures alone, a large-scale deployment of advanced liquid biofuels is needed in parallel [8]. There is a huge potential to significantly and realistically improve the sustainability of IC engines in the short- and medium-term through the development and deployment of renewable liquid fuels. Extensive existing distribution infrastructure can support such initiatives without modification or investment [4].

Hydrotreating vegetable oils or waste animal fats is a sustainable way to produce high-quality bio-based diesel fuel [10]. To clarify the distinction between first-generation biodiesels (fatty acid methyl esters, FAME), these fuels are referred to as 'renewable diesel' [11]. Renewable diesel is chemically identical to its petroleum counterpart, making it a complete drop-in replacement for fossil diesel fuel [12]. It works on all diesel engines without blending limits or modifications to the engines or fuel distribution infrastructure.

Renewable diesel overcomes many of the sustainability issues associated with first-generation biofuels. Notably, they do not compete with food resources, as they are produced from non-food crops, including agricultural and forest residues, dedicated energy crops, and industrial wastes [13, 14]. Moreover, paraffinic, high cetane, sulfur- and aromatic-free renewable diesel does not have the detrimental effects typical for ester-type biodiesels, such as deposit formation, storage stability problems, or poor cold properties [10]. Major CO_2 savings are based on the fact that the production of biofuels from organic waste results in fuels that contain only biogenic carbon [15], i.e., atmospheric carbon that was captured via biomass growth. Combustion of these fuels is considered carbon-neutral, as it does not release any new CO_2 into the atmosphere.

The development of renewable HVO type diesel fuels has been active in recent years, and many studies have confirmed the emissions benefits of HVO type fuels. Considerable reductions in engine-out CO, unburnt HC, and particulate matter (PM) emissions have been reported by [16, 17, 18, 19]. For example, Kuronen et al. [16] examined neat HVO on two heavy-duty engines and two city buses. The reference fuel was sulfur-free EN 590 diesel fuel. For HVO, PM was reduced by 28-46%, CO by 5-78%, and HC by 0-48%. In [19], a non-road diesel engine was driven with different fuel blends of traditional fossil diesel fuel and CTO based renewable diesel. With neat renewable diesel, a reduction of 21% in HC, 15% in CO, and 27% in PN compared with fossil diesel was reported. The main reasons for reduced CO and HC emissions were assumed to be the low aromatic content and the higher cetane number of the CTO renewable fuel, also suggested by [20].

The reductions in NO_x emissions from using HVO are reported more inconsistently in the open literature, with considerable reductions reported by some researchers, while others [19,21,22] did not measure meaningful differences between the fuels. Both NO_x reduction and improvements in PM formation using HVO have been reported, e.g., by [10, 23]. Nylund et al. [23] examined 17 city buses and found average reductions of 10% for NO_x, 30% for PM, 30% for CO, and 40% for unburned HC when switching from regular diesel to 100% HVO. In [10], smoke emissions were reduced by 35% with HVO without any modifications to the engine control. At the same time, a 6% decrease in NO_x emissions was detected. Bohl et al. [24] reported a simultaneous NO_x reduction of 10% and PM reduction of 36% after optimizing injection parameters.

The present study aimed to investigate how HVO-type renewable fuel affects a high-speed, non-road diesel engine´s performance and exhaust emissions. The renewable BVN was studied as neat and restrictedly as a 50% blend with conventional fossil diesel. Neat low-sulfur DFO served as the reference fuel. During a thorough test bench campaign, the engine was driven at eight steady state load points which were based on the loads of the ISO 8178-4 standard´s non-road steady-state cycle C1. The test engine had no exhaust after-treatment system, meaning that raw engine-out emissions were recorded during the experiments. In addition to gaseous emissions, PN emissions and particle size distributions (PSD) were determined. All fuels were studied with similar engine settings, and no engine modifications or parameter optimizations were made during the tests.

2. Experimental Setup

The engine experiments were performed by the University of Vaasa at the IC engine laboratory of the Technobothnia laboratory unit in Vaasa, Finland.

2.1. Fuels

The studied HVO was BioVerno supplied by a Finnish forestry company UPM. The fuel batch examined in this study represents UPM's normal commercial production. UPM´s renewable diesel production process is based on hydrotreatment of CTO, a wood-based residue of the chemical pulping process. CTO is a mixture of fatty acids with a carbon chain of 16 to 20 carbons (36-58%), rosin acids (10-42%), and sterols and neutral substances (10-38%). The composition varies depending on many factors, such as tree species and the growing cycle and age of the tree, geographical location, time of the year, and the pulping conditions. [25]

The production process of CTO-based renewable diesel fuel is presented in Figure 1. At first, crude tall oil - an organic, water-immiscible liquid from a pulp mill - is purified from solid particles, elements and metals, and other contaminants. These impurities have to be reduced to ppm level or less to ensure the hydrogenation catalysts' functionality. Hydrotreatment is carried out in the biorefinery's hydrotreatment unit at a pressure range of 2-12 MPa and a temperature

FIGURE 1 CTO-based renewable fuel production process.

range of 280-430 °C. The actual hydrotreating is performed in a plug flow reactor using catalysts capable of simultaneous hydro-deoxygenation, hydrodesulfurization, isomerization, hydrogenation, and cracking. Next, the remaining hydrogen sulfide and incondensable gases are removed. Finally, the hydrotreated CTO "raw diesel" containing mid-distillate diesel components and lighter naphtha components is distilled, i.e., fractionated to renewable diesel and naphtha. [25] Table 1 shows the main specification of the three studied fuels and also lists the limits of the European diesel specification EN 590.

The BVN-DFO blend fully met the requirements of the EN 590. For neat BVN, however, the density was slightly below the minimum limit of 820 kg/m^3, and 95% distillation slightly exceeded the maximum of 360°C defined in EN 590. The PAH content of BVN and the blend was significantly lower than that of DFO. The cetane number - an ignitability indicator for diesel fuels - of BVN and the blend was higher than that of the reference fuel. A high cetane number is advantageous in terms of cold start, noise and emissions [26].

TABLE 1 Properties of the test fuels analyzed by ASG Analytik-Service GmbH.

Parameter	Test method	Unit	DFO	BVN-DFO 50/50	BVN	Specification EN 590:2014	
						min	max
Cetane Number	DIN EN 17155	-	57.5	61.5	65.2	51.0	-
Cetane Index	DIN EN ISO 4264	-	57.0	63.4	71.2	46.0	-
Density (15°C)	DIN EN ISO 12185	kg/m^3	836	826	815	820	845
PAH content	DIN EN 12916	% (m/m)	2.7	1.4	0.1	-	8.0
Total aromatics	DIN EN 12916	% (m/m)	23.8	12.9	2.0		
Sulphur content	DIN EN ISO 20884	mg/kg	7.9	<5	<5	-	10
Flash Point	DIN EN ISO 2719	°C	67.5	73.0	77.0	>55	-
Carbon residue (10% Dist.)	DIN EN ISO 10370	% (m/m)	<0.10	<0.01	<0.1	-	0.30
Ash Content (775°C)	DIN EN ISO 6245	% (m/m)	<0.001	<0.001	<0.001	-	0.1
Water content	DIN EN ISO 12937	mg/kg	32	19	21	-	200
Total contamination	DIN EN 12662	mg/kg	<12	<12	<12	-	24
Copper strip corrosion	DIN EN ISO 2160	Korr. Grad.	1	1	1	-	1
FAME content	DIN EN 14078	% (V/V)	<0.1	<0.1	<0.1	-	7.0
Oxidation stability	DIN EN ISO 12205	g/m^3	<1	<1	<1	-	25
filterable insolubles		g/m^3	<1	<1		-	-
adherent insolubles		g/m^3	<1	<1		-	-
HFRR (Lubricity at 60°C)	DIN EN ISO 12156	µm	<460	<460	<460	-	460
Kin. Viscosity (40°C)	DIN EN ISO 3104	mm^2/s	3.3	3.4	3.5	2.0	4.5
% (V/V) recovery at 250°C	DIN EN ISO 3924	% (V/V)	22.7	19.8	15.9	-	<65
% (V/V) recovery at 350°C		% (V/V)	93.4	93.1	92.2	85	-
95% (V/V) recovery		°C	354	358	372	-	360
CFPP	DIN EN 116	°C	-12	-14	-14	-	*
Manganese (Mn)	DIN EN 16576	mg/l	<0.5	<0.5	<0.5	-	2.0
Surface tension (20°C)	DIN EN 14370	mN/m	28.3	28.1	27.9		
Calorific value, lower	DIN 51900-2	MJ/kg	42.8	43.2	43.4	-	-

* According national specifications

2.2. Engine

The experiments were performed with a four-cylinder, turbocharged, intercooled non-road diesel engine, equipped with a common-rail fuel injection system. The test engine was mounted on a test bench and loaded with a Horiba eddy-current dynamometer WT 300. A Horiba SPARC controller platform was used to control engine speed, torque and throttle. The engine was not equipped with exhaust gas after-treatment devices, meaning that raw engine-out emissions were recorded during the experiments. The main specification of the test engine is given in Table 2.

2.3. Analytical Procedures

The measurement setup for regulated gaseous emissions consisted of typical type-approval grade methods: a non-dispersive infrared (NDIR) analyzer to record CO and CO_2 concentrations, a chemiluminescence detector (CLD) for recording NO_x, and a heated flame ionization detector for HC. In addition, several unregulated gaseous compounds were recorded using a Fourier transformation infrared (FTIR) analyzer. PN and PSD were measured using an engine exhaust particle sizer (EEPS) spectrometer. Prior to emission measurements, the analyzers were calibrated according to the instrument manufacturer's instructions. The brake-specific emissions results were calculated from the recorded data of the pollutant concentrations according to the ISO 8178 standard.

For the determination of the exhaust PN, the raw exhaust was sampled. The sample was diluted with a rotating disc diluter (MD19-E3, Matter Engineering AG) using a constant dilution ratio of 60:1. For the EEPS, the diluted sample was further diluted by purified air with a dilution ratio of 2:1. Thus, the overall dilution ratio was 120:1. The sample flow rate of EEPS was adjusted at 5.0 dm^3/min before the measurement. Periods of three minutes were chosen for the PN and size distribution results, during which the total concentration of particles was as stable as possible. Mean values with standard deviations were calculated from the particle numbers measured during these three-minute time intervals. For gaseous emission, only momentary values at the time of measurement for each load point were available. Therefore, due to the lack of continuous measurement data, the standard deviations of gaseous emissions could not be determined.

TABLE 2 Test engine specification.

Engine	AGCO POWER 44 AWI
Cylinder number	4
Bore (mm)	108
Stroke (mm)	120
Swept volume (dm^3)	4.4
Rated speed (rpm)	2200
Rated power (kW)	103
Rated maximum torque at rated speed (Nm)	446
Maximum torque at 1500 rpm (Nm)	560

Table 3 summarizes the methods and instruments adopted for the measurements. The schematic representation of the experimental setup is shown in Figure 2.

The sensor data were collected using software made in the LabVIEW system-design platform. In addition to gaseous and PN emissions, the recorded quantities included engine speed and torque and several fluid temperatures and fluid pressures, such as temperatures of cooling water, intake air and exhaust gas, and intake air and exhaust pressures. The engine control functions were monitored with AGCO SISU Power WinEEM4 software. No engine parameter optimizations were applied during the tests, and all fuels were studied using similar engine settings. Engine warm-up and measurement procedures were identical for all fuels.

For combustion analysis, the heat release rate (HRR) and the mass fraction burned (MFB) were determined based on the in-cylinder pressure data, measured with a piezoelectric Kistler 6125C pressure sensor. The signal was filtered and amplified by a charge amplifier and transferred to a Kistler KIBOX combustion analyzer. A Kistler 2614B1 crank angle encoder recorded the crankshaft position. To smooth out irregular combustion, the cylinder pressure data were averaged over 100 consecutive cycles.

TABLE 3 Analytical instruments.

Parameter	Measuring device	Technology
NO_x	Eco Physics CLD 822 M hr	Chemiluminescence
CO, CO_2	Siemens Ultramat 6	NDIR
HC	J.U.M. VE7	HFID
O_2	Siemens Oxymat 61	Paramagnetic
PN and PSD	TSI EEPS 3090	Spectrometer
Smoke	AVL 415 S	Optical filter
Unregulated gaseous emissions	Gasmet DX4000	FTIR
Air mass flow	ABB Sensyflow P	Hot-film anemometer
Cylinder pressure	Kistler KiBox	

FIGURE 2 Experimental set-up.

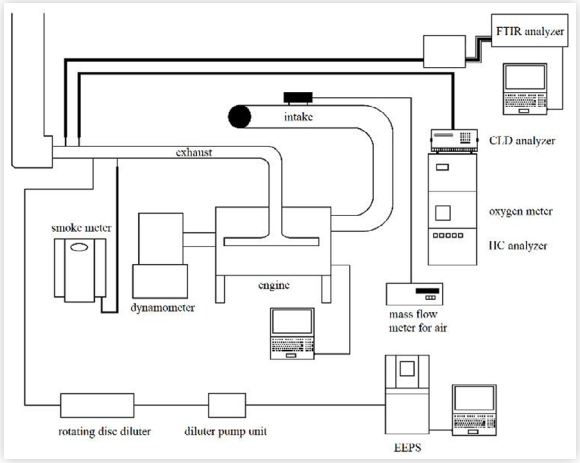

HRR and MFB were calculated using the AVL Concerto data post-processing tool. The average values of in-cylinder pressures and the Thermodynamics2 macro with a calculation resolution of 0.2°CA were used to calculate HRR values. Thereafter, the HRR curves were filtered with a DigitalFilter macro and a frequency of 4,000 Hz. For MFB results, the cylinder pressure values were first filtered, and after that, the macro was used. For MFB calculations, the pressure values were not averaged to determine the standard deviations for 100 consecutive cycles.

2.4. Experimental Matrix

Performance and emission measurements were conducted at eight steady state load points following the modes of the ISO 8178-4 C1 test cycle. The C1 cycle is also referred to as the non-road steady cycle (NRSC). The test engine's rated speed was 2200 rpm, and the intermediate speed was chosen to be 1500 rpm. At idle, the engine speed was 860 rpm. Table 4 lists the loading points or modes, the corresponding engine speeds, loads and torques, and the NRSC weighting factors (WF) for the different modes.

Before initiating the measurements, it was always waited that the engine run had stabilized. The main criteria were that the intake air and exhaust gas temperatures were stable.

3. Results and Discussion

3.1. Measurement Conditions

The range of ambient temperature variation was 2-4°C between the test runs. The relative humidity ranged from 13 to 18%. The ambient pressure was 97 kPa for the blend and 100-101 kPa for DFO and BVN during the measurements. The ambient conditions were not considered to noticeably affect the results as they were very similar for each fuel.

3.2. Combustion Analysis

Maximum cylinder pressures for DFO and BVN were very similar at all speed and load configurations. The BVN-DFO blend consistently showed slightly lower peaks of cylinder pressure compared to the other two fuels. Figure 3 depicts cylinder pressure at rated speed at 75% load. Maximum cylinder pressure at this point for DFO and BVN was 106 bar and for the blend 105 bar. Nonetheless, the pressure curves were very similar, indicating that combustion propagated quite similar way with all three fuels.

TABLE 4 Experimental matrix.

Mode	1	2	3	4	5	6	7	8
Speed (rpm)	2200	2200	2200	2200	1500	1500	1500	860
Load (%)	100	75	50	10	100	75	50	0
Torque (Nm)	446	334	223	45	560	420	280	1
WF	0.15	0.15	0.15	0.1	0.1	0.1	0.1	0.15

FIGURE 3 Cylinder pressure against crank angle at rated speed at 75% load for the studied fuels.

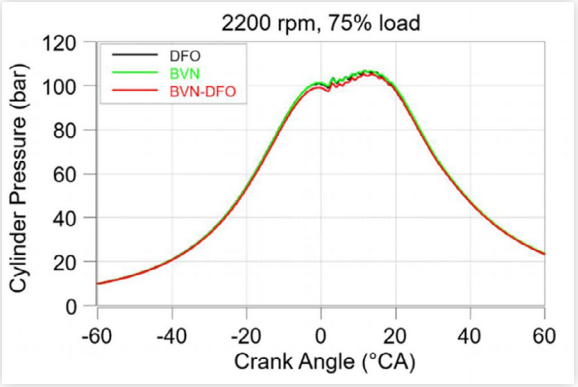

Table 5 illustrates 10%, 50%, and 90% MFB points for each fuel at rated speed at 75% load and intermediate speed at 50% load. Standard deviations of crank angles at MFB 10%, MFB 50% and MFB 90%, calculated from 100 consecutive engine cycles, are also given. BVN had the earliest crank angle positions of MFB 10% at both load points. This was consistent with the highest cetane number of BVN and presumably a shorter ignition delay. The latest MFB 90%, and a shade longer combustion duration (CD), was measured for the BVN-DFO blend. This was also evident in the cylinder pressures, which were slightly lower with the blend than with the other fuels (Figure 3). Otherwise, no significant differences in combustion durations were detected, defined herein as the crank angle duration from MBF 10% to MBF 90%. MFB 50% values were very similar for all fuels studied.

Figure 4 illustrates HRR at rated speed at 75% load. No pilot injection was used at this load point. Despite the differences in cetane numbers (Table 1), the HRR curves were quite similar for all fuels studied. A slightly lower peak in premixed combustion was observed for BVN and the blend compared to DFO.

TABLE 5 Mass fraction burned, standard deviations and combustion durations at rated speed at 75% load and intermediate speed at 50% load.

	MFB 10%	Stdev	MFB 50%	Stdev	MFB 90%	Stdev	CD MFB10-90%
	°CA	°CA	°CA	°CA	°CA	°CA	°CA
Mode 2							
DFO	8.0	0.090	17	0.12	32	0.47	24
BVN-DFO	8.0	0.095	17	0.12	33	0.48	25
BVN	7.8	0.094	17	0.11	32	0.39	24
Mode 7							
DFO	8.7	0.063	14	0.078	27	0.27	18
BVN-DFO	8.7	0.065	14	0.089	27	0.32	19
BVN	8.6	0.072	14	0.078	27	0.24	18

FIGURE 4 HRR as a function of crank angle at rated speed at 75% load for the studied fuels.

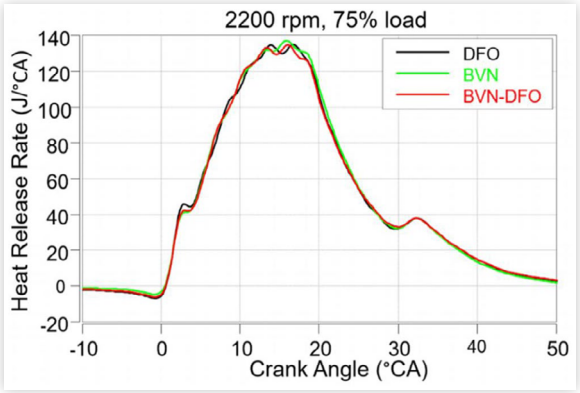

3.3. Efficiency

The engine brake thermal efficiency (BTE) was very similar for all fuels at all load and speed configurations. Figure 5 illustrates the efficiency at intermediate speed. At a brake mean effective pressure (BMEP) of 16 bar, the BTE varied from 40.5% for blend to 40.8% for BVN and DFO.

3.4. Gaseous Emissions

Over the eight-mode cycle, both BVN and BVN-DFO blend slightly reduced NO_x emissions, as shown in Figure 6. The largest reduction was achieved with the blend emitting 3.4% less NO_x than the baseline DFO. With BVN, the NO_x reduction was 2.6% compared to fossil diesel. Throughout the cycle with weightings, the NO_x for DFO was 7.9 g/kWh, for BVN 7.7 g/kWh and for blend 7.6 g/kWh, also showing that the engine was tuned for high NO_x - and high efficiency - and intended for the later use of an efficient catalyst system for clear NO_x reduction.

The improved NO_x outcome with BVN could be explained by the fuel properties. NO_x formation is reduced with fuels having lower aromatic content as aromatic compounds have higher adiabatic flame temperature and thereby produce higher local combustion temperatures [27, 28]. In the case of the BVN-DFO blend, the lower NO_x could be attributed to a slightly longer combustion duration resulting in lower cylinder pressure and temperature peaks.

In general, HC and CO emissions are low for lean-burn engines. However, the use of CTO-based renewable diesel reduced them further compared to conventional diesel fuel, as shown in Figure. 7. Throughout the cycle with weightings, the CO emissions were 0.24 g/kWh for neat BVN, 0.26 g/kWh

FIGURE 5 Engine brake thermal efficiency against engine load at intermediate speed.

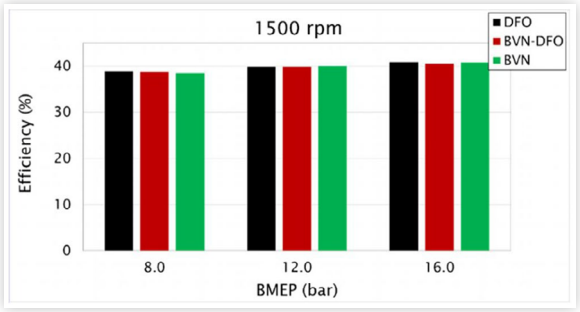

FIGURE 6 Cycle-weighed NO_x emissions for the studied fuels.

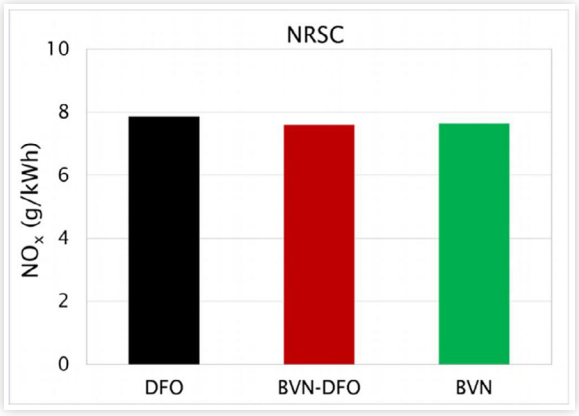

FIGURE 7 Cycle-weighted CO and HC emissions with the studied fuels.

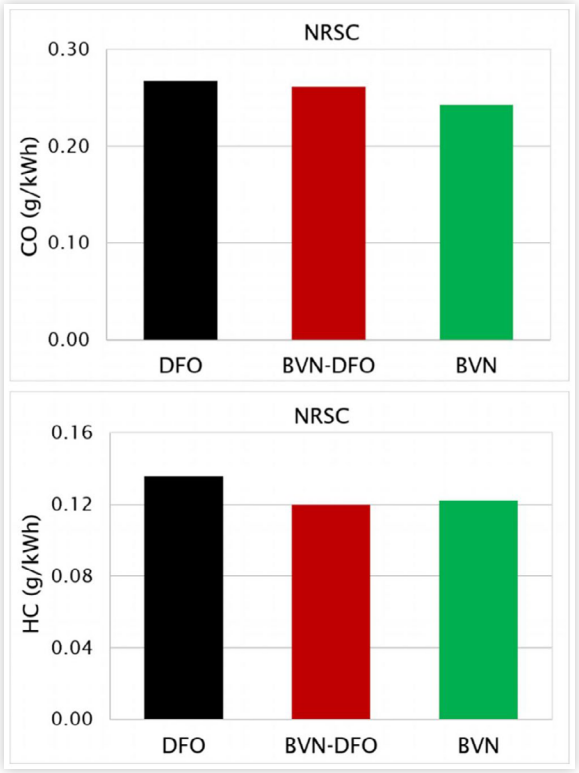

FIGURE 8 Relative changes in cycle-weighted brake specific emissions. DFO forms the baseline.

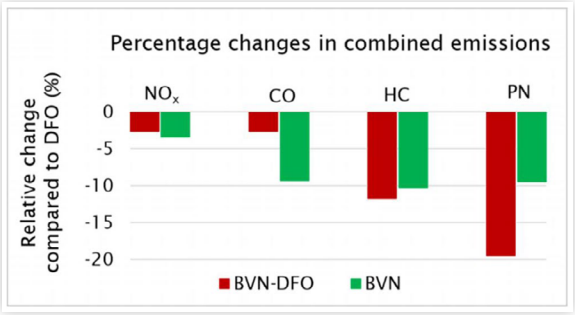

for BVN-DFO blend and 0.27 for DFO. Compared to fossil diesel, the percentage reduction for neat BVN was 9%.

Quite similar trend was observed for HC emissions. BVN and the blend produced the lowest HC, 0.12 g/kWh for both fuels. DFO´s HC emissions were 0.14 g/kWh. The percentage reduction for neat BVN was 10% compared to fossil diesel. The reason for lower HC emissions were assumed to be the better ignitability of HVO, limiting the overmixing effect. The absence of aromatics can also be expected to reduce HC emissions in the exhaust gas [24].

HC and CO emissions for all fuels were well below the EU Stage V and US Tier 4 emission limits for non-road engines (0.19 g/kWh for HC and 5.00 g/kWh for CO).

Figure 8 summarizes the percentage changes in regulated emissions. DFO forms the baseline. In addition to gaseous emissions, relative changes in particle numbers are presented. PN results are discussed in more detail in Section 3.5.

From the recorded unregulated gaseous emissions, nitrous oxide (N_2O) concentrations were low at all loads and almost equal for all three fuels. N_2O generally ranged from 0.4 to 0.8 ppm, but at full load at 1500 rpm, it was 0.1 ppm.

The wet exhaust methane (CH_4) contents were also low at all loads. The highest concentrations were recorded at 10% load at 2200 rpm (0.9 ppm for DFO, 0.6 ppm for the blend, and 0.7 ppm for BVN) and at half load at 2200 rpm (0.4 ppm for DFO, <0.1 ppm for the blend, and 0.3 ppm for BVN). At higher loads, CH_4 content was always below 0.1 ppm for all fuels.

The wet exhaust formaldehyde concentrations peaked at half load at 2200 rpm (3.0 for DFO and the blend, and 2.2 for BVN). Otherwise, it varied between 0.1 and 2.1 ppm, BVN having the lowest formaldehyde concentration at all loads.

Overall, with regard to unregulated emissions, the differences between fuels were negligible, and the recorded levels were close to the measuring accuracy.

3.5. PN Emission and Smoke

The effect of CTO-based renewable diesel on PSD at four different load points is shown in Figure 9. The averages of PN concentrations are presented as data points and combined with lines. The shaded area depicts the standard deviation. One peak of the bimodal PSD was detected at a particle diameter of 10 nm, the other at approx. 35 nm, even though the latter was not observed at all loads.

At higher loads, no consistent trend was observed in PSD between the fuels. In contrast, at idle, both BVN and the blend resulted in a clear reduction of nuclei mode (10 nm) PN emissions. This can be explained by near-zero sulfur and low aromatics content of BVN, also concluded by [29]. Marasri et al. [30] also pointed out that, at low temperatures, lower density fuel might be more easily atomized, vaporized, and mixed with air in the combustion chamber, leading to improved combustion.

Figure. 10 depicts the weighted total PN emission within the size range of 5.6-560 nm over the eight-mode test cycle following the NRSC. When looking at these results, the blend was the most beneficial. Fueling with the BVN-DFO blend produced a total particle number (TPN) reduction of 20% compared with DFO. With neat BVN, TPN decreased by 10% compared with reference fuel.

The main reason for decreased PN was interpreted to be the beneficial hydrocarbon structure and low aromatics content of CTO renewable fuel. The more complete combustion was assumed to be due to the higher H/C ratio, also concluded by [31, 32]. Furthermore, BVN's aromatic free composition implies that less PAH, acting as soot precursors, are formed [33, 34]. On the other hand, as shown by [35], high-cetane fuels can also lead to lower soot emissions as a result of improved ignition quality and, thus, cleaner combustion.

With all fuels, smoke was low at all loads. For DFO, filter smoke number (FSN) values varied from 0.01 to 0.07, for the blend from 0.02 to 0.05, and for BVN from 0.01 to 0.05.

In the present study, the engine settings were not optimized for the combustion of paraffinic fuel. Further reductions in exhaust emissions could be achieved by adjusting engine parameters to take advantage of the properties of paraffinic fuel, as evidenced by [10,24,36].

4. Conclusions

This study investigated the effect of CTO-based renewable diesel fuel on the performance and exhaust emissions of a non-road diesel engine over the eight-mode steady state cycle that followed a standardized NRSC driving cycle C1. A combustion analysis was performed as well. Renewable diesel was studied as neat and as a 50% blend with conventional fossil diesel. Neat DFO served as the baseline fuel. All fuels were studied with similar engine settings, and no engine parameter optimizations were made during the tests.

Based on the performed research work, the main conclusions were:

- According to the combustion analysis, combustion propagated quite similar way with all three fuels. BVN and the blend generated a shade lower peaks of premixed combustion. MFB 50% values were, however, very similar for all fuels.

FIGURE 9 Particle size distributions at high load and low load conditions.

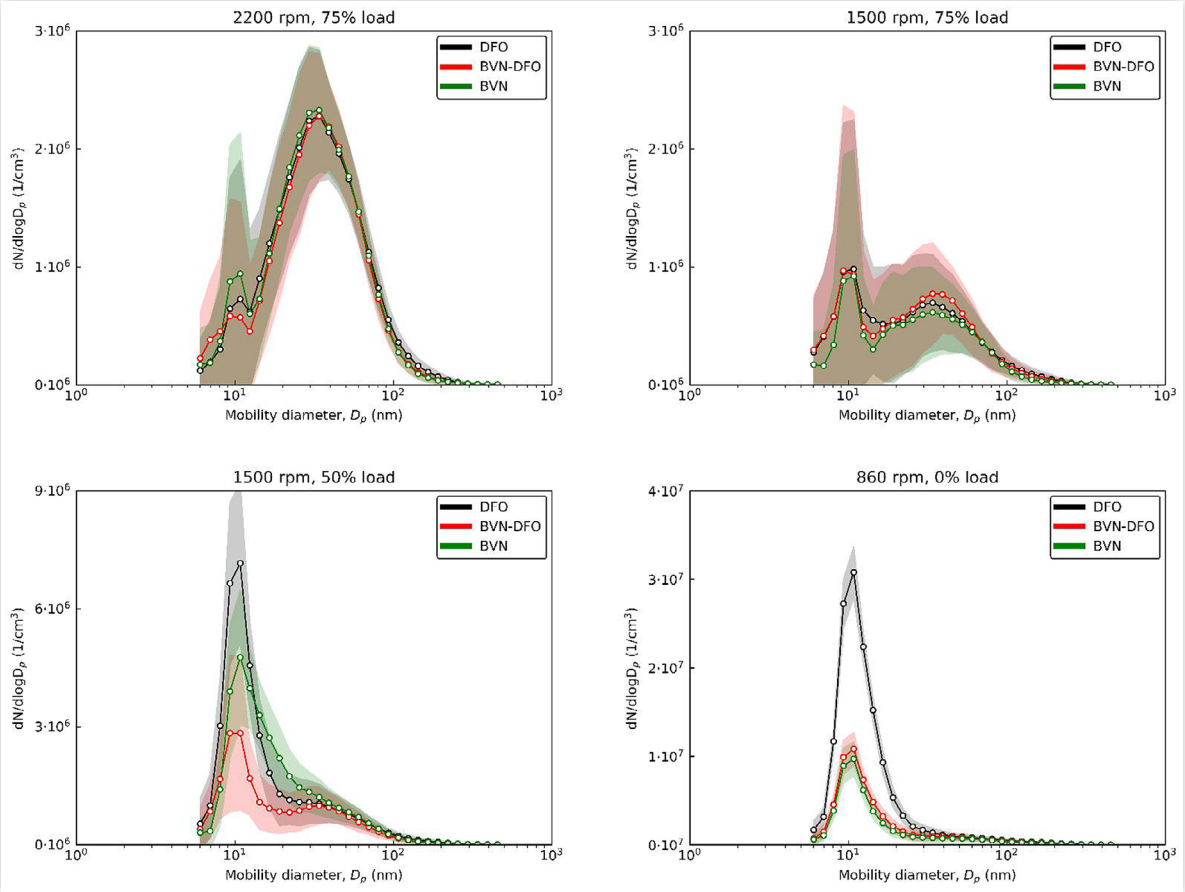

FIGURE 10 Total PN emission within the particle size range of 5.6 to 560 nm, weighted over the eight-mode cycle.

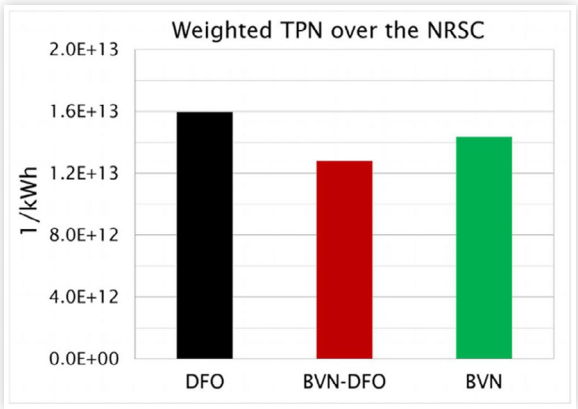

- The engine brake thermal efficiency was almost identical for all fuels throughout the load-speed range of the test engine.
- Over the eight-mode cycle, both BVN and BVN-DFO blend reduced NO_x emissions by approx. 3% compared to fossil DFO.
- The cycle-weighted CO emissions reduced by 9% with BVN and 3% with the blend. HC emissions reduced by 10% with BVN and 12% with the blend. The reason for lower HC emissions were assumed to be the better ignitability of CTO renewable fuel.
- The wet exhaust gas concentrations of nitrous oxide, methane, and formaldehyde were negligible with all fuels.
- Fueling with the BVN-DFO blend produced a TPN reduction of 20% compared with the reference fuel. With neat BVN, TPN decreased by 10% compared with DFO. The main reason for decreased PN was interpreted to be the beneficial hydrocarbon structure and near-zero sulfur and low aromatics content of CTO renewable fuel.

References

1. Niemi, S., Hissa, M., Ovaska, T., Sirviö, K. et al., "Performance and Emissions of a Non-Road Diesel Engine Driven with a Blend of Renewable Naphtha and Diesel Fuel Oil," in: Schubert, N. (Eds), *Fuels: Conventional and Future Energy for Automobiles: 12th International Colloquium Fuels - Conventional and Future Energy for Automobiles*, (Ostfildern, Deutschland: Technische Akademie Esslingen, 2019).
2. Kalghatgi, G., "Is it Really the End of Internal Combustion Engines and Petroleum in Transport?" *Applied Energy* 225 (2018): 965-974, doi:10.1016/j.apenergy.2018.05.076.
3. Gabiña, G., Martin, L., Basurko, O.C., Clemente, M. et al., "Performance of Marine Diesel Engine in Propulsion Mode with a Waste-Oil Based Alternative Fuel," *Fuel* 235 (2019): 259-268, doi:10.1016/j.fuel.2018.07.113.
4. Leach, F., Kalghatgi, G., Stone, R., and Miles, P., "The Scope for Improving the Efficiency and Environmental Impact of Internal Combustion Engines," *Transportation Engineering* 1 (2020): 100005, doi:10.1016/j.treng.2020.100005.
5. EU COM/2020/562. Communication from the Commission to the European Parliament, the Council, the European Economic and Social Committee and the Committee of the Regions. Stepping up Europe's 2030 Climate Ambition. Investing in a Climate-Neutral Future for the Benefit of our People. EU COM/2020/562 Final. https://eur-lex.europa.eu/legal-content/EN/ALL/?uri=CELEX:52020DC0562.
6. Reitz, R.D., Ogawa, H., Payri, R., Fansler, T. et al., "The Future of the Internal Combustion Engine," *Int. J. Engine Res.* 21, no. 1 (2020): 3-10, doi:10.1177/1468087419877990.
7. Lajunen, A., Sainio, P., Laurila, L., Pippuri-Mäkeläinen, J. et al., "Overview of Powertrain Electrification and Future Scenarios for Non-Road Mobile Machinery," *Energies* 11 (2018): 1184, doi:10.3390/en11051184.
8. ERTRAC, "Future Light and Heavy Duty ICE Powertrain Technologies," ERTRAC Working Group Energy and Environment, 2016, https://www.ertrac.org/uploads/documents_publications/Roadmap/2016-04-05_ICE_roadmap_edited%20version.pdf.
9. Hao, H., Geng, Y., Tate, J.E. et al., "Impact of Transport Electrification on Critical Metal Sustainability with a Focus on the Heavy-Duty Segment," *Nat Commun* 10 (2019): 5398, doi:10.1038/s41467-019-13400-1.
10. Aatola, H., Larmi, M., Sarjovaara, T., and Mikkonen, S., "Hydrotreated Vegetable Oil (HVO) as a Renewable Diesel Fuel: Trade-off between NOx, Particulate Emission, and Fuel Consumption of a Heavy Duty Engine," *SAE Int. J. Engines* 1, no. 1 (2009): 1251-1262. https://doi.org/10.4271/2008-01-2500.
11. Sarjovaara, T., "Studies on Heavy Duty Engine Fuel Alternatives," Doctoral dissertation, Department of Energy Technology, Aalto University, Finland, 2015, ISBN 978-952-60-6561-8.
12. Engman, A., Gauthier, Q., Hartikka, T., Honkanen, M., et al., "Neste Renewable Diesel Handbook," Neste Proprietary publication, Neste Corporation, Espoo, 2020, https://www.neste.com/sites/default/files/attachments/neste_renewable_diesel_handbook.pdf
13. Fokaides, P.A. and Christoforou, E., "Life Cycle Sustainability Assessment of Biofuels," in: Luque, R., Lin, C.S.K., Wilson, K. and Clark, J. (Eds), *Handbook of Biofuels Production*, 2nd ed., (Woodhead Publishing, 2016), 41-60, doi:10.1016/B978-0-08-100455-5.00003-5.
14. Sathitsuksanoh, N., Zhu, Z., Rollin, J., and Zhang, Y.-H.P., "Solvent Fractionation of Lignocellulosic Biomass," in: Waldron, K. (Eds), *Bioalcohol Production*, (Woodhead Publishing, 2010), 122-140, doi:10.1533/9781845699611.1.122.
15. Edwards, R., Larivé, J.F., Rickeard, D. and Weindorf, W., JEC Well-to-Wheels Analysis: Well-to-Wheels Analysis of Future Automotive Fuels and Powertrains in the European context, Well-to-Tank Report Version 4.0, JRC Technical reports, Publications Office of the European Union, July 2013, doi:10.2788/40526.
16. Kuronen, M., Mikkonen, S., Aakko, P., and Murtonen, T., "Hydrotreated Vegetable Oil as Fuel for Heavy Duty Diesel Engines," SAE Technical Paper 2007-01-4031 (2007). https://doi.org/10.4271/2007-01-4031.
17. Dimitriadis, A., Natsios, I., Dimaratos, A., Katsaounis, D. et al., "Evaluation of a Hydrotreated Vegetable Oil (HVO) and Effects on Emissions of a Passenger Car Diesel Engine," *Front. Mech. Eng.* 4, no. 7 (2018): 1-19, doi:10.3389/fmech.2018.00007.
18. Murtonen, T. and Aakko-Saksa, P., "Alternative Fuels with Heavy-Duty Engines and Vehicles: VTT's Contribution," VTT Technical Research Centre of Finland. VTT Working Papers No. 128, 2009, http://www.vtt.fi/inf/pdf/workingpapers/2009/W128.pdf
19. Niemi, S., Vauhkonen, V., Mannonen, S., Ovaska, T. et al., "Effects of Wood-Based Renewable Diesel Fuel Blends on the Performance and Emissions of a Non-Road Diesel Engine," *Fuel* 186 (2016): 1-10, doi:10.1016/j.fuel.2016.08.048.
20. Sugiyama, K., Goto, I., Kitano, K., Mogi, K. et al., "Effects of Hydrotreated Vegetable Oil (HVO) as Renewable Diesel Fuel on Combustion and Exhaust Emissions in Diesel Engine," *SAE Int. J. Fuels Lubr* 5, no. 1 (2012): 205-217.
21. Pflaum, H., Hofmann, P., Geringer, B., and Weissel, W., "Potential of Hydrogenated Vegetable Oil (HVO) in a Modern Diesel Engine," SAE Technical Paper 2010-32-0081 (2010). https://doi.org/10.4271/2010-32-0081.
22. Pirjola, L., Rönkkö, T., Saukko, E., Parviainen, H. et al., "Exhaust Emissions of Non-Road Mobile Machine: Real-World and Laboratory Studies with Diesel and HVO Fuels," *Fuel* 202 (2017): 154-164, doi:10.1016/j.fuel.2017.04.029.
23. Nylund, N.-O., Erkkilä, K., Ahtiainen, M., Murtonen, T. et al., "Optimized Usage of NExBTL Renewable Diesel Fuel OPTIBIO," VTT Technical Research Centre of Finland, Research notes 2604, ISBN 978-951-38-7795-8.
24. Bohl, T., Smallbone, A., Tian, G., and Roskilly, A.P., "Particulate Number and NOx Trade-off Comparisons Between HVO and Mineral Diesel in HD Applications," *Fuel* 215 (2018): 90-101, doi:10.1016/j.fuel.2017.11.023.

25. Heuser, B., Vauhkonen, V., Mannonen, S., Rohs, H. et al., "Crude Tall Oil-Based Renewable Diesel as a Blending Component in Passenger Car Diesel Engines," *SAE Int. J. Fuels Lubr.* 6, no. 3 (2013): 817-825, doi:10.4271/2013-01-2685.
26. Hartikka, T., Kuronen, M., and Kiiski, U., "Technical Performance of HVO (Hydrotreated Vegetable Oil) in Diesel Engines," SAE Technical Paper 2012-01-1585 (2012). https://doi.org/10.4271/2012-01-1585.
27. Glaude, P., Fournet, R., Bounaceur, R., and Molière, M., "Adiabatic Flame Temperature from Biofuels and Fossil Fuels and Derived Effect on NOx Emissions," *Fuel Processing Technology* 91, no. 2 (2010): 229-235, doi:10.1016/j.fuproc.2009.10.002.
28. Huang, Y., Wang, S., and Zhou, L., "Effects of Fischer-Tropsch Diesel Fuel on Combustion and Emissions of Direct Injection Diesel Engine," *Front. Energy Power Eng. China* 2, no. 3 (2008): 261-267, doi:10.1007/s11708-008-0062-x.
29. Ovaska, T., "Exhaust Particle Numbers of High- and Medium-Speed Diesel Engines with Renewable and Recycled Fuels," Doctoral thesis, School of Technology and Innovations. University of Vaasa, 2020, ISBN 978-952-476-929-7.
30. Marasri, S., Ewphun, P.P., Srichai, P. et al., "Combustion Characteristics of Hydrotreated Vegetable Oil-Diesel Blends under EGR and Low Temperature Combustion Conditions," *Int.J Automot. Technol.* 20 (2019): 569-578, doi:10.1007/s12239-019-0054-3.
31. Rimkus, A., Žaglinskis, J., Rapalis, P., and Skačkauskas, P., "Research on the Combustion, Energy and Emission Parameters of Diesel Fuel and a Biomass-to-Liquid (BTL) Fuel Blend in a Compression-Ignition Engine," *Energy Conversion and Management* 106 (2015): 1109-1117, doi:10.1016/j.enconman.2015.10.047.
32. Dimitriadis, A., Seljak, T., Vihar, R., Baškovič, U.Z. et al., "Improving PM-NOx Trade-off with Paraffinic Fuels: A study Towards Diesel Engine Optimization with HVO," *Fuel* 265 (2020): 116921, doi:10.1016/j.fuel.2019.116921.
33. Gill, S.S., Tsolakis, A., Dearn, K.D., and Rodríguez-Fernández, J., "Combustion Characteristics and Emissions of Fischer-Tropsch Diesel Fuels in IC Engines," *Prog Energy Combust Sci* 37 (2011): 503-523, doi:10.1016/j.pecs.2010.09.001.
34. Pastor, J.V., García-Oliver, J.M., Micó, C., García-Carrero, A.A. et al., "Experimental Study of the Effect of Hydrotreated Vegetable Oil and Oxymethylene Ethers on Main Spray and Combustion Characteristics under Engine Combustion Network Spray A Conditions," *Applied Sciences* 10, no. 16 (2020): 5460, doi:10.3390/app10165460.
35. Labeckas, G., Slavinskas, S., and Kanapkienė, I., "The Individual Effects of Cetane Number, Oxygen Content or Fuel Properties on Performance Efficiency, Exhaust Smoke and Emissions of a Turbocharged CRDI Diesel Engine - Part 2," *Energy Conversion and Management* 149 (2017): 442-466, doi:10.1016/j.enconman.2017.07.017.
36. Happonen, M., Heikkilä, J., Murtonen, T., Lehto, K. et al., "Reductions in Particulate and NO(x) Emissions by Diesel Engine Parameter Adjustments with HVO Fuel," *Environ Sci Technol.* 46, no. 11 (2012): 6198-6204, doi:10.1021/es300447t.

Contact Information

Kindly contact
Mrs. Kirsi Spoof-Tuomi
the University of Vaasa
PO Box 700, FI-65101 Vaasa, Finland
kirsi.spoof-tuomi@uwasa.fi

Acknowledgments

The authors wish to thank the company UPM for delivering renewable diesel fuel for the research.

Abbreviations

BMEP - brake mean effective pressure
BTE - brake thermal efficiency
CH_4 - methane
CLD - chemiluminescence detector
CA - crank angle
CD - combustion duration
CFPP - cold filter plugging point
CO - carbon monoxide
CTO - crude tall oil
DFO - diesel fuel oil
EEPS - engine exhaust particle sizer
EU - European Union
FAME - fatty acid methyl ester
FSN - filter smoke number
FTIR - Fourier-transform infra-red
GHG - greenhouse gas
HC - total hydrocarbons
HDV - heavy-duty vehicles
HFID - heated flame ionization detector
HFRR - high frequency reciprocating rig
HRR - heat release rate
HVO - hydrotreated vegetable oil
ICE - internal combustion engine
ISO - International Standard Organization
MFB - mass fraction burned
N_2O - nitrous oxide
NDIR - non-dispersive infra-red
NO_x - oxides of nitrogen

NRMM - non-road mobile machinery
NRSC - non-road steady cycle
PAH - polyaromatic hydrocarbons
PM - particulate matter
PN - particle number
PSD - particle size distributions
TPN - total particle number
WF - weighting factor

ISSN 0148-7191

2021-01-1208 Published 21 Sep 2021

Crude Tall Oil based Renewable Diesel: Performance, Emission Characteristics and Storage Stability

Kirsi Spoof-Tuomi Univ Of Vaasa

Ville Vauhkonen UPM-Kymmene Corp

Seppo Niemi, Teemu Ovaska, Vilja Lehtonen, Sonja Heikkilä, and Olav Nilsson Univ Of Vaasa

Citation: Spoof-Tuomi, K., Vauhkonen, V., Niemi, S., Ovaska, T. et al., "Crude Tall Oil based Renewable Diesel: Performance, Emission Characteristics and Storage Stability," SAE Technical Paper 2021-01-1208, 2021, doi:10.4271/2021-01-1208.

Abstract

International policies aiming at replacing fossil fuels with bio-components are getting stronger. Hydrotreating of bio-oils is a sustainable way to produce premium quality diesel fuels from completely renewable feedstocks. The Finnish forestry company UPM has developed an innovative production process based on hydrotreatment to convert crude tall oil (CTO) into a high-quality renewable diesel fuel that can be used as a blending component or as 100% fuel in all diesel engines without modifications. Paraffinic, high cetane CTO renewable diesel allows efficient and clean combustion, reducing harmful air emissions in addition to not releasing any new CO_2 into the atmosphere during their combustion. This study investigated the effect of CTO renewable diesel (BVO) on engine performance and exhaust emissions. Conventional market diesel served as a reference fuel. The research engine was a common-rail off-road diesel engine, operated by using the load points of the non-road steady state cycle C1 of the ISO8178 standard. The use of BVO reduced all regulated gaseous emissions (NO_x -10%, CO -7%, HC -7%). A significant 26% reduction was obtained in cycle-weighted particulate number. In addition to low emissions, fuels are required to remain stable and of high quality even after long-term storage. Another target of the present study was to clarify the influence of long-term storage on CTO renewable diesel properties. In this context, the paper reports the comprehensive results of fuel analyses in a fresh state and after four years of storage, the focus being on parameters that may be affected by the formation of oxidation products. BVO did not show substantial storage stability problems.

1. Introduction

Today, most heavy-duty vehicles and non-road applications rely on diesel engine technology as their primary power source [1]. Liquid fossil fuels have become the predominant fuel for those segments due to their high energy density and ease of distribution and storage, and a vast global infrastructure has been built over the past century to support this system [2]. These segments will also be the most difficult to electrify due to the high energy demand [3]. The expected large battery capacity would burden vehicle weight and reduce the payload capacity. Moreover, the cost would be high, and the charging time would be long. For non-road machinery operating for extended periods far away from charging infrastructure, the issue of battery technology is even more complicated. Thereby, robust and efficient diesel engines are expected to continue to play a central role as a power source for heavy-duty and off-road applications [2,3,4,5].

At the same time, concerns on climate change and global warming are growing, and international policies aiming to reduce greenhouse gas (GHG) emissions are getting stronger. In September 2020, the European Commission decided on increasingly stringent GHG emission reduction targets. The new goal is to reduce EU GHG emissions by at least 55% by 2030, compared to 1990 levels [6]. This is a substantial increase from the earlier target of 40%. This level of ambition for the next ten years is expected to set Europe on a balanced pathway to becoming climate neutral by 2050 - an economy with net-zero GHG emissions.

There are still no real alternatives in non-road transportation that could compete with an internal combustion (IC) engine throughout the entire application range. Besides, IC engines are still undergoing continuous further improvements with, e.g., advances in combustion technologies [5]. However, the GHG reductions of the required magnitude cannot be achieved through energy efficiency measures alone, and large-scale deployment of advanced liquid biofuels is needed in parallel [3]. There is a huge potential to significantly and realistically improve the sustainability of IC engines in the short- and medium-term through the development and deployment of renewable liquid fuels. Extensive existing distribution infrastructure can support such initiatives without modification or investment [2].

In recent decades, various biofuels have been introduced to the existing fuel markets [7]. First-generation biofuels, such as biodiesels derived from corn, sugarcane or soybean [8], symbolize the step towards fossil-free energy production. However, from the sustainability perspective, first-generation biofuels face a number of sustainability challenges, the biggest drawback being the competition with food production through excessive land use [7, 8]. There are also concerns about potential negative impacts on biodiversity [9] and competition for water in certain areas.

Advanced (second and third-generation) biofuels overcome many of the sustainability issues associated with first-generation biofuels. Notably, they do not compete with food resources, as they are produced from non-food crops, such as agricultural and forest residues, and industrial wastes [10, 11]. Additional benefits of biofuels produced from residues and waste streams are improved process energy efficiency [11] and substantially reduced CO_2 production [9]. Major CO_2 savings are based on the fact that the production of biofuels from organic waste results in fuels that contain only biogenic carbon [12], i.e., atmospheric carbon that was captured via biomass growth. Combustion of these fuels is considered carbon neutral, as it does not release any new CO_2 into the atmosphere. A recent study by Soam & Börjesson [13] showed that substitution of fossil diesel by higher-generation biofuels produced from by- and waste products may result in GHG emission reductions of up to 90% over their life cycle.

Various types of fuels can be derived from renewable feedstock, such as fats and vegetable oils [14]. A common biofuel is fatty acid methyl ester (FAME), also referred to as biodiesel, produced via transesterification of vegetable oils [15]. Due to many disadvantages of FAME biodiesel, such as deposit formation and storage stability problems [16], alternative routes for producing a diesel substitute have been developed. One of the alternative processes to esterification is hydrotreating. Hydrotreating vegetable oils or animal fats leads to a deoxygenated and thus stable product that is fully compatible with petroleum diesel fuel [17]. To clarify the difference from ester-type biodiesels, the term 'renewable diesel' is used for hydrotreated vegetable oils (HVO) [16].

The development of hydrotreated vegetable oil type diesel fuels have been strong particularly in the Nordic countries. Several studies have proved the emission benefits of these types of fuels. In Niemi et al. [18], a non-road diesel engine was driven with different fuel blends of traditional fossil diesel fuel and CTO based renewable diesel. With neat renewable diesel, a reduction of 21% in HC, 15% in CO, and 27% in particle number (PN) compared with fossil diesel were reported. Dimitriadis et al. [19] and Murtonen & Aakko-Saksa [20] also reported remarkable reductions in engine-out HC, CO and soot emissions with HVO. In Aatola et al. [16], smoke emissions were reduced by 35% with HVO without any modification to the engine control. At the same time, a 6% decrease in NO_x emissions was detected. Sarjovaara [21] reported similar results. The opposite behavior compared to the traditional NO_x-PM trade-off outlined the benefits of this kind of fuel [16, 21].

In addition to emission efficiency, maintaining fuel quality during long-term storage is an important aspect [22]. Fuel storage stability is crucial especially for vehicles and stationary engines that are out of use for extended periods with fuel in their tanks, such as seasonal machinery, or military equipment and emergency generator sets. Thereby, the stable quality of diesel fuel even after years of storage is also relevant in terms of the security of supply. The term 'fuel storage stability' refers to fuel's resistance against degradation processes that can alter its physicochemical properties and form undesirable compounds upon prolonged storage [23]. For biodiesel, the degradative processes are largely related to the degree of unsaturation in the fatty acid alkyl ester chain, water content and environmental factors such as temperature and exposure to air during storage [24, 25]. Biodiesels are more susceptible to oxidative attack than fossil diesel fuel [25], and oxidative degradation, caused by exposure to oxygen in the air, is the primary concern for them. Oxidative degradation of biodiesel can lead to the formation of short-chain carboxylic acids, aldehydes, ketones, and polymeric sediments [22,25,26,27] that impair fuel quality. It may cause problems with, e.g., fuel filter clogging and reduce the lifespan of fuel delivery components due to increased metal corrosion and elastomer degradation [27]. In addition, biodiesel's storage stability may include issues of water contamination and microbial growth [26]. Currently, EN 590 diesel standard limits the maximum allowable FAME content at 7% [28].

Instead, the storage stability properties of hydrotreated oils are considered almost similar to those of fossil diesel. As those fuels contains little or no oxygen, the long-term oxidation stability remains fairly steady, resulting in good storage behavior [19]. Generally, hydrotreated fuels also has low tendency to incorporate dissolved water. As a result, the risk of microbial growth is similar to that of fossil diesel fuel, and no extra precautions regarding microbiological growth, water separation, or storage stability are required [29]. Hydrotreated renewable diesel fuels, with their chemical composition almost similar to fossil-based paraffinic fuels (e.g., n-, iso-, and cyclic paraffin), also have similar compatibility with fuel delivery components and materials as fossil diesel [30]. Extensive field trials, both at 100% hydrotreated fuels and various blending ratios, have not led to any operability issues or need for extra maintenance regarding fuel systems, engines, or exhaust after-treatment devices [29].

The first target of the present study was to examine engine performance and exhaust emissions with renewable diesel. The renewable diesel under investigation was CTO based diesel fuel (BVO) produced by the Finnish forestry company UPM. Conventional market diesel (DFO) served as a reference fuel. The experiments were carried out using a commercial diesel engine, AGCO 44 AWI, designed for off-road use. During a thorough test bench campaign, the test engine was run using the loads of the ISO8178 standard´s non-road steady-state cycle C1. The engine had no exhaust after-treatment system. Both fuels were studied using similar engine settings, and no engine or parameter optimizations were applied with the studied fuels. Alongside the gaseous emissions, PN and particle size distributions (PSD) and the basic engine performance were determined. In addition, the study examined the influence of long-term storage on CTO renewable diesel properties. In this context, the paper reports the comprehensive results of fuel analyses in a fresh state and after

four years of storage, the focus being on parameters that may be affected by the formation of oxidation products.

2. Experimental Setup

The engine experiments were performed by the University of Vaasa at the IC engine laboratory of the Technobothnia laboratory unit in Vaasa, Finland.

2.1. Fuels

Hydrotreated fuel for this study was delivered by UPM, Finland. The studied CTO based renewable diesel fuel was produced at the end of 2016 in UPM´s biorefinery in Lappeenranta. The production process of UPM´s renewable diesel - known as UPM BioVerno - is based on hydrotreatment of crude tall oil, a wood-based residue of chemical pulping process. CTO is a mixture of fatty acids with a carbon chain of 16 to 20 carbons (36-58%), rosin acids (10-42%), and sterols and neutral substances (10-38%). The composition varies depending on many factors, such as tree species and the growing cycle and age of the tree, geographical location, time of the year, and the pulping conditions [7].

The CTO-based renewable fuel production process includes several phases, shown in Figure 1. In the process, crude tall oil - an organic, water-immiscible liquid from a pulp mill - is first pretreated to remove solid particles, elements and metals, and other contaminants before introducing it into the hydrogenation reactor. The amounts of these impurities have to be reduced to ppm level or less to ensure the hydrogenation catalysts' functionality. The actual hydrotreating is carried out in a plug flow reactor at the pressure range of 2-12 MPa and at the temperature range of 280-430 °C, using commercial catalysts capable of simultaneous hydrodeoxygenation, hydrodesulfurization, isomeri-zetion, hydrogenation and cracking, Next, the remaining hydrogen sulfide and incondensable gases are removed. Finally, the hydrotreated CTO "raw diesel" containing mid-distillate diesel components and lighter naphtha components is distilled, i.e., fractionated to renewable diesel and naphtha. [7].

In the present study, BVO was studied as neat. Commercial Finnish low-sulfur diesel fuel oil served as a reference fuel. Table 1 shows the main specification of the studied fuels and also lists the limits of the European diesel specification EN 590. The fuel analyses came from the fuel supplier. For BVO, two different analytical results are presented. The newer fuel analysis was performed in 2020 in the context of this study, i.e., after four years of storage. The older fuel analysis was conducted in a fresh state in 2016. A key part of the study was to examine the impact of long-term storage on BVO quality.

BVO mainly met the requirements of the EN 590. The density was slightly below the minimum limit of 820 kg/m^3, and 95% distillation slightly exceeded the maximum of 360°C defined in EN 590. BVO was treated with a lubricity additive.

Oxidation stability, a key parameter of diesel fuel quality in terms of its storage stability, was determined following the DIN EN ISO 12205 [44]. ISO 12205 describes the procedure for measuring the inherent stability of middle-distillate petroleum fuels by bubbling oxygen through the heated sample (95°C) for 16 hours. The test simulates the storage of diesel fuel for one year. Following the exposure to accelerated oxidizing conditions, the fuel is filtered, and the level of insoluble material is measured. BVO resulted in an insoluble concentration well below the maximum limit of 25 g/m^3 specified in the EN 590.

The results of fuel analyzes are further discussed in Section 3.1

2.2. Engine

The test engine, an AGCO Power 44 AWI, was a high-speed four-cylinder diesel engine designed for off-road applications. It is turbocharged, intercooled and has Bosch common-rail fuel-injection system with a maximum pressure of 160 MPa.

Table 2 gives the main specification of the test engine. The engine was loaded with a Horiba eddy-current dynamometer WT 300. A Horiba SPARC controller platform was used to control engine speed, torque and throttle.

The engine was not equipped with devices for exhaust gas after-treatment, meaning that raw engine-out emissions were recorded during the experiments.

2.3. Analytical Procedures

The measurement setup for regulated gaseous emissions consisted of a chemiluminescence detector (CLD), used to measure the NO_x, a non-dispersive infrared (NDIR) analyzer to measure CO and CO_2, and a heated flame ionization

FIGURE 1 CTO-based renewable fuel production process.

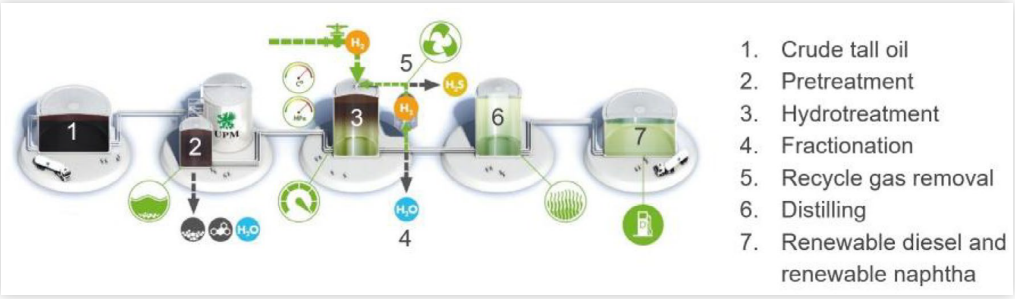

TABLE 1 Properties of the test fuels analyzed by ASG Analytik-Service GmbH. Abbreviations HFRR = High frequency reciprocating rig, CFPP = Cold filter plugging point.

	Test method	Unit	DFO	BVO in 2020	BVO in 2016	Specification EN 590:2014	
						min	max
Cetane Number	DIN EN 17155 [31]*	-	57.5	61.6	60.8	51.0	-
Cetane Index	DIN EN ISO 4264 [33]	-	57.0	66.1	66.4	46.0	-
Density (15°C)	DIN EN ISO 12185 [34]	kg/m^3	836.4	812.7	812.6	820	845
PAH content	DIN EN 12916 [35]	% (m/m)	2.7	0.1	1.0	-	8.0
Total aromatics	DIN EN 12916	% (m/m)	23.8	4.6			
Sulphur content	DIN EN ISO 20884 [36]	mg/kg	7.9	<5	<5(<1)	-	10
Flash Point	DIN EN ISO 2719 [37]	°C	67.5	73.0	72.0	>55	-
Carbon residue (10% Dist.)	DIN EN ISO 10370 [38]	% (m/m)	<0.10	<0.10	0.02	-	0.30
Ash Content (775°C)	DIN EN ISO 6245 [39]	% (m/m)	<0.001	<0.001	<0.005	-	0.1
Water content	DIN EN ISO 12937 [40]	mg/kg	32	22	<30	-	200
Total contamination	DIN EN 12662 [41]	mg/kg	<12	<12	6	-	24
Copper strip corrosion	DIN EN ISO 2160 [42]	Korr.Grad.	1	1	1	-	1
FAME content	DIN EN 14078 [43]	% (V/V)	<0.1	<0.01	<0.1	-	7.0
Oxidation stability	DIN EN ISO 12205 [44]	g/m^3	<1	<1	7	-	25
filterable insolubles	DIN EN ISO 12205	g/m^3	<1		4	-	-
adherent insolubles	DIN EN ISO 12205	g/m^3	<1		3	-	-
HFRR (Lubricity at 60°C)	DIN EN ISO 12156-1 [45]	µm	380	380	361	-	460
Kin. Viscosity (40°C)	DIN EN ISO 3104 [46]	mm^2/s	3.3	2.8	2.8	2.0	4.5
% (V/V) recovery at 250°C	DIN EN ISO 3924 [47]	% (V/V)	22.7	33.2	33.1	-	<65
% (V/V) recovery at 350°C	DIN EN ISO 3924	% (V/V)	93.4	92.8	92.6	85	-
95% (V/V) recovery	DIN EN ISO 3924	°C	354	367	369	-	360
CFPP	DIN EN 116 [48]	°C	-12	-8	-9	-	**
Manganese (Mn)	DIN EN 16576 [49]	mg/l	<0.5	<0.5	<0.5	-	2.0
Surface tension (20°C)	DIN EN 14370 [50]	mN/m	28.3	27.3			
Calorific value, lower	DIN 51900-2 [51]	MJ/kg	42.8	43.6	43.3	-	-

* *In 2016: DIN EN 15195 [32]*

** *According national specifications*

detector (HFID) for HC. In addition, several unregulated gaseous compounds were measured using Fourier transformation infrared (FTIR) equipment. PN and PSD were measured using an engine exhaust particle sizer (EEPS) spectrometer.

For the determination of the exhaust PN, the exhaust sample dilution before the EEPS was organized using a rotating disc diluter (model Matter Engineer MD19-3E). After the disk diluter using the constant dilution ratio of 60:1, the diluted sample was further diluted for the EEPS by purified air with a dilution ratio of 2:1. Thus, the overall dilution ratio was 120:1. Table 3 summarizes the methods and instruments adopted for the measurements. The schematic representation of the experimental setup is shown in Figure 2.

TABLE 2 Test engine specification.

Engine	AGCO POWER 44 AWI
Cylinder number	4
Bore (mm)	108
Stroke (mm)	120
Swept volume (dm^3)	4.4
Compression ratio	16.5:1
Rated speed (rpm)	2200
Rated power (kW)	103
Rated maximum torque at rated speed (Nm)	446
Maximum torque at 1500 rpm (Nm)	560

TABLE 3 Analytical instruments.

Parameter	Measuring device	Technology
NO_x	Eco Physics CLD 822 M hr	Chemiluminescence
CO, CO_2	Siemens Ultramat 6	NDIR
HC	J.U.M. VE7	HFID
O_2	Siemens Oxymat 61	Paramagnetic
PN and PSD	TSI EEPS 3090	Spectrometer
Smoke	AVL 415 S	Optical filter
Unregulated gaseous emissions	Gasmet DX4000	FTIR
Air mass flow	ABB Sensyflow P	Hot-film anemometer
Cylinder pressure	Kistler KiBox	

FIGURE 2 Experimental set-up.

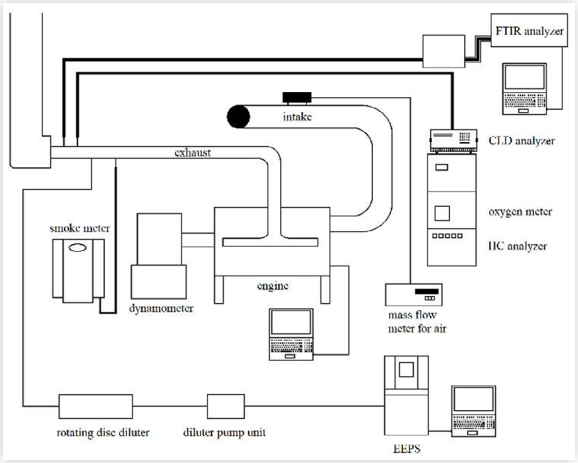

The sensor data were collected using software made in the LabVIEW system-design platform, published by National Instruments, Austin, Texas. In addition to gaseous and particulate emissions, the recorded quantities included engine speed and torque and several fluid temperatures and fluid pressures, such as temperatures of cooling water, intake air and exhaust gas, and intake air and exhaust pressures. The engine control functions were monitored with AGCO SISU Power WinEEM4 software. No engine parameter optimizations were applied during the tests, and both fuels were studied using similar engine settings.

Engine warm-up and measurement procedures were identical for both fuels. Prior to measurements, the analyzers were manually calibrated once a day according to the instrument manufacturers' instructions. The brake-specific emissions results were calculated from the measured pollutant concentration data according to the ISO 8178 standard [52].

For combustion analysis, the heat release rate (HRR) and the mass fraction burned (MFB) were determined based on the in-cylinder pressure data, measured with a piezoelectric Kistler 6125C pressure sensor. The signal was filtered and amplified by a charge amplifier and transferred to a Kistler KIBOX combustion analyzer. A Kistler 2614B1 crank angle encoder recorded the crankshaft position. To smooth out irregular combustion, the cylinder pressure data were averaged over 100 consecutive cycles.

HRR and MFB were calculated using the AVL Concerto data post-processing tool. The average values of in-cylinder pressures and the Thermodynamics2 macro with a calculation resolution of 0.2°CA were used to calculate HRR values. Thereafter, the HRR curves were filtered with a DigitalFilter macro and a frequency of 4,000 Hz. For MFB calculations, the pressure values were not averaged to determine the standard deviations for 100 consecutive cycles.

2.4. Experimental Matrix

The performance and emission measurements were conducted at eight steady state load points. The loads were selected according to the ISO 8178-4 C1 test cycle, known as the non-road steady cycle (NRSC) [53]. The test engine's rated speed was 2200 rpm, and the intermediate speed was 1500 rpm. At idle, the speed was 860 rpm. The loading points or modes and the corresponding engine speeds, loads and torques, as well as the NRSC weighting factors for the different modes, are listed in Table 4.

Before initiating the measurements, it was always waited that the engine run had stabilized. The main criteria were that the intake air and exhaust gas temperatures were stable.

3. Results and Discussion

3.1. CTO Renewable Fuel Storage Stability

The CTO based renewable diesel fuel was produced at the end of 2016, in Lappeenranta biorefinery. The fuel sample was then taken from a storage tank to be used in engine tests conducted by the VTT Technical Research Centre of Finland in the project that had a goal to optimize engine for paraffinic diesel fuels. The fuel batch used in these tests was stored in a chemical container that had a constant temperature of 20 °C. The fuel was kept in a 230-liter plastic barrel with an airtight lid through the four-years ageing period. Prior to storage, the fuel was treated with a lubricity additive

Renewable diesel used in these engine tests showed slight unstable behavior in the oxidation tests made in 2016, see Table 1. There was a small amount of deposit formation in the oxidation stability test of EN ISO 12205, where the sample is at an elevated temperature of 95°C and treated with oxygen. However, the result was well inside the limits set by the EN590 standard.

When the fuel was analyzed in autumn 2020, there was no deposit formation. The amount of measured polyaromatics in the sample had decreased from 1.0 m-% to 0.1 m-%.

Overall, the changes in the fuel properties were small, partly negligible, which shows that hydrotreated CTO-based renewable diesel can be stored under controlled conditions for extended periods without compromising the fuel quality. The next sections show, what kind of engine results this stored fuel generated.

TABLE 4 Experimental matrix.

Mode	1	2	3	4	5	6	7	8
Speed (rpm)	2200	2200	2200	2200	1500	1500	1500	860
Load (%)	100	75	50	10	100	75	50	0
Torque (Nm)	446	334	223	45	560	420	280	1
Weighting factor	0.15	0.15	0.15	0.1	0.1	0.1	0.1	0.15

3.2. Combustion Analysis

In general, combustion progressed in a quite similar manner with both fuels, as shown in Figures 3 and 4. However, BVO consistently showed a slightly lower peak of heat release rate (HRR) in the premixed combustion phase. Presumably, the higher cetane number of BVO resulted in better fuel ignition in the cylinder and a shorter ignition delay, resulting in a lower premixed peak. At rated speed at 75% load, main and post-injections were in use, while at intermediate speed at 50% load, the pilot injection was also adopted.

Table 5 shows 10%, 50%, and 90% mass fraction burned (MFB) points at rated speed at 75% load (Mode 2) and intermediate speed at 50% load (Mode 7). Standard deviations of crank angles at MFB 10%, MFB 50% and MFB 90%, calculated from 100 consecutive engine cycles, are also given. No significant differences in combustion durations (CD) were detected, defined herein as the crank angle duration from MBF 10% to MBF 90%. MFB 50% values were also very similar for both fuels.

The differences in maximum cylinder pressures between the studied fuels were minimal, as shown in Figure 5, also indicating that combustion propagated quite similar way with both fuels.

FIGURE 3 HRR as a function of crank angle at rated speed at 75% load.

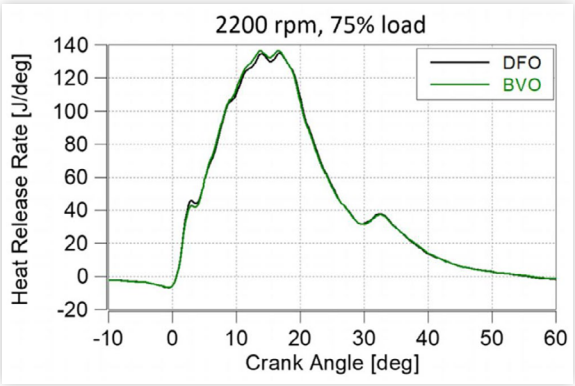

FIGURE 4 HRR as a function of crank angle at intermediate speed at 50% load.

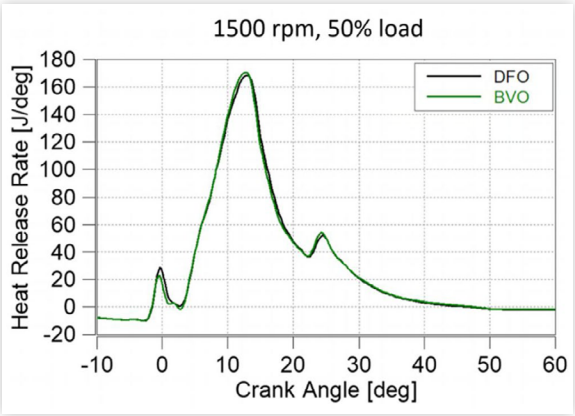

TABLE 5 Mass fraction burned, standard deviations and combustion durations at rated speed at 75% load and intermediate speed at 50% load.

	MFB 10%	Stdev	MFB 50%	Stdev	MFB 90%	Stdev	CD MFB10-90%
	°CA	°CA	°CA	°CA	°CA	°CA	°CA
Mode 2							
DFO	7.7	0.085	16	0.12	31	0.50	23
BVO	7.7	0.093	16	0.12	31	0.60	23
Mode 7							
DFO	8.7	0.063	14	0.078	27	0.27	18
BVO	8.8	0.065	14	0.084	27	0.33	18

FIGURE 5 Maximum cylinder pressure versus engine load at rated speed.

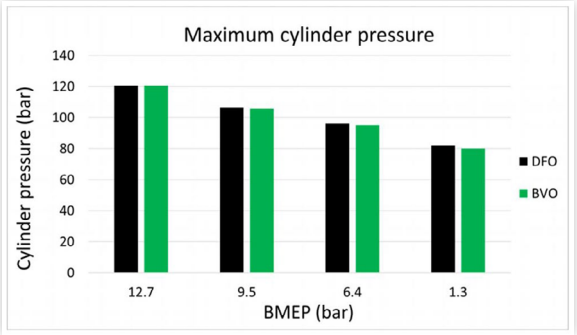

3.3. Efficiency

The engine brake thermal efficiency was very similar for both fuels at all loads (Fig. 6). DFO produced slightly higher values, but the difference was marginal by no more than 0.6 percentage points, and thus of the order of magnitude of the measurement accuracy.

3.4. Gaseous Emissions

The use of BVO resulted in lower brake-specific NO_x emissions on all measured speed and load configurations compared to DFO, as seen in Figure 7. Over the measurement cycle, BVO reduced NO_x by 10% (Fig. 8). Throughout the cycle with weightings, the NO_x for DFO was 7.9 g/kWh and for BVO 7.1 g/kWh, also indicating that the engine was tuned for high NO_x - and high efficiency - and intended for the later use of various catalysts for thorough NO_x reduction.

The main reason for improved NO_x outcome is that BVO is an exclusively paraffinic fuel with a high H/C ratio and low aromatic content. NO_x formation is reduced with fuels having lower aromatic content as aromatic compounds have higher adiabatic flame temperature and thereby produce higher local combustion temperatures [54, 55]. In addition, the higher cetane number of BVO most probably resulted in a shorter ignition delay, also concluded by [56]. A shorter ignition delay reduces

FIGURE 6 Brake thermal efficiency of the engine against engine load and speed. CTO renewable diesel after four-years ageing. Baseline fuel DFO.

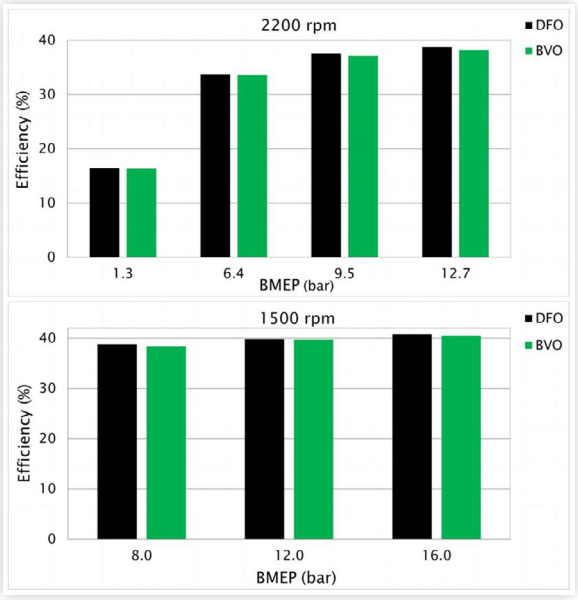

FIGURE 7 NO_x emissions at different speeds and loads. CTO renewable diesel after four-years ageing. Baseline fuel DFO.

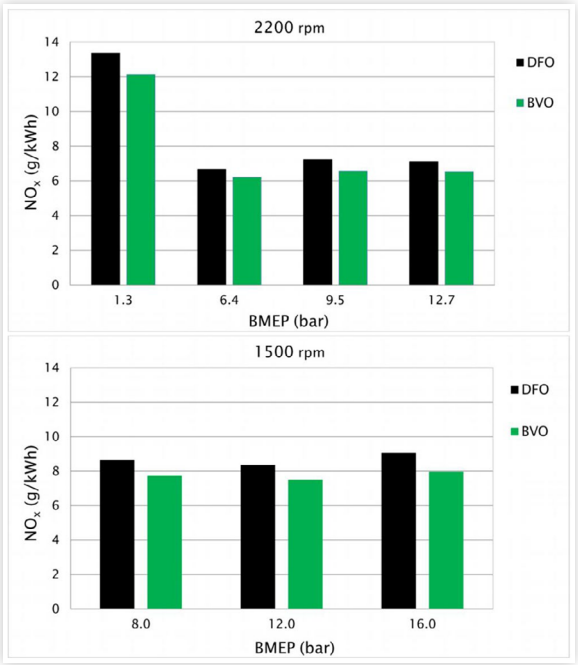

FIGURE 8 Cycle-weighed NO_x emissions for aged CTO renewable diesel. Baseline fuel DFO.

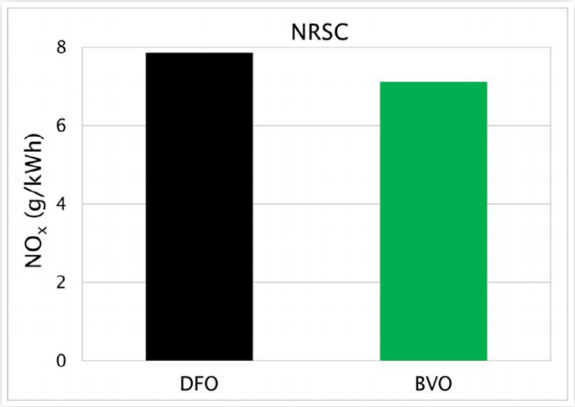

the energy released during the premixed combustion phase resulting in lower maximum combustion pressure and temperature in the cylinder, which in turn leads to lower NO_x formation [55].

CTO renewable diesel also proved to be beneficial in terms of CO and HC emissions (Fig. 9). Cycle-averaged CO emissions decreased by 7% from 0.27 to 0.25 g/kWh. In absolute terms, the reduction was reasonably small because

FIGURE 9 Cycle-weighted CO and HC emissions for aged CTO renewable diesel. Baseline fuel DFO.

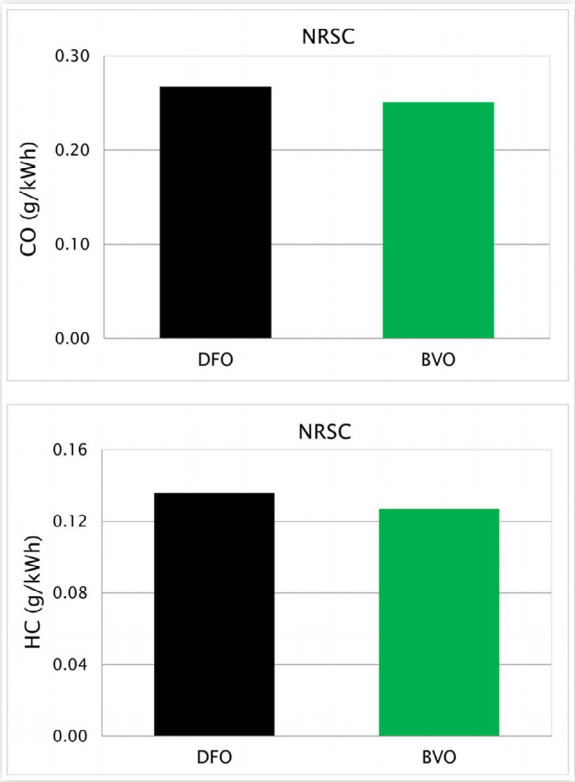

of the already low CO values. The percentage reduction of brake-specific HC emissions was also 7%, from 0.14 to 0.13 g/kWh. HC reductions were more pronounced at lower loads.

HC and CO emissions for both fuels were well below the EU Stage V and US Tier 4 emission limits for non-road engines (0.19 g/kWh for HC and 5.00 g/kWh for CO).

The main reasons for lower CO and HC emissions were assumed to be the higher cetane number and the lower aromatic content of BVO, and thus better combustion characteristics. BVO's high cetane number reduces ignition delay, which favors the oxidation process of CO emissions and limits overmixing of fuel, and consequently, HC emissions [19].

From the recorded unregulated gaseous emissions, nitrous oxide (N_2O) concentrations were low at all loads and almost equal for both fuels. N_2O generally ranged from 0.4 to 0.8 ppm, but at full load at 1500 rpm, it was below 0.1 ppm.

The wet exhaust methane (CH_4) contents were also low at all loads. The highest concentrations were recorded at 10% load at 2200 rpm (0.9 ppm for DFO and 0.5 ppm for BVO) and at half load at 2200 rpm (0.4 ppm for DFO and 0.1 ppm for BVO). At higher loads, CH_4 content was always below 0.1 ppm for both fuels.

The wet exhaust formaldehyde concentrations peaked at 3.0 ppm (at half load at 2200 rpm). Otherwise, it varied between 0.6 and 2.1 ppm. No significant difference between fuels was detected.

3.5. PN Emission and Smoke

The total PN emissions within the particle size range of 5.6 to 560 nm for BVO and fossil EN590 diesel at different speed and load combinations are shown in Figure 10. Each bar represents the mean value of the total PN. Depending on the load, the total PN decreased by 1-74% with CTO renewable fuel. The largest reductions were detected at low loads.

FIGURE 10 Total PN emission within the particle size range of 5.6 to 560 nm at different speeds and loads. CTO renewable diesel after four-years ageing. Baseline fuel DFO.

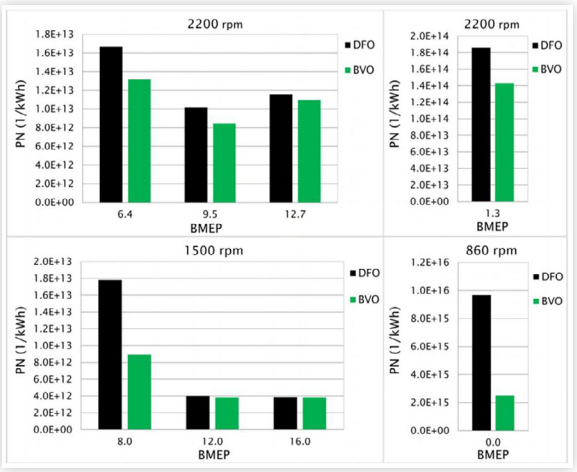

FIGURE 11 Total PN emission for the aged CTO renewable fuel and DFO within the particle size range of 5.6 to 560 nm, weighted over the eight-mode cycle.

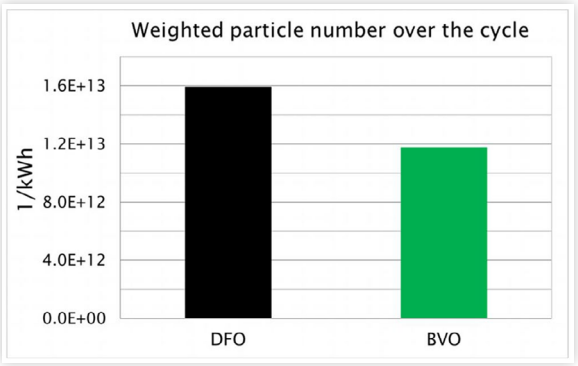

Figure 11 depicts the weighted total PN over the ISO8178 C1 driving cycle. Compared with DFO, CTO renewable fuel produced a reduction of 26% in the total PN emission. The result comes in agreement with previous studies [18, 56].

PSD at high load and low load conditions are depicted in Figures 12 and 13. The averages of PN concentrations are presented as data points and connected by lines. The shaded area depicts the standard deviation. The first peak of the bimodal PSD was detected at a particle diameter of 10 nm, and the other at approx. 35 nm. BVO generally produced a lower PN average in the larger particle size range, but the average number of smaller particles (10 nm) was slightly higher than that of DFO at some loads. With BVO, the decrease in particle number at the size category of 10 nm was evident at half load at 1500 rpm and at low idle.

The improvement in the total PN emission can be explained by examining the fuel properties. The higher H/C ratio of BVO most likely led to a more complete combustion, also concluded by [57, 58]. Furthermore, due to the BVO´s almost aromatic free composition, less PAH, i.e., precursors of soot, was formed [59, 60]. The significant PN reduction at the particle size category of 10 nm at low idle can be explained by BVO´s near-zero sulfur and low aromatics content [61] and the improved ignition quality [62].

With both fuels, smoke was very low at all loads. For DFO, filter smoke number (FSN) values varied from 0.018 to 0.070 and for BVO from 0.013 to 0.037, respectively. The reason for lower engine smoke with CTO renewable diesel was assumed to be the lower aromatic content of the fuel. According to Aatola et al. [16], a high cetane number can also have a beneficial effect on engine smoke.

4. Conclusions

This paper investigated CTO-based renewable diesel. The main target was to examine the effect of renewable diesel on the performance and exhaust emissions of an off-road diesel

FIGURE 12 Particle size distributions at high load conditions for CTO renewable diesel after four-years ageing. Baseline fuel DFO.

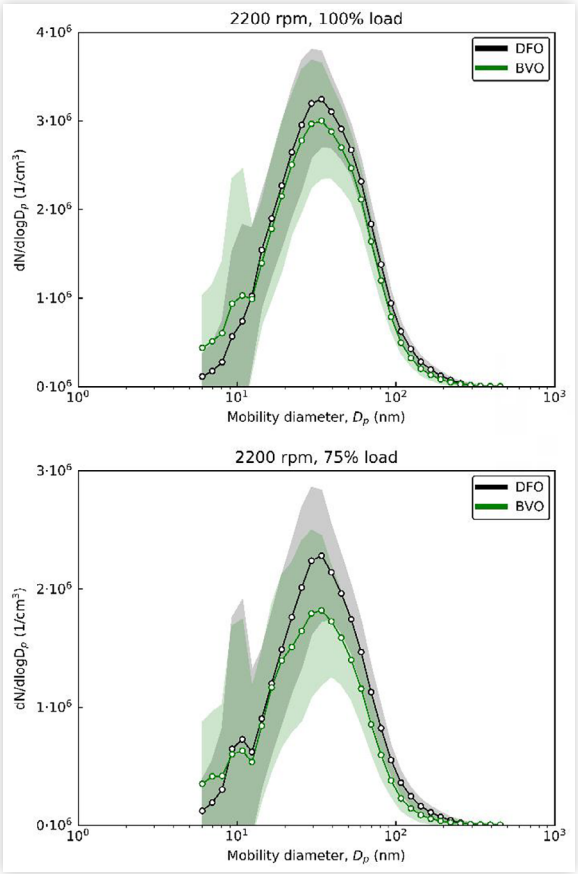

FIGURE 13 Particle size distributions at low load conditions for aged CTO renewable diesel. Baseline fuel DFO.

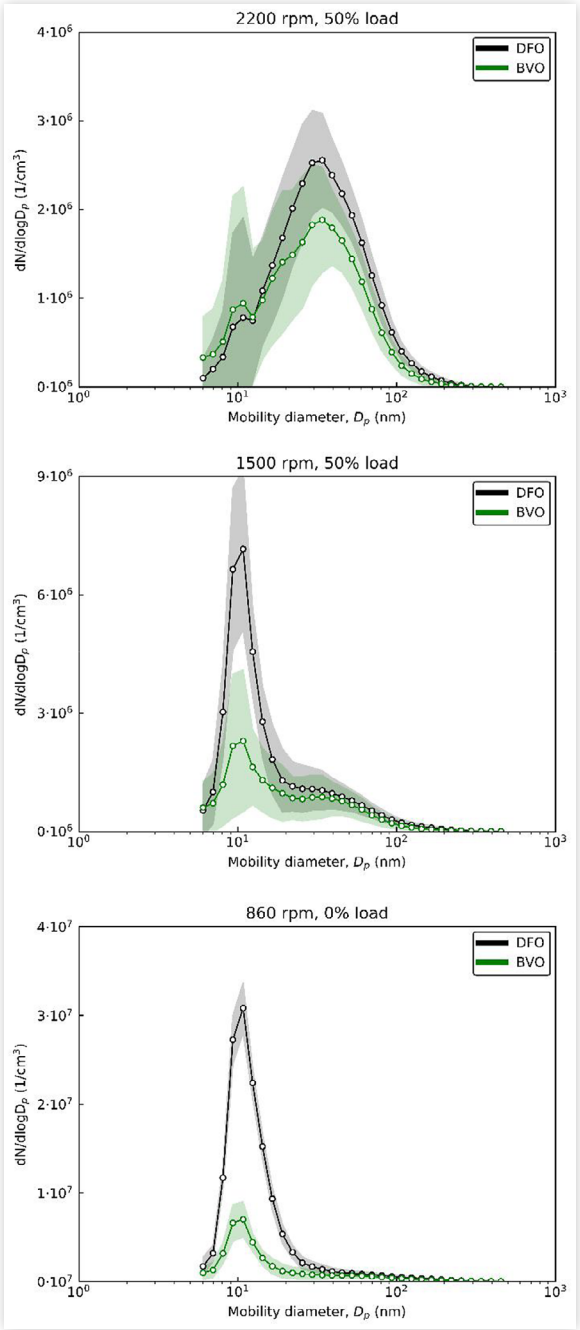

engine. In this context, raw engine-out emissions were recorded. CTO-based renewable fuel was studied in neat form, and conventional fossil diesel was used as the baseline fuel. An additional goal was to examine the effect of long-term storage on the properties of this renewable diesel.

From the fuel analyzes, the following conclusion could be drawn:

- After four years of storing, the changes in the fuel properties were negligible and showed that hydrotreated CTO-based renewable diesel fuel can be stored under controlled conditions for extended periods of time without compromising the fuel quality.

Engine performance and exhaust emissions were characterized over the eight-mode steady state cycle that followed a standardized NRSC driving cycle C1. Based on the measurements, the main findings were:

- The engine´s brake thermal efficiency was very similar for both fuels.
- The use of BVO resulted in lower brake-specific NO_x emissions on all measured speed and load configurations compared to DFO. Over the NRSC cycle, BVO reduced NO_x by 10%.
- The main reason for lower NO_x emissions was assumed to be the high H/C ratio and low aromatics content of BVO. In addition, the higher cetane number of BVO

most probably resulted in a shorter ignition delay, leading to lower NO_x formation.

- Over the eight-mode cycle, CO emissions decreased by 7% with BVO. HC emissions also decreased by 7%. HC reductions were more pronounced at lower loads.
- The main reasons for lower CO and HC emissions were assumed to be the higher cetane number and the lower aromatic content of BVO, and thus better combustion characteristics.
- The wet exhaust gas concentrations of nitrous oxide, methane, and formaldehyde were negligible with both fuels.
- Fueling with CTO renewable fuel produced a reduction of 26% in the total PN emission compared with DFO. The main reasons for decreased total PN emission were assumed to be the improved ignition quality, the beneficial hydrocarbon structure and near-zero sulfur and low aromatics content of BVO.

References

1. Niemi, S., Hissa, M., Ovaska, T., Sirviö, K., and Vauhkonen, V., "Performance and Emissions of a Non-Road Diesel Engine Driven with a Blend of Renewable Naphtha and Diesel Fuel Oil," In: Schubert, N., (ed.), *Fuels: Conventional and Future Energy for Automobiles: 12th International Colloquium Fuels - Conventional and Future Energy for Automobiles* (2019), Ostfildern, Deutschland, 25.06.2019-26.06.2019. Technische Akademie Esslingen.
2. Leach, F., Kalghatgi, G., Stone, R., and Miles, P., "The Scope for Improving the Efficiency and Environmental Impact of Internal Combustion Engines," *Transportation Engineering* 1 (2020): 100005, doi:10.1016/j.treng.2020.100005.
3. ERTRAC, "Future Light and Heavy Duty ICE Powertrain Technologies," *ERTRAC Working Group Energy and Environment* 05.04.2016, https://www.ertrac.org/uploads/documents_publications/Roadmap/2016-04-05_ICE_roadmap_edited%20version.pdf.
4. Lajunen, A., Sainio, P., Laurila, L., Pippuri-Mäkeläinen, J. et al., "Overview of Powertrain Electrification and Future Scenarios for Non-Road Mobile Machinery," *Energies* 11 (2018): 1184, doi:10.3390/en11051184.
5. Reitz, R.D., Ogawa, H., Payri, R., Fansler, T. et al., "The Future of the Internal Combustion Engine," *Int. J. Engine Res.* 21, no. 1 (2020): 3-10, doi:10.1177/1468087419877990.
6. EU COM/2020/562, Communication from the Commission to the European Parliament, the Council, the European Economic and Social Committee and the Committee of the Regions. Stepping up Europe´s 2030 Climate Ambition, Investing in a Climate-Neutral Future for the Benefit of Our People, EU COM/2020/562 Final, https://eur-lex.europa.eu/legal-content/EN /ALL/?uri=CELEX:52020DC0562.
7. Heuser, B., Vauhkonen, V., Mannonen, S., Rohs, H. et al., "Crude Tall Oil-Based Renewable Diesel as a Blending Component in Passenger Car Diesel Engines," *SAE Int. J. Fuels Lubr.* 6, no. 3 (2013): 817-825. https://doi.org/10.4271/2013-01-2685.
8. Naqvi, M. and Yan, J., "First-Generation Biofuels," in: Yan, J. (Eds), *Handbook of Clean Energy Systems*. Vol. 1, (John Wiley & Sons, Ltd., 2015), doi:10.1002/9781118991978.hces207.
9. Naik, S.N., Goud, V.V., Rout, P.K., and Dalai, A.K., "Production of First and Second Generation Biofuels: A Comprehensive Review," *Renewable and Sustainable Energy Reviews* 14, no. 2 (2010): 578-597, doi:10.1016/j.rser.2009.10.003.
10. Fokaides, P.A. and Christoforou, E., "Life Cycle Sustainability Assessment of Biofuels," in: Luque, R., Lin, C.S.K., Wilson, K. and Clark, J. (Eds), *Handbook of Biofuels Production*, Second ed., (Woodhead Publishing, 2016), 41-60, doi:10.1016/B978-0-08-100455-5.00003-5.
11. Sathitsuksanoh, N., Zhu, Z., Rollin, J., and Zhang, Y.-H.P., "Solvent Fractionation of Lignocellulosic Biomass," in: Waldron, K. (Eds), *Bioalcohol Production*, (Woodhead Publishing, 2010), 122-140, doi:10.1533/9781845699611.1.122.
12. Edwards, R., Larivé, J.F., Rickeard, D., and Weindorf, W., "JEC Well-to-wheels Analysis: Well-to-wheels Analysis of Future Automotive Fuels and Powertrains in the European Context," Well-to-tank report version 4.0, July 2013, JRC Technical reports, Publications Office of the European Union, doi:10.2788/40526.
13. Soam, S. and Börjesson, P., "Considerations on Potentials, Greenhoude Gas, and Energy Performance of Biofuels Based on Forest Residues for Heavy-Duty Road Transport in Sweden," *Energies* 13 (2020): 6701, doi:10.3390/en13246701.
14. Knothe, G., "Biodiesel and Renewable Diesel: A Comparison," *Prog. Energy Combust. Sci.* 36, no. 3 (2010): 364-373, doi:10.1016/j.pecs.2009.11.004.
15. Bezergianni, S. and Dimitriadis, A., "Comparison between Different Types of Renewable Diesel," *Renew. Sustain. Energy Rev.* 21 (2013): 110-116, doi:10.1016/j.rser.2012.12.042.
16. Aatola, H., Larmi, M., Sarjovaara, T., and Mikkonen, S., "Hydrotreated Vegetable Oil (HVO) as a Renewable Diesel Fuel: Trade-off between NOx, Particulate Emission, and Fuel Consumption of a Heavy Duty Engine," *SAE Int. J. Engines* 1, no. 1 (2009): 1251-1262. https://doi.org/10.4271/2008-01-2500.
17. Sebos, I., Matsoukas, A., Apostolopoulos, V., and Papayannakos, N., "Catalytic Hydroprocessing of Cottonseed Oil in Petroleum Diesel Mixtures for Production of Renewable Diesel," *Fuel* 88, no. 1 (2009): 145-149, doi:10.1016/j.fuel.2008.07.032.
18. Niemi, S., Vauhkonen, V., Mannonen, S., Ovaska, T. et al., "Effects of Wood-Based Renewable Diesel Fuel Blends on the Performance and Emissions of a Non-Road Diesel Engine," *Fuel* 186 (2016): 1-10, doi:10.1016/j.fuel.2016.08.048.
19. Dimitriadis, A., Natsios, I., Dimaratos, A., Katsaounis, D. et al., "Evaluation of a Hydrotreated Vegetable Oil (HVO) and Effects on Emissions of a Passenger Car Diesel Engine," *Front. Mech. Eng.* 4, no. 7 (2018): 1-19, doi:10.3389/fmech.2018.00007.
20. Murtonen, T. and Aakko-Saksa, P., "Alternative Fuels with Heavy-Duty Engines and Vehicles: VTT's Contribution," *VTT Technical Research Centre of Finland, VTT Working*

Papers No. 128 (2009), http://www.vtt.fi/inf/pdf/workingpapers/2009/W128.pdf.

21. Sarjovaara, T., "Studies on Heavy Duty Engine Fuel Alternatives," Doctoral dissertation, Department of Energy Technology, Aalto University, Finland, 2015, ISBN 978-952-60-6561-8.
22. Owczuk, M. and Kołodziejczyk, K., "Liquid Fuel Ageing Processes in Long-term Storage Conditions," in *Storage Stability of Fuels*, Biernat, K. (ed.), IntechOpen, 2015, doi:10.5772/59798
23. Pölczmann, G., Tóth, O., Beck, A., and Hancsók, J., "Investigation of Storage Stability of Diesel Fuels Containing Biodiesel Produced from Waste Cooking Oil," *Journal of Cleaner Production* 111 Part A (2016): 85-92, doi:10.1016/j.jclepro.2015.08.035.
24. de Siqueira Cavalcanti, E.H., Zimmer, A.R., Bento, F.M., and Ferrão, M.F., "Chemical and Microbial Storage Stability Studies and Shelf Life Determinations of Commercial Brazilian Biodiesels Stored in Carbon Steel Containers in Subtropical Conditions," *Fuel*, 236: 993-1007, 2019, doi:10.1016/j.fuel.2018.09.043
25. Farahani, M., Pagé, D.J.Y.S., Turingia, M.P., and Tucker, B.D., "Storage Stability of Biodiesel and Ultralow Sulfur Diesel Fuel Blends," *ASME. J. Energy Resour. Technol.* 131, no. 4 (2009): 04180, doi:10.1115/1.4000177.
26. Pullen, J. and Saeed, K., "An Overview of Biodiesel Oxidation Stability," *Renewable and Sustainable Energy Reviews* 16, no. 8 (2012): 5924-5950, doi:10.1016/j.rser.2012.06.
27. Chandran, D., "Compatibility of Diesel Engine Materials with Biodiesel Fuel," *Renewable Energy* 147, no. 1 (2020): 89-99, doi:10.1016/j.renene.2019.08.040.
28. DIN EN 590, "Automotive Fuels - Diesel - Requirements and Test Methods (includes Amendment 2017)," DIN German Institute for Standardization, Standard DIN EN 590, Rev. Oct. 2017.
29. Engman, A., Gauthier, Q., Hartikka, T., Honkanen, M., et al., "Neste Renewable Diesel Handbook," Neste Proprietary publication, Neste Corporation, Espoo, 2020, https://www.neste.com/sites/default/files/attachments/neste_renewable_diesel_handbook.pdf.
30. Hartikka, T., Kuronen, M., and Kiiski, U., "Technical Performance of HVO (Hydrotreated Vegetable Oil) in Diesel Engines," SAE Technical Paper 2012-01-1585 (2012), https://doi.org/10.4271/2012-01-1585.
31. DIN EN 17155, "Liquid Petroleum Products - Determination of Indicated Cetane Number (ICN) of Middle Distillate Fuels - Primary Reference Fuels Calibration Method using a Constant Volume Combustion Chamber," DIN German Institute for Standardization, Standard DIN EN 17155.
32. DIN EN 15195, "Liquid Petroleum Products - Determination of Ignition Delay and Derived Cetane Number (DCN) of Middle Distillate Fuels by Combustion in a Constant Volume Chamber," DIN German Institute for Standardization, Standard DIN EN 15195, Rev. Feb 2015.
33. DIN EN ISO 4264, "Petroleum Products - Calculation of Cetane Index of Middle-Distillate Fuels by the Four Variable Equation," DIN-adopted European-adopted ISO Standard DIN EN ISO 4264.
34. DIN EN ISO 12185, "Crude Petroleum and Petroleum Products - Determination of Density using the Oscillating U-tube Method (ISO 12185:1996)," DIN-adopted European-adopted ISO Standard DIN EN ISO 12185, Rev. Nov. 1997.
35. DIN EN 12916, "Petroleum Products - Determination of Aromatic Hydrocarbon Types in Middle Distillates - High Performance Liquid Chromatography Method with Refractive Index Detection," DIN German Institute for Standardization, Standard DIN EN 12916.
36. DIN EN ISO 20884, "Petroleum Products - Determination of Sulfur Content of Automotive Fuels - Wavelength-dispersive X-ray Fluorescence Spectrometry," DIN-adopted European-adopted ISO Standard DIN EN ISO 20884.
37. ISO 2719, "Determination of Flash Point - Pensky-Martens Closed Cup Method," ISO Standard ISO 2719, Rev. Jun. 2016.
38. DIN EN ISO 10370, "Petroleum Products - Determination of Carbon Residue - Micro Method (ISO 10370:2014)," DIN-adopted European-adopted ISO Standard DIN EN ISO 10370, Rev. Mar. 2015.
39. DIN EN ISO 6245, "Petroleum Products - Determination of Ash (ISO 6245:2001)," DIN-adopted European-adopted ISO Standard DIN EN ISO 6245, Rev. Jan. 2003.
40. DIN EN ISO 12937, "Petroleum Products - Determination of Water - Coulometric Karl Fischer Titration Method (ISO 12937:2000)," DIN-adopted European-adopted ISO Standard DIN EN ISO 12937, Rev. Mar. 2002.
41. DIN EN 12662, "Liquid Petroleum Products - Determination of Total Contamination in Middle Distillates, Diesel Fuels and Fatty Acid Methyl Esters," DIN German Institute for Standardization, Standard DIN EN 12662, Rev. Jul. 2014.
42. DIN EN ISO 2160, "Petroleum Products - Corrosiveness to Copper - Copper Strip Test (ISO 2160:1998)," DIN-adopted European-adopted ISO Standard DIN EN ISO 2160, Rev. Apr. 1999.
43. DIN EN 14078, "Liquid Petroleum Products - Determination of Fatty Acid Methyl Ester (FAME) Content in Middle Distillates - Infrared Spectrometry Method," DIN German Institute for Standardization, Standard DIN EN 14078, Rev. Sept. 2014.
44. DIN EN ISO 12205, "Petroleum Products - Determination of the Oxidation Stability of Middle-Distillate Fuels (ISO 12205:1995)," DIN-adopted European-adopted ISO Standard DIN EN ISO 12205, Rev. Nov. 1996.
45. DIN EN ISO 12156-1, "Diesel Fuel - Assessment of Lubricity using the High-Frequency Reciprocating Rig (HFRR) - Part 1: Test Method (ISO 12156-1)," DIN-adopted European-adopted ISO Standard DIN EN ISO 12156-1.
46. DIN EN ISO 3104, "Petroleum Products - Transparent and Opaque Liquids - Determination of Kinematic Viscosity and Calculation of Dynamic Viscosity (ISO 3104:1994)," DIN-adopted European-adopted ISO Standard DIN EN ISO 3104, Rev. Oct. 1994.
47. DIN EN ISO 3924, "Petroleum Products - Determination of Boiling Range Distribution - Gas Chromatography Method (ISO 3924)," DIN-adopted European-adopted ISO Standard DIN EN ISO 3924.
48. DIN EN 116, "Diesel and Domestic Heating Fuels - Determination of Cold Filter Plugging Point - Stepwise

Cooling Bath Method," DIN German Institute for Standardization, Standard DIN EN 116.

49. DIN EN 16576, "Automotive Fuels - Determination of Manganese and Iron Content in Diesel - Inductively Coupled Plasma Optical Emission Spectrometry (ICP OES) Method," DIN German Institute for Standardization, Standard DIN EN 16576, Rev. Feb. 2015.
50. DIN EN 14370, "Surface Active Agents - Determination of Surface Tension," DIN German Institute for Standardization DIN EN 14370, Rev. Nov. 2004.
51. DIN 51900-2, "Determining the Gross Calorific Value of Solid and Liquid Fuels using the Isoperibol or Static Jacket Calorimeter and Calculation of Net Calorific Value," DIN German Institute for Standardization, Standard DIN 51900-2, Rev. May 2003.
52. ISO 8178-1, "Reciprocating Internal Combustion Engines - Exhaust Emission Measurement - Part 1: Test-bed Measurement Systems of Gaseous and Particulate Emissions," International Organization for Standardization, Standard ISO 8178-1:2020.
53. ISO 8178-4, "Reciprocating Internal Combustion Engines -Exhaust Emission Measurement - Part 4: Steady-state and Transient Test Cycles for Different Engine Applications," International Organization for Standardization, Standard ISO 8178-4:2020.
54. Glaude, P., Fournet, R., Bounaceur, R., and Molière, M., "Adiabatic Flame Temperature from Biofuels and Fossil Fuels and Derived Effect on NOx Emissions," *Fuel Processing Technology* 91, no. 2 (2010): 229-235, doi:10.1016/j.fuproc.2009.10.002.
55. Huang, Y., Wang, S., and Zhou, L., "Effects of Fischer-Tropsch Diesel Fuel on Combustion and Emissions of Direct Injection Diesel Engine," *Front. Energy Power Eng. China* 2, no. 3 (2008): 261-267, doi:10.1007/s11708-008-0062-x.
56. Pettinen, R., Murtonen, T., and Söderena, P., "Performance Assessment of Various Paraffinic Diesel Fuels," in *Proceedings of Fuels for Efficiency, Annex 52, IEA-AMF Technology Collaboration Programme on Advanced Motor Fuels*, October 2017, https://www.iea-amf.org/app/webroot/files/file/Annex%20Reports/AMF_Annex_52.pdf.
57. Rimkus, A., Žaglinskis, J., Rapalis, P., and Skačkauskas, P., "Research on the Combustion, Energy and Emission Parameters of Diesel Fuel and a Biomass-to-liquid (BTL) Fuel Blend in a Compression-Ignition Engine," *Energy Conversion and Management* 106 (2015): 1109-1117, doi:10.1016/j.enconman.2015.10.047.
58. Dimitriadis, A., Seljak, T., Vihar, R., Baškovič, U.Z. et al., "Improving PM-NOx Trade-off with Paraffinic Fuels: A Study Towards Diesel Engine Optimization with HVO," *Fuel* 265 (2020): 116921, doi:10.1016/j.fuel.2019.116921.
59. Gill, S.S., Tsolakis, A., Dearn, K.D., and Rodríguez-Fernández, J., "Combustion Characteristics and Emissions of Fischer-Tropsch Diesel Fuels in IC Engines," *Prog Energy Combust Sci* 37 (2011): 503-523, doi:10.1016/j.pecs.2010.09.001.
60. Pastor, J.V., García-Oliver, J.M., Micó, C., García-Carrero, A.A. et al., "Experimental Study of the Effect of Hydrotreated Vegetable Oil and Oxymethylene Ethers on Main Spray and Combustion Characteristics under Engine Combustion Network Spray A Conditions," *Applied Sciences* 10, no. 16 (2020): 5460, doi:10.3390/app10165460.
61. Ovaska, T., "Exhaust Particle Numbers of High- and Medium-Speed Diesel Engines with Renewable and Recycled Fuels," Ph.D. thesis, School of Technology and Innovations. University of Vaasa, 2020, ISBN 978-952-476-929-7.
62. Erman, A.G., Hellier, P., and Ladommatos, N., "The Impact of Ignition Delay and Further Fuel Properties on Combustion and Emissions in a Compression Ignition Engine," *Fuel* 262 (2020): 116155, doi:10.1016/j.fuel.2019.116155.

Contact Information

Mrs. Kirsi Spoof-Tuomi
the University of Vaasa, PO Box 700, FI-65101 Vaasa, Finland
kirsi.spoof-tuomi@uwasa.fi.

Acknowledgments

The authors wish to thank the company UPM for delivering renewable diesel fuel for the research.

Abbreviations

CA - crank angle
CD - combustion duration
CFPP - cold filter plugging point
CH_4 - methane
CLD - chemiluminescence detector
CO - carbon monoxide
CTO - crude tall oil
DFO - diesel fuel oil
EEPS - engine exhaust particle sizer
EU - European Union
FAME - fatty acid methyl ester
FSN - filter smoke number
FTIR - Fourier-transform infra-red
GHG - greenhouse gas
HC - total hydrocarbons
HFID - heated flame ionization detector
HFRR - high frequency reciprocating rig
HRR - heat release rate
HVO - hydrotreated vegetable oil
IC - internal combustion
ISO - International Standard Organization
MFB - mass fraction burned
N_2O - nitrous oxide

NDIR - non-dispersive infra-red
NO_x - oxides of nitrogen
NRSC - non-road steady cycle
PAH - polyaromatic hydrocarbons
PN - particle number
PSD - particle size distributions

ISSN 0148-7191